APPLICATION OF CERAMIC MEMBRANE BIOREACTORS IN TREATING DOMESTIC WASTEWATER

JIN LE

(*B. Sci., QDU*)

A THESIS SUBMITTED

FOR THE DEGREE OF DOCTOR OF PHILOSOPHY

DIVISION OF ENVIRONMENTAL SCIENCE AND ENGINEERING

NATIONAL UNIVERSITY OF SINGAPORE

2011

ACKNOWLEDGEMENTS

First of all, I would like to express my sincere gratitude to my supervisors, Prof. Ong Say Leong and A/P Ng How Yong for their constant supports and engorgement; invaluable patience and guidance throughout the whole course of my study and research.

My sincere thanks also go to the members of the examination committee (internal and external) of this thesis.

Special thanks to all the laboratory staffs in Centre for Water Research: Mr. Chandrasegaran, Ms. Lee Leng Leng, Ms. Tan Hwee Bee and Ms. Tan Xiaolan, for their kind assistance in the experimental set-up and the lab equipment. My thanks also go to the final year students Ms Nguyen Thi Huong Tra, Mr Chong Yee Siong and Ms Lau Eng Tong who have contributed to this research project.

I also wish to express my deepest thanks to my family, and my good friends in the lab, especially Dr Ng Tze Chiang, Albert, Dr Huang Zhi, Dr Mo Huajuan, Dr Lee Lai Yoke, and Ms Li Jiaxuan for their continuous support.

Last but not least, I wish to thank my entire extended family, my parents Jin Huiliang and Le Minglang, and my husband Wang Kai, for their unflagging love and unfailing support throughout my life.

Jin Le

TABLE OF CONTENTS

SUMMARY

Membrane fouling, the key disadvantage that inevitably occurs continuously in the membrane bioreactor (MBR), baffles the wide-scale application of MBR. Ceramic membrane, which possesses higher chemical, biological, mechanical and thermal resistance compared to the polymeric counterparts, has seldom been used in MBR to treat municipal wastewater due to the high price involved in membrane fabrication process. Four ceramic membranes with the same materials but different pore size, ranging from 80 to 300 nm, were studied in parallel using four lab-scale submerged MBRs in Phase 1 (i.e., one type of ceramic membrane in one MBR). Total chemical oxygen demand (COD) and ammonia nitrogen removal efficiencies were observed to be consistently above 94.5% and 98%, respectively, in all submerged ceramic membrane bioreactors. The experimental results showed that fouling was mainly affected by membrane's microstructure, surface roughness and membrane pore size. Ceramic membrane with the roughest surface and biggest pore size (300 nm) had the highest fouling potential with respect to the transmenberane pressure (TMP) increment profile, and reached a TMP of 30 kPa on Day 72 and Day 80 of the two fouling cycles. The 80 nm membrane with a smoother surface and relatively uniform smaller pore openings experienced least membrane fouling with respect to TMP increase, and reached a TMP of 30 kPa on Day 150 in Cycle 1, and it never experienced serious fouling in Cycle 2. The effects of the molecular weight

distribution, particle size distribution and other biomass characteristics such as extracellular polymeric substances, zeta potential and capillary suction time, were also investigated in this study. Results showed that no significant differences of these attributes were observed. These observations indicated that the membrane surface properties, especially the surface roughness, were the dominant factors leading to different fouling potential observed in this study.

An in-depth study of fouling mechanisms for different pore-sized ceramic membranes in MBR were conducted in Phase 2 with four different pore–sized membranes being placed in one SCMBR in order to have a same mixed liquor condition for all the membranes. Results showed that M80 was able to reject more organics and experienced more serious initial fouling within the first 7 days. However, from Day 10 onwards, significant TMP increase was observed for all the membranes, where M300 has the highest TMP increase rate (dp/dt) of 2.31 and M80 has the lowest dp/dt of 0.96. Based on the LC-OCD, EEM spectra and HPLC results of the membrane permeates and mixed liquor supernatant of the sample after 1 h and 14 d operation duration, it was found that a bioflm/biocake layer was formed on the membrane surface after a period of time. This biofilm/biocake layer enhanced the organic rejection for ceramic membranes, especially for M300. The biofilm/biocake development on the membrane surface was also monitored by scanning the membrane surface using a high-resolution scanner at each sampling point. Obtained images analyzed by ISA-2 software showed that the overall biofilm/biocake coverage ratio increase rate on the membrane surface was related to the membrane surface roughness, which was M300 > M100 > M200 > M80. This finding indicates that the biofim/biocake coverage ratio could be a good indicator for membrane fouling.

Membrane fouling has been noted as the main obstacle for the widespread application of MBR. In order to alleviate membrane fouling, in Part 1 of Phase 3 a porous suspended biofilm carrier was introduced into submerged ceramic membrane bioreactors (SCMBR) treating domestic wastewater. Results showed that biofilm carrier addition was very efficient in mitigate cake formation on the membrane surface, resulting in lesser fouling in SCMBR with carrier. SCMBR without carriers had 5 times higher cake resistance (147.00×10^{11} m^{-1}) and 2.5 times higher total resistance(177.98×10^{11} m^{-1}) than that of the one with carriers, indicating that the addition of biofilm carriers in SCMBR reduced the cake resistance by 72.7% after a same operation period. Both the higher concentration of biomass and inorganic matters in cake layer facilitated TMP increment in SCMBR without carriers due to the bridging interaction of biopolymers and inorganic matters. Although the solutes compositions occupied fewer proportions in the biofilm/cake layer, their fouling contribution could not be ignored. The liquid chromatography - organic carbon detector (LC-OCD) results indicated that a higher concentration of low molecular weight (LMW) compounds (less than 1000 daltons) in the cake layer contributed to the faster fouling in R2 (without carriers). The excitation emission matrix (EEM) florescence spectra of the cake layer showed that there were two obvious protein-like substance peaks at the wavelength of Ex/Em =250-270/390 and Ex/Em=250/420-430 in both SCMBRs. However, relative dominance of the protein-like substance was relatively high in R2 (without carriers) with intensity of 284.9 in the first peak and intensity of 244.7 in the second peak, which confirmed that higher biopolymer contents were detected in cake layer in SCMBR without carriers. Other characteristics of the cake as well as the biomass suspensions were also evaluated in this study. The evaluation of optimum biofilm carrier dosage in the SCMBR system with mixed

liquor suspended solids (MLSS) concentration of 6,000 mg/L showed that the optimum biofilm carrier dosage was 5.70% based on the dosage selection of 2.85% and 5.70% by volume ratio of carrier volume to reactor working volume.

In addition to the biofilm carrier addition, three times higher backwash flux than that of the membrane permeate was adopted in R2 (with backwash) in Part 2 of Phase 3. Results showed that backwash applied was very efficient in alleviating membrane fouling by partially removing the biocake/biofilm on the membrane surface and foulants in the membrane pores. The reactor with backwash system could extend operation duration by 14 days, which was half of the total duration of the SCMBR without backwash (R1). In R1 (without backwash), exponential TMP increase was found, while a linear relationship between the time and the TMP was observed in R2 (with backwash). SEM images showed that a thick and non-porous fouling layer consisting of various bacteria covered by a cluster of biopolymer was found on membrane surface in R1 (without backwash). On the contrary, no obvious fouling layer was observed and the clusters of microbial cells were much fewer on the membrane surface in R2 (with backwash). Analysis of the elemental composition on the membrane surface by SEM-EDX technology showed that elements of C, O, Mg, Al, S, Si, P, Ca, and Fe were detected, indicating the initiation of inorganic fouling on the membrane surface. The higher intensity of these elements (Mg, Al, Ca, Fe) on the membrane surface in R1 (without backwash) suggested the existing of a cation bridge between Mg^{2+}, Fe^{3+}, Al^{3+}, Ca^{2+} and COO- and become the major component of biopolymers. The investigation of the organic composition of the cake layer by traditional protein and carbohydrate analysis, LC-OCD, FTIR and EEM spectra indicated that biopolymer and clay materials were the major membrane foulants. The

higher concentration of these components in cake layer contributed to the faster membrane fouling observed in R1 (without backwash).

Keywords: backwash, biofilm carrier, cake layer, EEM, fouling minimization, FTIR, LC-OCD, membrane fouling, pore size, SCMBR, surface roughness.

NOMENCLATURE

ASP	activated sludge process
BCR	biofilm/biocake coverage ratio
BWP	backwash pressure (Pa)
CI	chloroform: isoamyl alcohol
CMBR	ceramic membrane bioreactor
CST	capillary suction time (s•L/g)
DOM	dissolved organic matter
EEM	excitation emission matrix
EPS	extracellular polymeric substances
FTIR	frustrated total internal reflection
HMW	high molecular weight
HPLC	high performance liquid chromatography
HRT	hydraulic retention time (h)
LC-OCD	liquid chromatography – organic carbon detector
LMW	low molecular weight
MBR	membrane bioreactor
MBR	membrane bioreactor
MF	microfiltration

MLSS	mixed liquor suspended solids (gL^{-1})
MLVSS	mixed liquor volatile suspended solids (gL^{-1})
MWCO	molecular weight cut-off (Da)
MWD	molecular weight distribution
PCI	phenol: chloroform: isoamyl alcohol
PCR	polymerase chain reaction
PSD	particle size distribution
RO	reverse osmosis
SCMBR	submerged ceramic membrane bioreactor
sdH_2O	sterilized distill water
SEM	scanning electron microscopy
SEM-EDX	scanning electron microscopy- energy diffusive x-ray
SMP	soluble microbial products
SRT	sludge retention time (d)
TCOD	total chemical oxygen demand
TDS	total dissolved solids
TMP	transmembrane pressure (Pa)
TOC	total organic carbon
TSS	total suspended solids
UF	ultrafiltration
VSS	volatile suspended solids

LISTS OF FIGURES

LIST OF TABLES

Chapter 1. Introduction

1.1 Water Reclamation and MBR Application

Water is an essential life-sustaining element and is yet a finite resource. There is only 1.7% drinking water resource out of the total water resource available on planet earth. Of this 1.7%, 30.1% is ground water and slightly more than half of it is saline. This distribution indicates that only less than 1.5% of the total water supply is available as fresh water for the world population. On the other hand, the world population has experienced a tremendous increase in the last few decades. The rapid increase in world population, together with the global issues of water scarcity and land shortages, has called for water reclamation as one of the alternative water sources.

Currently, there are two sources of water that can be commonly reclaimed or reused with our present level of technology: seawater and municipal wastewater. Comparing both, seawater desalination is relatively costly and energy consumptive, and can merely be applied in coastal areas. On the contrary, reusing wastewater is a sustainable water management approach that would contribute to a stable supply of water source in the long term (Ghayeni *et al*., 1998). This is because typically a large proportion of the cities' public water supply would end up as domestic wastewater, and the domestic wastewater produced by human activities can be reclaimed or reused

by the current technology. This water-wastewater cycle provides a reliable supply of water with slight variations and at lower costs throughout the year as compared to seawater desalination (Khawaji, 2008). It was reported that total life cycle cost of producing reverse osmosis (RO) water from secondary effluent was about 1.2 times cheaper than seawater desalination (Cote *et al*., 2005). This difference is due to the lower total dissolved solids (TDS) present in the secondary effluent compared to seawater, thus lowering the osmotic pressure required to produce an equal amount of fresh water (Cote *et al*., 2005). In Singapore, reclaimed water called NEWater is a main water supplier for the water usage in the semi-conductor industry and a small quantity of NEWater has been fed into reservoirs for in-direct potable usage. This NEWater was reclaimed from the municipal wastewater by purifying secondary effluent (treated by activated sludge process (ASP)) via MF/UF - RO system.

With heightened awareness in public health and environmental protection, regulations for better wastewater effluent quality have been implemented for both municipal and industrial wastewater discharges. The increasing need to reclaim treated wastewater for reuse purposes makes the conventional activated sludge process (ASP) inadequate or not cost-effective to meet the stringent water quality requirement. This emerging development has led to the popularity of some novel wastewater treatment systems. A more compact and efficient treatment system capable of producing treated effluents of excellent quality- membrane bioreactor (MBR) - has thus become as a solution for the new era.

MBR is a combination of the conventional ASP and membrane separation technology (microfiltration (MF) or ultrafiltration (UF)) to give a compact system. It uses the membrane separation system to replace the secondary settling tank in an ASP system

and therefore reduces the footprint of the whole treatment system. With membrane pore sizes ranging from a few micronmeters to a few nanometres, MF and UF membranes can remove most particulates, bacteria and viruses and makes it possible to achieve high-grade clarification and disinfection of the effluent (Judd, 2006). This attribute enables MBR to eliminate all the constraints associated with biomass sedimentation. As a result, MBR can consistently provide high quality effluent continuously. In addition to the effluent quality, MBR system can also provide greater operation flexibility than ASP as the control of sludge retention time (SRT) is independent of hydraulic retention time (HRT). The advantages of MBR over the conventional ASP lead MBR to gain increasing popularity in the municipal wastewater and industrial wastewater treatment and water reclamation.

According to a report of technical market research from Business Communications Company, the global MBR market is rising at an average annual growth rate of 10.9% and is expected to approach US$363 million in 2010 (Hanft, 2006). In another market research conducted by Frost & Sullivan (2005), it is predicted that the US and Canadian MBR markets sum up to US$32.2 million, and projected to reach US$89 million in 2010. Hence, the potential growth of MBR market can be perceived as optimistic. On the other hand, in the last decade, the advancement of MBR technology has made the MBR more efficient and economical than the existing aerobic biological wastewater treatment processes, especially for a country with very limited space like Singapore. MBR has been proven to be an effective solution to transform wastewater into an environmentally friendly product suitable for discharge and reuse, as the relative ease of retention of biomass by a membrane makes it possible to treat the wastewater effectively.

MBR is capable of treating various waste streams (Chiemchaisri *et al*., 1994; Rahman and Al-Malack, 2006; Ueda *et al*., 1997) and has in fact been used to upgrade existing wastewater treatment plants. Its can accommodate high mixed liquor concentration of up to 30 g/L in industrial applications and at high SRT of beyond 50 days, giving better removal of refractory organic matter and making the system more robust to load variations and toxic shocks (Lesjean *et al*, 2004). It is not feasible to operate the conventional ASP at such high mixed liquor concentrations and SRTs because of its limitations in achieving good sludge settleability. Moreover, in recent years, a new concept of coupling a reverse osmosis (RO) process after MBR has been developed for municipal wastewater reclamation (Qin *et al*., 2006). This reveals yet another promising area for MBR applications.

While MBR has obvious advantages over ASP, it also has its share of problems. Negative aspects of MBR, however, include high capital, maintenance and operating costs, which are to some extent exacerbated by membrane fouling. Membrane fouling is a result of the interaction between membrane and activated sludge suspensions, and it is a process of accumulation of organics or inorganic onto the membrane surface or into the membrane pores. The occurring of membrane fouling in turn requires frequent membrane cleaning, leading to higher operational costs in MBR system. Therefore, the issue of membrane fouling, which inevitably occurs continuously in the MBR, hinders the widespread applications of MBR. In order to promote the MBR application, the identification, investigation, controlling, and modeling of membrane fouling have become the focus of most MBR studies in recent years. However, a need for understanding the fouling mechanisms of MBR remains as there are many unknowns regarding the fouling mechanisms in a system with such complex biomass components.

1.2 Ceramic Membrane in MBR System

Currently, there are two types of membranes used in MBR – polymeric and ceramic ones. Polymeric membrane is a membrane with both thin selective layer and support layer, while ceramic membrane is a kind of membrane made of inorganic materials with a thin selective layer and a very thick support layer. Due to the different characteristics of these two membranes, they are applied in different areas. Polymeric membranes are largely applied in domestic wastewater treatment (Chiemchaisri *et al*, 1994). However, they are sensitive to caustic cleaning regents, especially when the membrane module is seriously fouled during industrial operation (Xing, 1998). On the contrary, ceramic membrane is usually applied in treating industrial wastewater, such as fermentation liquid (Li *et al*., 2006), refinery wastewater (Rahman and Al-Malack, 2006), degreasing solution (Blöche *et al*., 2004) and landfill leachate (Visvanathan *et al*., 2007) owing to its excellent selectivity, permeability as well as thermal and chemical stability. The stable compositions of the ceramic membranes enable the production of high quality permeate, and that the membrane will not be damaged by the solution during the operation. Although ceramic membranes are comparatively more expensive than those polymeric counterparts, cleaning of ceramic membrane is relatively easy and backwash/backflush/backpulse can be conveniently implemented in situ because ceramic membranes possess a higher degree of mechanical resistance. In addition, due to the resistance to chemical abrasion and biological degradation, ceramic membrane can also withstand a higher pH and temperature range. These merits would facilitate a good permeate flux recovery after maintenance cleaning and a longer life-span that cannot be easily matched by polymeric membranes, which in turn, leads to a lower cost from a long-term point of view.

It is noted that ceramic membrane may facilitate the MBR to achieve the advantages of having a lower operation cost from the viewpoint of long-term operation. Reviewed from the published literature also showed that the application of ceramic membrane was able to produce stable and high-quality membrane permeate. However, to date, most of the studies concerning the CMBR performance employed side-stream configurations (Xing *et al*., 2000; Tardieu *et al*., 1999) and treatment of synthetic wastewater (Sun *et al*., 2006), although all of which revealed that excellent carbonaceous and ammonia removals could be obtained. The high energy consumption involved in the side-stream MBR makes it less and less popular in recent years. In addition, the usage of the synthetic wastewater cannot fully represent the results of treatment performance for domestic wastewater in submerged ceramic MBR (SCMBR). Hence, there is a need to investigate the treatment performance of SCMBR in domestic wastewater treatment. Given the water scarcity of the world and the higher energy requirement involved in the side-stream MBR system, it is desirable to investigate the performance of SCMBR for the treatment of domestic wastewater.

In addition, although many efforts have been invested to investigate the membrane fouling and optimize the operating conditions of polymeric MBR, inadequate attention have thus far been paid to the inorganic membrane such as ceramic membranes. Even less information are available on fouling mechanisms in SCMBR in treating domestic wastewater. The lack of the information on the fouling characteristics of ceramic membrane might be a main constraint for the application of SCMBR in treating domestic wastewater. Given the potential advantages of the ceramic membrane for MBR system, the application of SCMBR in treating the domestic wastewater is meaningful, and it is desirable to conduct an in-depth study on

SCMBR for treating domestic wastewater as it would enable one to lower operation costs and to exploit water reclamation in a sustainable manner.

1.3 Conflicting Influence of Membrane Surface Property on Submerged MBR Performance

All parameters involved in the design and operation of MBR processes have an influence on membrane fouling (Le-Clech *et al*., 2006a). Some well-known factors controlling fouling include particle size distribution (PSD), extracellular polymeric substances (EPS), soluble microbial products (SMP) and the floc-structure of activated sludge (Chang and Lee, 1998; Chang *et al*., 1999; Kim *et al*., 1999; Wisniewski and Gransmik, 1998). In addition, fouling is in close association with membrane materials and morphologies, because membrane properties of different membrane materials would induce different fouling characteristics on the membrane surface and into the membrane pores (Chang *et al*., 2001; Chen, 1998). Among the factors affecting membrane fouling, the effect of membrane pore size is seldom reported, especially in MBR system with ceramic membranes (i.e., SCMBR). A review of literature of polymeric membrane systems revealed that conflicting trends have been reported with respect to the effect of membrane pore size on fouling. There are no consistent general trends noted between pore size and membrane performances. Some researchers reported that a smaller pore-sized membrane was easier to induce fouling in the early stage of the operation due to a higher potential for cake layer formation (Chang *et al*., 2001), and pore blocking was the main contributor to the poor performance associated with bigger pore-sized membrane in long-term operation (He *et al*., 2005). Gander *et al*. (2000), however, reported the opposite trend. In addition, some studies have also demonstrated that it was not the membrane pore size,

but the surface structure and membrane pore openings that were dominating the fouling phenomenon (Madaeni *et al*., 1999; Fang and Shi, 2005). The different fouling propensities reported in these studies might be due to the effects of different membrane and operating conditions applied; therefore, a comprehensive study by adopting ceramic membranes with the same materials but different pore sizes for a long-term operation simultaneously would lead to an understanding on the effects of membrane pore size and surface properties on fouling in MBR.

Up to now, numerous studies have been conducted in the polymeric MBRs in order to elucidate membrane fouling; however, the fouling characteristics of the SCMBR and the factors leading to the different fouling propensity for different pore-sized SCMBRs remain unclear especially when SCMBR are applied to treat domestic wastewater. In addition, the contradicted results reported pertaining to the effect of membrane pore size on membrane fouling due to the complex and changing nature of the biological suspension in MBR systems and membrane pore size distribution used in the various studies also suggests a need for a systematic study to elucidate the relationship between pore size and fouling behavior using real wastewater. In view of the above, it is desirable to evaluate the fouling mechanism for SCMBR and systematically investigate the effect of pore size on membrane fouling characteristics for domestic wastewater treatment.

1.4 Fouling Minimization Strategies

In order to widen the MBR application, most MBR studies performed aimed to identify, investigate and model membrane fouling. Based on that, a number of studies have been conducted to control membrane fouling, including operating condition optimization (Defrance *et al*., 1999a; Liu *et al*., 2000; Bourgeous *et al*., 2001; Sofia *et*

al., 2004), biomass characteristics optimization (Chang and Fane, 2002; Holbrook *et al*., 2004) and membrane surface property optimization (Chang and Fane, 2002; Holbrook *et al*., 2004; Le Roux *et al*., 2005). Recently, adding certain carriers with specific characteristics in order to absorb biomass and small molecules became another attempt for membrane fouling control. Kim *et al*. (1998) reported that the adsorption of DOM by activated carbon greatly enhanced the membrane permeability of biological activated carbon sludge. Similar results were also reported in other studies (Kim and Lee, 2003; Li *et al*., 2005) that mitigating the cake layer formation was an effective method to relieve membrane fouling. Cake layer was proved to be the main contributor to membrane fouling in MBR (Chiemchaisri and Yamamoto, 1994; Choo and Lee, 1996; Meng *et al*., 2007). Thus, fouling control by reducing the cake layer formation by scouring effect provided by suspended biofilm carrier addition became a worthwhile idea. The addition of porous and suspended carriers was proven to enhance the membrane performance, indicating that biofilm carrier dosage could be a good attempt for cake layer control (Yang *et al*., 2006; Wei *et al*., 2006; Huang *et al*., 2008). Since the cake layer were considered as the main contributor in membrane fouling, the evaluation of the cake characteristics in terms of its volatile suspended solids (VSS), colloidal, solutes and inorganic matters compositions is a meaningful step in order to elucidate the fouling control mechanisms by biofilm carrier addition. However, previous studies did not investigate the cake layer structure and components, it remains unclear how suspended carriers will affect cake layer compositions.

In view of the above, there is a need to illustrate the fouling control mechanism by porous suspended carriers in SCMBR by studying the biomass characteristics and cake layer properties. A comparative study needs to be conducted in SCMBR with

and without suspended biofilm carriers under the same operating conditions. The characteristics of the cake layer and the major components of biomass in cake layer needs to be identified.

It was reported that in addition to operating condition optimization, system optimization and suspended carrier addition, backwash is also an alternative for relieving membrane fouling (Kuberkar *et al*., 1998; Hong *et al*., 2005). In the MBR with backwash system, most of the reversible fouling leading to pore blocking and cake layer was found to be removed by the backwash (Le-Clech *et al*., 2006b).This is because the backwash pressure was able to partially dislodge the loosely attached foulants on the membrane surface and loosen pore clogging near the membrane surface. As a result, the membrane filtration flux can be partially recovered through a backwash operation, and eventually the filtration period could be prolonged.

As discussed in section 1.2, the in situ membrane backwash can be realized in a system with flat-sheet ceramic membrane. However, so far no study has been conducted regarding the influence of backwash in the SCMBR treating domestic wastewater. Therefore, an investigation of the impact of backwash on the membrane performance in an SCMBR is meaningful, which will provide information for designers and operators to optimize the operating condition. The different fouling mechanism elucidation of SCBMR with or without backwash by investigating the cake layer characteristics (biomass contents, soluble contents, inorganic contents and microbial observation) will also give an insight into the system optimization in SCMBR.

1.5 Research Objectives

In view of the research needs discussed above, the goal of this study was to investigate the property of the ceramic membranes for successful application in a submerged MBR for domestic wastewater treatment. Both the treatment performance of SCMBR and the effect of pore sizes on membrane fouling for domestic wastewater treatment were systematically investigated. Backwash and biofilm carrier addition were also conducted in the third phase of the study to explore an effective way to delay membrane fouling. Figure 1.1 shows the experimental planning for the three-phase study. The detailed objectives are:

- To investigate the treatment performance of SCMBR in treating domestic wastewater.
- To investigate the fouling propensity of four different pore-sized membranes and to elucidate the factors attributing to membrane fouling.
- To investigate the affecting mechanisms of biofilm carriers and backwash and to explore an effective way to minimize membrane fouling in SCMBR.

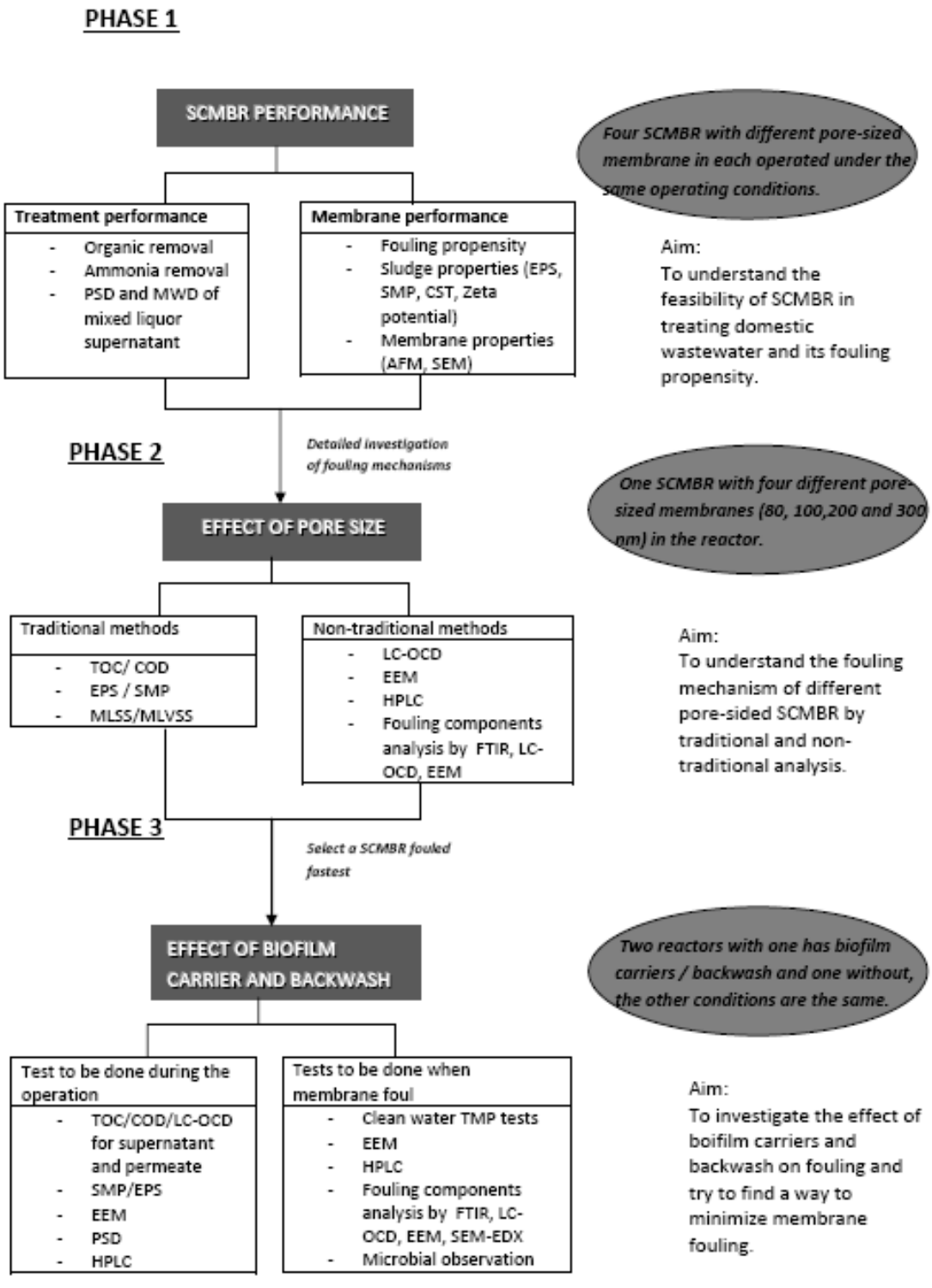

Figure 1.1 Experimental designs for the three-phase study.

Phase 1 was designed to study the performance of the SCMBR and to illustrate the different fouling potential of the four types of ceramic membrane with different pore sizes by recording the TMP increase profiles. The effect of the ceramic membrane pore size on the biomass properties, membrane permeability, and fouling potential for each type of membrane were studied. In this phase, four lab-scale SCMBRs, with volume of 7 L each, were operated in parallel to investigate the fouling potential of different pore-sized (80, 100, 200 and 300 nm) ceramic membranes. For each SCMBR, three flat sheet ceramic membrane modules were mounted between two baffles, and each module were placed above a diffuser with an effective aeration rate of 2 L air/min per membrane module. The specific objectives of the study of this phase are:

- To illustrate the treatment performance such as the carbonaceous removal and ammonia removal of SCMBR in treating domestic wastewater.
- To investigate the fouling propensity of different pore-sized membranes in SCMBRs operated in parallel.
- To investigate the effects of pore size on biomass properties and membrane permeability.

In Phase 2, the main objective was to understand the conflicting impact of membrane pore size on membrane fouling. In order to rule out the effect of biomass properties, all four membranes with the different pore size of 80, 100, 200 and 300 nm were mounted in a single SCMBR. Therefore, all four ceramic membranes were operating under the same environmental conditions throughout the operation period. The MBR has been monitored for around one year after the biomass acclimation period. The specific aims of this phase of study are:

- To elucidate the fouling propensity of different pore-sized membranes in one SCMBR.
- To understand the biofilm formation and its effect on organic rejection by non-traditional analysis of high performance liquid chromatography (HPLC), LC-OCD and EEM. The effect of dissolved organic matters (DOM) on fouling was also evaluated.
- To evaluate the effect of biofilm/biocake formation on the membrane surface on membrane fouling by investigating development of biofilm microbial communities.

Phase 3 was designed to evaluate the influence of biofilm carrier addition and backwash system on membrane fouling. In part 1 of this phase, two reactors (one with biofilm carriers and one without) were operated simultaneously. A daily de-sludge of 700 ml was conducted in the reactor of 7 L in order to maintain an SRT of 10 d. In part 2 of this phase, two reactors (one with backwash system and one without) were operated in parallel to evaluate the effect of backwash on the biomass properties and membrane fouling. The backwash flux was set at three times higher than that of the membrane permeate flux, and was applied in the SCMBR with backwash system. Both reactors were operated under the conditions of 6 h HRT and 12 d SRT. The specific aims of this phase of study are:

- To evaluate the effect of biofilm carriers on the biomass properties (i.e. SMP; EPS; PSD and MWD)
- To elucidate the cake layer composition of the reactor with biofilm carriers and without biofilm carriers.

- To evaluate the effect of soluble organic contents on the membrane surface and the inorganic contents in the cake layer.
- To dose different dosage of biofilm carriers to investigate the optimal dosage of biofilm carrier under similar operating conditions.
- To evaluate the components of the cake layer and the microscopic observation of the membrane surface for the reactor with backwash and without backwash system.

1.6 Organization of Thesis

The rest of this thesis is divided into following chapters:

- Chapter 2 - Literature Review

  This chapter included a comprehensive review of the books and published literatures, which are relevant to this study. The various topics included treatment performance in ceramic membrane systems, effects of membrane properties on fouling and fouling mechanism elucidations. It presents some findings, highlights the strength of these studies and the research gaps and needs based on these studies.

- Chapter 3 – Materials and Methods

  This chapter described lab-scale experimental set-up and operating conditions for the three-phase studies. The characteristics of the membrane were also explained in this chapter. The detailed sampling methods, the analytical methods and the equipment involved in these tests were described in this chapter.

- Chapter 4 – 6 Results and Discussions in 3-phase study

  These three chapters presented the experimental findings, and based on these findings, comparisons between the current studies and the published literatures were provided. Chapter 4 focused on treatment performance elucidation, such as carbonaceous removal and ammonia removal. The preliminary fouling propensities of different pore-sized membranes were also discussed. Chapter 5 presented the detailed fouling mechanisms illustration. Chapter 6 evaluated the influence of the biofilm carrier addition and backwash on membrane fouling, and discussed the optimal dosage of bioflm carrier in SCMBR under similar operating condition.

- Chapter 7 - Conclusions and Recommendations

  This chapter summarized the main conclusions obtained from the experimental data. Based on the current findings and the experimental constrains, recommendations for future studies were also suggested.

Chapter 2. Literature Review

2.1 Application of Ceramic membrane in MBR

2.1.1 Ceramic Membrane Characteristics

Most of current MBR systems employed in municipal wastewater treatment are using polymeric membranes. In the application of MBR that is based on polymeric materials, the leading country is Japan, where most MBR systems are used for water recycling in buildings (Yamamoto *et al*., 1989; Chiemchaisri *et al*, 1994). As these polymeric membranes are normally sensitive to caustic cleaning reagents, the difficulty encountered in membrane cleaning is a common phenomenon in MBR operation, especially when the membrane module is seriously fouled during industrial operation (Xing, 1998). This is because although chemical cleaning removes fouling, it may change the properties of the membrane and consequently, influence their performance. It was demonstrated by Mattias *et al*. (2008) that after the chemical cleaning by acid, the membrane permeability increased while the retention decreased for aromatic polyamide membranes; and the similar behavior was observed with alkaline cleaning of the semi-aromatic polyamide (polypiperazine) membranes. In addition, physical cleaning such as air backwashing is also an efficient method for flux recovery. However, it may also present potential issue of membrane breakage and rewetting for polymeric membrane. Compared to polymeric, the ceramic

membrane is more robust than the polymeric counterparts. To explore the potential advantage of ceramic membranes, an MBR system equipped with ceramic membranes was first developed in France (Trouve *et al*., 1994). Although ceramic membranes are comparatively more expensive than those polymeric counterparts, they make the in situ cleaning of membrane easy and convenient as these inorganic membranes possess a higher degree of chemical abrasion and biological degradation. Ceramic membranes have a great chemical stability in a wider range of pH and temperature (White and Asaadi, 1989), which makes them very popular in treating industrial wastewater. In addition, they can also withstand a higher suction range and can be backwashed/backflushed/backpulsed more readily. This would facilitate excellent permeate flux recovery after maintenance cleaning and attain a longer life-span that could not be matched by flat sheet polymeric membranes, leading to a lower operation cost from the viewpoint of long-term operation.

Compared to ASP, there is a major concern for MBR – high cost that includes both capital for membrane cost and operating costs. With the advancing of the membrane fabrication technology, the MBR will eventually be an alternative for wastewater treatment process if the membrane cost could be further reduced. In this case, the operating cost of the MBR system will be the main concern for its future application. The ceramic membrane, which will not only make the in situ cleaning possible during the operation, but also sustain chemical abrasion, and lengthen the membrane life-span. This will to some extent lower the total operation cost. As such, to investigate the application of the ceramic membrane in MBR is a necessity given its robustness nature.

2.1.2 CMBR Treatment Performance

Owing to its excellent selectivity, permeability as well as thermal, mechanical, biological and chemical stability, ceramic membrane filtration is an advanced method widely applied in beverage, brewing soy sauce and dairy industries for separating the substrate (Li *et al*., 2006; Wang *et al*., 2004). In addition, ceramic membrane is also widely used in MBR for treating industrial wastewater, such as refinery wastewater (Rahman and Al-Malack, 2006), high strength wastewater (Sun *et al*., 2006), degreasing solution (Blöcher *et al*., 2004), and landfill leachate (Visvanathan *et al*., 2007).

A review of literature revealed that application of the ceramic membrane bioreactor for treating municipal wastewater is rarely reported (Xing *et al*., 1999, 2000, 2001; Defrance *et al*., 2000; Tardieu *et al*., 1999). Xing *et al*. (2000) reported that 97% of COD, 96.2% of ammonia nitrogen (NH_3-N), and 100% of SS were removed by operating the CMBR at SRTs of 5-, 15- and 30-d, respectively, which fulfill the urban wastewater reuse standard adapted in China. Similarly, Sun and his co-workers (Sun *et al*., 2006) used submerged CMBR to treat high strength synthetic wastewater at a prolonged SRT of 200 d. They noted that CMBR could achieve both COD and TOC overall removal efficiency at 96%. These researchers have demonstrated that like polymeric membrane, CMBR performance is independent of its hydraulic loading rate as well as the organic loading rate. However, most of these studies dealing with the domestic wastewater were employing the side-stream MBR configuration. The use of recirculation loops in cross-flow configurations leads to increased energy costs. In addition, the high shear stresses in the tubes and recirculation pumps can contribute to the destruction of bioflocs and this has been linked to a loss of biological activity

(Brockmann and Seyfried, 1997), while the submerged MBR can overcome these setbacks. In addition, the performance of submerged system (i.e., SCMBR) for treating raw sewage water is still unclear, as the available information is mostly extracted from the side-stream system (Xing *et al*., 1999) or synthetic wastewater (Sun *et al*., 2006). Therefore, given the water scarcity of the world and higher energy requirement in a side-stream MBR system, it is desirable to investigate the performance of SCMBR for the treatment of domestic wastewater. Moreover, as the membrane performance influence the MBR economy, the initiation of a comprehensive investigation on performance of the submerged membrane modules is necessary.

2.2 Factors Affecting Membrane Fouling

All the parameters involved in the design and operation of MBR processes have an influence on membrane fouling. In the operation of the MBR, there are four major types of causes for membrane fouling (Figure 2.1), which include feed characteristics (Chae *et al*., 2006; Ng *et al*., 2005; Rojas *et al*., 2005), biomass characteristics (Ahmed *et al*., 2007), membrane characteristics (Fang and Shi, 2005) and the operating conditions (Ng *et al*., 2006; Ng and Hermanowicz, 2005). Each of them contributes to the membrane fouling in a different way.

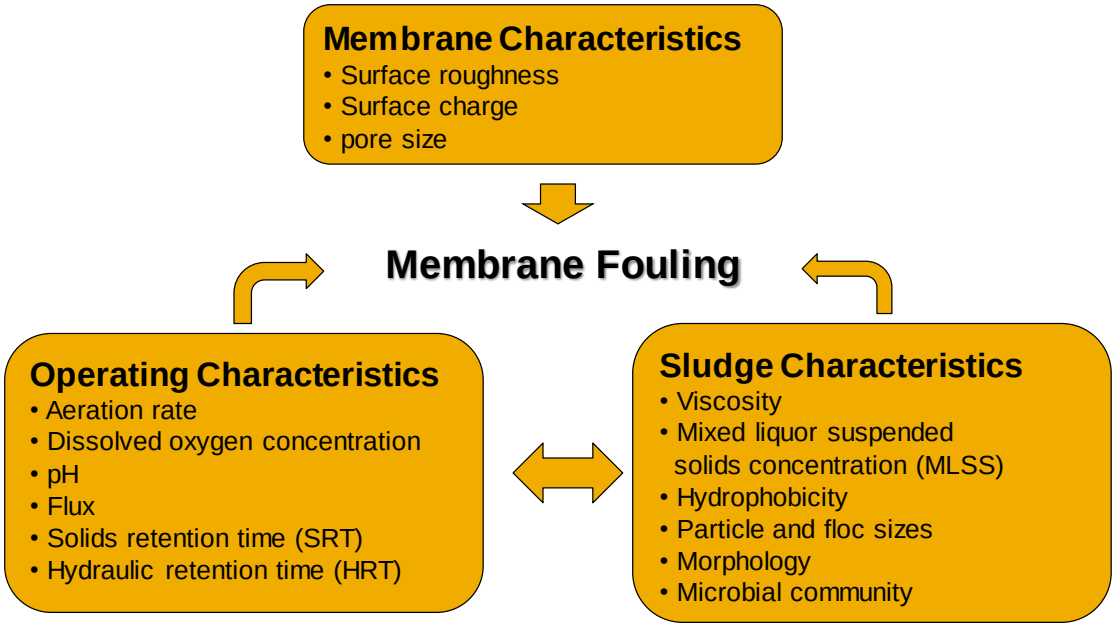

Figure 2.1 Factors affecting fouling in submerged MBRs.

2.2.1 Effect of Biomass Characteristics on Fouling

MLSS Concentration

Mixed liquor suspended solids (MLSS) is considered as the main contributor to membrane fouling, its concentration indeed has a complex interaction with membrane filtration. However, the effect of MLSS concentration on MBR fouling is variable, mainly because of the complexity and variability of the components (both organic like extracellular polysaccharides and soluble microbial products and inorganic like Mg^{2+}, Ca^{2+}, Fe^{3+}). Controversial findings about the effect of MLSS on membrane have been reported. Some authors demonstrated that if the other biomass characteristics were not accounted for, the increase in MLSS concentration seemed to have a negative effect on the MBR performance (Cicek *et al*., 1999; Chang and Kim, 2005). However, some other authors reported positive effect (Defrance and Jaffrin, 1999b; Brookes *et al*., 2006), and some observed insignificant impacts (Le-clech *et al*., 2003; Hong *et al*., 2002). The lack of a clear correlation between MLSS concentration and

characteristics of other foulants suggested that the MLSS concentration alone is a poor indicator of membrane fouling propensity (Jefferson *et al*., 2004).

EPS and SMP Components

Extracellular polymeric substances (EPS), which is often identified as the most significant biological factor attributing to membrane fouling, has shown different relationships with the membrane fouling in different studies (Lee *et al*., 2003; Fawehinmi *et al*., 2004; Yamoto *et al*., 2006). This phenomenon might be attributed to the different operating conditions applied in the individual study. Another contribution to the controversial results reported is that there is no standard method of EPS extraction existing. EPS was found to have no impacts on the flux specific resistance below 20 and above 80 mgEPS/gMLVSS, but played a significant role on fouling between these two limits in MBR (Le-Clech *et al*., 2006a). This was confirmed by another study reporting no clear relation between bound EPS (or eEPS) and membrane fouling for concentrations lower than 10 mg/gSS (Yamoto *et al*., 2006). However, in another example obtained with an anaerobic MBR, specific resistance increased linearly with eEPS rising from 20 to 130 mg/gSS (Fawehinmi *et al*., 2004).

Protein, humic substances and polysaccharide are the major polymeric constituents in both extracted EPS and sludge flocs (Wilén *et al*., 2003). However, the chemical constituents in extracted EPS under different conditions were slightly different. Table 2.1 summarizes EPS (extracted EPS) concentrations as well as compositions reported in various MBR set-ups and reveal a relatively narrow range of the EPS_p and EPS_c measured. In most cases, EPS_p (with a maximum concentration of 120 mg/gSS) was greater than EPS_c (maximum concentration of 40 mg/gSS) (Le-Clech *et al*., 2006a).

In addition, it can be seen from the table that the concentration of the humic substances is also higher than that of carbohydrate. This observation showed that the predominant organic components in extracted EPS were protein and humic substances. However, due to the constrains of humic substances detection (LC-TOC is involved in the fractionization of humic substances, while the LC-TOC is only available in several laboratories all over the world), protein and carbohydrate were usually taken as the major components for EPS (Brookes *et al*., 2003; Meng *et al*., 2006).

Table 2.1 Chemical compositions of extracted EPS (units are in mg/g MLVSS by default).

EPS	**EPS_p**	**EPS_c**	**EPS_h**	**Others**	**Details**	**Reference**
	25-30	7-8	12-13		R(10)	Cabassud *et al*.(2004)
108±14	45±3.6	7.8±0.6	28±9.0	Uronic acids 1.6±0.6	Batch Filtration Test	Wilén *et al*.(2003)
	31-116	6-15	-	TOC:37-65	Four pilot-scale plants	Brookes *et al*.(2003)
	30-36	33-28	-	-	S (20-60)	Lee *et al*. (2003)
	73 60	30 17	-	-	S (∝) R (∝)	Le-Clech *et al*.(2003)

Note: S, synthetic wastewater; R, real wastewater; SRT are given in the days in bracket; ∝, infinite SRT (i.e. no wastage).
EPS_p: protein in EPS EPS_c: carbohydrate in EPS EPS_h: humics in EPS

EPS affected the membrane fouling in a complex way due to its complex composition. In previous studies it has been found that there was a positive correlation between the total amount of the EPS and negative surface charge (SC) (Mikkelsen and Keiding, 2001; Jia *et al*., 1996; Morgan *et al*., 1990), which would correspondingly affect the membrane fouling. Little information can, however, be found in the literature

pertaining to the influence of the individual components on the SC. Mikkelsen and Keiding (2001) found a positive relationship between the charge density of extracted EPS and its protein content, which supported the findings reported by Wilén *et al*. (2003) that the proteins had a significant effect on the SC. From another aspect, it was found by Morgan *et al*. (1990) and Liao *et al*. (2001) that the SC of biomass flocs was more influenced by the proportions between proteins and carbohydrates (protein/carbohydrate or protein/(carbohydrate + DNA)) than by the concentrations of the individual components of the EPS. This phenomenon was explained by a neutralization of positive charges on the proteins by negative charges on the carbohydrates. On the other hand, no such correlations between ratios of different components in extracted EPS and the biomass were reported by Wilén *et al*. (2003). These findings suggested that the various polymer fractions affect the SC in a more complex way than preciously suggested. Therefore, it should be noted that the compositions of the EPS could be more important than the total amount of the EPS in the biomass flocs.

Soluble microbial products (SMP), was defined as soluble cellular components that are released during cell lysis, diffuse through the cell membrane and lost during synthesis (Laspidou and Rittmann, 2002) or are excreted for some purposes (Li *et al*., 2005). In an attempt to protect the membrane from direct contact with MLSS, a dual compartment MBR (bioreactor coupled with settling tank in which membrane filters biomass supernatant) has been built in Singapore (Ng *et al*., 2005). In this set-up, a higher filtration resistance was observed from the membranes filtering supernatant rather than those filtering 4 g/L of biomass. This example clearly indicated that the composition and concentration of the dissolved matters present in the biomass supernatant (i.e., SMP) had a large impact on membrane filtration; tentatively affect

the performance and the membrane fouling. Comparison between acclimatized sludge obtained from MBR and CASP pilot plants revealed similar levels in terms of $_{e}EPS_{p}$, $_{e}EPS_{c}$ and $_{e}EPS_{humic}$ (Cabassud *et al*., 2004). The presence of the membrane in the MBR process does not seem to affect the content of $_{e}$EPS within the flocs. However, SMP_{p}, SMP_{c} and SMP_{humic} levels were significantly greater than those of the MBR biomass, presumably due to the retention of large macromolecules by the membrane. During filtration it was expected that SMP would adsorb onto the membrane surface, block membrane pores and/or form a gel structure on the membrane surface where they provided a possible nutrient source for biofilm formation and a hydraulic resistance to permeate flow. In this case, the formation of organic layer exclusively exists in MBR.

It was recently reported by Ng *et al*. (2006) that membrane rejection range changed from 28 to 52% and from 32 to 21% for carbohydrates and proteins, respectively, when SRT was changed from 3 d to 20 d. These observations confirmed that the membrane had high rejection efficiency for dissolved organic matters like SMP, and the rejected organics would either deposit inside the membrane pores to induce pore clogging, or form a layer on the membrane surface which is defined as biofilm/biocake sometimes. However, the effect of the biofilm structure on membrane fouling are still unclear (will be discussed in later section). Thus, further study on the effect of SMP in term of the biofilm/biocake components on membrane surface will enhance our understanding regarding the fouling mechanisms in MBR.

In order to obtain better control of the feed water characteristics and other environmental conditions, many research studies were based on the use of synthetic/analogue solutions, which attempted to model real wastewaters (Lee *et al*.,

2003; Cho *et al*. 2005). These solutions were sometimes very basic (mainly composed of glucose) and therefore are very easily biodegradable. As a result, it is expected that SMP levels in such systems are lower than those in real systems. As it may be assumed that there are almost no substrate residuals from glucose in the supernatant, the less biodegradable SMP induced by cell lysis or cell release would account for most of the SMP measured in synthetically fed MBRs. This could explain the lower influence of SMP compared to those of $_{e}$EPS reported in some MBR studies using synthetic wastewater. Using synthetic substrate, Cho *et al*. (2005) concluded that the membrane fouling was affected more by the bound EPS of activated sludge flocs than the dissolved organic matter. Similar results were also reported by Lee *et al*. (2003) that no remarkable factor was found in fouling caused by supernatant. SUVA measurement carried out from supernatant of MBR fed with synthetic solution confirmed the presence of a portion of larger, more aromatic, more hydrophobic and double-bond-rich organics, which originated from the decayed biomass rather than the feed (Shin and Kang, 2003). Another important study (Lee *et al*., 2001), also based on synthetic wastewater, revealed that soluble organics alone could not predict MBR fouling. Thus, for application purpose, the effect of SMP on membrane fouling in the real case might be better understood if the raw domestic wastewater can be applied as the feed.

EPS on Membrane Surface

Although many studies have been conducted on the concentration and composition of EPS in the bulk solution, relatively less attention have been paid to the effect of EPS on membrane surface. Different mechanisms for the interaction between the macromolecules present in the supernatant and the membrane surface have been

proposed recently. Rosenberger *et al*. (2006) proposed that high polysaccharide concentrations in the supernatant correspond to high fouling rates while low concentrations correspond to low fouling rates. In addition, the increase of the fouling rate was mainly due to the retention of the polysaccharides by the membrane since no polysaccharide peak could be detected in permeates by the liquid chromatography – organic carbon detector (LC-OCD). The concentration difference between the mixed liquor supernatant and permeate can be partly attributed to physical retention due to the size of the organic compounds and probably partly due to the organic adsorption onto the membrane surface or into the membrane pores. It is remarkable that 30% of the original polysaccharide peak could penetrate the membrane, while these organic substances were always completely retained by the submerged membrane modules in the MBR (Rosenberger *et al*., 2006). Therefore, the fouling mechanisms of filtration between the solutes and the membrane in a biological system are different. The complexity of the system and the importance of the interactions between the membrane and microorganisms cannot be overlooked. Several interaction mechanisms between membrane material, soluble substances and microorganisms are possible:

i) Concentration polarization leads to enhanced concentrations of both biomass and organic macromolecules near the membrane surface. The creation of the fouling layer on the membrane surface would act as a secondary membrane, increasing the retention and/or the adsorption of macromolecules.

ii) The formation of a biofilm/biocake on the membrane surface, which is composed primarily of microbial cells and EPS, feeds on the dissolved macromolecules. As reported by Donlan (2002), EPS may account for 50 to 90% of the total organic

carbon of biofilms, and can be considered the primary matrix material of the biofilm. The formation of a biofilm could also lead to the degradation of the macromolecules as the permeate flows through the membrane.

iii) Finally, interaction between the macromolecules and other solutes (humics, divalent cations) within the membrane pores may be responsible for the reduction of the actual membrane pore size over time, eventually deteriorate the membrane permeability.

Flemming *et al*. (1994) summarized the negative effects of membrane biofouling attributed to the formation of biofilm/biocake as:

i. Increased separation system resistance by the biofilm

   This leads to a decrease in the product effluent production, as well as an increase in the TMP, with a subsequent increase in energy consumption.

ii. Formation of a gel phase between water and membrane surface

   Due to the diffusion resistance of the gel matrix, convective mass transport next to the membrane surface is inhibited. This leads to an increase in concentration polarization on the membrane, which may lead to scaling problems.

iii. Microbial attack on membranes

   Biofilms excrete acids and exoenzymes that attack membranes and their support materials. This is especially true for cellulose acetate membranes

which can hydrolyze directly. Such membrane deterioration leads to microbial contamination of the effluent quality.

iv. Increased costs

Direct and indirect costs incurred via the loss of product quality and quantity, higher energy demands and higher pre-treatment and cleaning demands, are all due to the negative effects of biofilms.

However, the studies done by Flemming *et al*. (1994) were on the basis of the biofouling on membrane other than that in membrane bioreactors. The fouling mechanisms in different systems are always different even with the same type of membranes. In particular, fouling mechanisms associated with MBR have not been systematically studied in terms of biofilm structure and components analysis. Given so many effects which are probably caused by the biofilm/biocake on the membrane surface, further study on the biofilm structure (morphologies, surface structures, etc.) and the compositions (protein, polysaccharide, inorganic matters, etc.) is necessary to elucidate the fouling mechanisms in MBR systems. A study on the source of the fouling in MBR will enhance the membrane life-span and the performance of MBR, and it will also help the operators to better optimize MBR systems in terms of operating conditions. In addition, though some efforts have been made to investigate the effect of the biofilm/biocake on the polymeric membrane performance in MBR, to date no information is available on the effect of biofilm/biocake on the inorganic membranes, such as ceramic membrane. The ceramic membranes, which possesses a hydraulic and rougher (compared to polymeric one) surface, might have a different fouling mechanism from that of the polymeric counterpart. It is therefore essential to investigate the fouling mechanism of ceramic membrane in submerged MBR.

2.2.2 Effect of Membrane Characteristics on Fouling

Effect of Membrane Pore Size

The effects of pore size on membrane fouling are strongly related to the feed solution characteristics and in particular the particle size distribution of the solution. It is expected that smaller pore membranes would reject a wider range of materials, and the resulting cake layer features a higher resistance compared to large pore membranes. As the pore size decreases, hindered transport of macromolecules exacerbates local polarization and the potential for aggregation and fouling. However, this type of fouling is more reversible and is more easily removed during the maintenance cleaning than fouling which is attributed to internal pore clogging occurring in larger pore-sized membrane systems.

Depending on the pore size and the types of the biomass filtered, results on the effect of membrane pore size on fouling reported in the literature have shown conflicting trends. During tests with a side-stream MBR, Madaeni *et al*. (1999) observed permeate flux (J_c) to be similar for membranes with different pore size (d_P). Chang *et al*. (2001), in comparing non-woven polypropylene membranes of three different d_P values, noted that the smallest pore (1.5 μm) exhibited greater initial fouling. Gander *et al*. (2000), however, found the larger d_P to be heavily fouled in the early stage of the filtration when they compared 0.4-μm polysulphone and 5-μm polypropylene membranes. These controversial results might be due to the different biological conditions applied in different systems. Another possible reason might be that the pore size of membranes used in these studies was in a large range, which was from 0.4 μm to several microns, while the particle with the size of larger than 0.45 μm is treated as suspended solids. In this case, the effect of the membrane pore size (less

than 0.45 μm) on fouling might be dramatically different from what have been reported in the studies using larger pore-sized membrane. For this reason, it seems appropriate to conduct tests under same feed and same operating conditions to isolate individual effect and only the effect of pore size on fouling. Besides, the range of membrane pore size should be a bit narrower for better comparison of the effects of membrane pore size on membrane fouling.

In addition, test duration is also an influencing factor on the effect of pore size on membrane permeability. In the microfiltration of 0.4% (weight) BSA solutions, Chen (1998) found that the critical flux increased with pore size when track-etched membranes of pore size 0.1, 0.2 and 0.4 μm were used., Wu *et al*. (1999) investigated the effect of membrane pore size (50 kDa, 100 kDa and 0.2 μm) on critical flux for three types of feed fluids (0.5% silica, 0.15% BSA and 5% yeast cell suspension). In contrast to Chen's study, for all feed fluids tested, the critical flux was found to decrease with increasing membrane pore size. It was also found that the membrane with smaller pore size had the highest initial fouling, while the larger pore-sized membrane has a greater long-term fouling potential (Chang *et al*., 2001). Similar trends showing the time dependency with respect to the effects of membrane pore size on membrane fouling were also reported for pore sizes ranging from 20 to 70 kDa (He *et al*., 2005). In this context, the test duration plays a vital role in the investigation of the effect of pore size on membrane performance, while the different durations employed in different studies make the comparison of different pore-sized membrane unreliable. However, to date few studies concerning the impacts of membrane pore size on membrane fouling have been focused on the long-term continuous filtration systems. Therefore, in order to solve this problem and comprehensively investigate the effect of pore size on membrane fouling, operating the MBRs simultaneously and

making the comparison concurrently between MBRs with different pore sizes for an extended period (e.g., over several months) is of great importance.

Another contributor to the discrepancies reported in various studies (Chang *et al*., 2001; Gander *et al*., 2000; Chen 1998; Wu *et al*., 1999) is that the membrane pore size will not only affect fouling directly, but also affects fouling indirectly by influencing membrane surface roughness. Evans *et al*. (2008) reported that increased fouling was present on rougher, more hydrophobic fluoropolymer (FP) surfaces, while if roughness, charge and hydrophobicity were similar, variation in pore size would not affect the filtration properties significantly over the range of 10, 30, and 100 kg/mol MWCO investigated when treating black tea liquor. Fang and Shi (2005) also reported that membrane roughness was the potential reason for the different fouling behaviors observed when four MF membranes with nominal sizes narrowly ranging from 0.20 to 0.22 μm were tested in parallel. Therefore, it was suspected that membrane microstructure, material and pore size distribution were all affecting MBR fouling significantly (Fang and Shi, 2005; He *et al*., 2005; Kang *et al*., 2006). As such, to conduct the MBR operation using membrane with the same material will help to isolate the effect of the membrane surface charge on membrane fouling. However, very few studies pertaining to the fouling of membrane with different pores but of the same materials have been reported in the MBR, and in fact no publication regarding this issue has been found in SCMBR. Therefore, it is necessary to investigate fouling mechanism of different pore-sized membranes in SCMBR in order to pave the way for exploration of SCMBR application.

Membrane Materials and Surface Property

Available membrane materials comprise of ceramic or polymeric. Ceramic materials such as alumina, zirconia, and titania (Al_2O_3, ZrO_2, and TiO_2, respectively) show superior hydraulic, thermal and chemical resistance, as indicated by the permeability data obtained at a maximum suction pressure of up to 2 bar (Germany, ItN)

Generally, it has been believed that hydrophobic membrane exhibited higher biofouling potentials than hydrophilic membranes (Leslie *et al*., 1993; Knoell *et al*., 1999; Pasmore *et al*., 2001). Other studies also confirmed that the increase of the hydrophobicity, both in cells and membranes, resulted in an increase of adhesion rate due to higher interaction energies between cells and membranes (Ghayeni *et al*., 1998; Knoell *et al*., 1999; Pasmore *et al*., 2001). The hydrophobicity of bacteria floc is the tendency of flocs to repel water. Chang and Lee (1998) demonstrated that higher biomass hydrophobicity could cause a stronger adherence to the membrane surface due to the interactions between them. It is also believed that hydrophobic interactions and polymeric entanglement contribute to increasing forces between the different floc fractions (Valin and Sutherland, 1982; Singh and Vincent, 1987; Eriksson *et al*., 1992).

Conventional wisdom generally attributes different fouling mechanisms for ceramic and polymeric membranes to properties of membrane materials, such as surface roughness, charge density, membrane morphology and hydrophobic/hydrophilic characteristics. This belief has been supported by some previous studies using various biological fluids (Matthiasson, 1983; Marshall *et al*., 1993; Fane and Fell, 1987). Reduction in the macromolecular adsorption with hydrophilic surfaces or by mitigating charge interactions will reduce the rate of the pore closure due to this

mechanism. Metsamuuronen *et al*. (2002) reported that much lower critical fluxes were observed for the ultrafiltration of baker's yeast when a hydrophobic polysulfone membrane was used as opposed to a hydrophilic regenerated cellulose membrane. Similar trends were also reported in anaerobic bioreactors (Kang *et al*., 2001; Yamagishi *et al*., 1990; Shimizu *et al*., 1989).

Kang and his co-workers (2001) have investigated the filtration characteristics of organic and inorganic membranes in a membrane-coupled anaerobic bioreactor. In their study it was found that for inorganic membrane, struvite was accumulated inside the membrane pore and played a key role in flux decline. For the organic membrane, however, a thick cake layer composed of biomass and struvite formed on the membrane surface, thus causing a major hydraulic resistance. This observation indicated that it might be more possible for inorganic to induce inorganic fouling than organic counterpart.

Therefore, low fouling in the bioreactor equipped with inorganic membrane might be attributed to their hydrophilic nature. However, there are also some contradictory results reported. Fang and Shi (2005) demonstrated that the polymeric membrane made of mixed cellulose esters (MEC) had a higher pore resistance than polyvinylidene fluoride (PVDF) membrane due to higher hydrophilicity of MEC membrane. This might be attributed to the reason that in mixed species feeds, the surface chemistry of the membrane might be masked by adsorption of the multitudes of macromolecular species. Thus, the benefits of hydrophilicity of MEC membrane might be obscured during the long-term fouling, and this hypothesis needs to be investigated. This finding, again, indicates that the effects of the membrane materials on the fouling potential highly depended on the operation durations.

Another contributor to such discrepancy is that not only the membrane hydrophilicity, but also the membrane surface charge and roughness will affect the membrane fouling. Evans *et al*. (2008) reported that increased fouling was present on rougher, more hydrophobic fluoropolymer (FP) surfaces, while if roughness, charge and hydrophobicity were similar (i.e., for the regenerated cellulose (RC) membrane), variation in pore size would not affect the filtration properties significantly over the range of 10, 30, and 100 kg/mol molecular weight cut-off (MWCO) investigated when treating black tea liquor. Fang and Shi (2005) also reported that membrane roughness was the potential reason for the different fouling behaviors observed when four MF membranes with nominal sizes narrowly ranged from 0.20 to 0.22 μm were tested in parallel. Therefore, it was suspected that membrane microstructure, material and pore size distribution were all affecting MBR fouling significantly (Fang and shi, 2005; He *et al*., 2005; Kang *et al*., 2006). As such, to conduct the MBR operation by applying the membrane with the same material will help to isolate the effect of the membrane surface charge on membrane fouling. However, comparatively fewer studies pertaining to the membrane fouling of hydrophilic membrane has been reported in the MBR, and even no publication regarding this issue has been found in SCMBR. In this context, it is necessary to investigate fouling mechanism in SCMBR—whether its hydrophilicity membrane property will relieve the fouling rate, and which factor (membrane roughness, membrane pre size) contributes most to the hydraulic resistance.

The different fouling propensity reported in these studies might be due to the effect of roughness on biofilm/biocake formation on membrane surface. However, the effect of roughness on adhesion of biological systems is poorly understood and has been discussed controversially. Quirynen *et al*. (1993) found that a rough surface harbored

25 times more bacteria and recommended to search for an optimal surface roughness for reducing intraoral plaque formation. An and Friedman (1998) found that the surface roughness produced with 120–1200 grit sand paper on titanium surface had virtually no effect on adhesion of *Staphylococcus epidermidis*. Similarly, Flint *et al.* (2000) found that adhesion of streptococci on stainless steel is largely independent of the surface topography. In contrast, Götzinger *et al*. (2007) noted that the effect of roughness on adhesion of the microorganism *S. cerevisiae* (soft) might be different from the effect of roughness on the adhesion of a hard inorganic particle. In a study regarding the effect of ultrafiltration membrane surface properties on biofilm initiation, Pasmore *et al*., (2001) demonstrated that those hydrophilic, electrically neutral and smooth surfaces are much less likely to foul with *P. aeruginosa* than hydrophobic, charged and rough surfaces. However, in order to avoid the interaction of bacteria itself and other hard inorganic particles, only one specific bacterium was chosen in this study, namely *Pseudomonas aeruginosa* (ATCC 27853, ATCC, Rockville, MD). In addition, Characklis and Marshall (1990) reported that Natural environment bacterial diversity led to an extremely complex biofilm system that is poorly understood. This further indicates that in a system with a complex composition of bulk solution like MBR, the effect of roughness on the particle adsorption should be more complex than previously suggested. In this case, the effect of surface roughness on biofilm formation in SCMBR is still unclear. A comprehensive study on the development and structure of biofilm/biocake along with the operation in MBR will lead to a clearer picture of how the roughness will affect the biofilm development in SMBR

2.2.3 Effect of Operating Conditions on Fouling

Effect of Aeration Rate

Since the introduction of the submerged MBR, bubbling has been accepted as the strategy of choice to induce flow circulation and shear stress on the membrane surface. Aeration used in MBR systems has three major roles: providing oxygen to the biomass, maintaining the activated sludge in suspension, and mitigating fouling by constant scouring of the membrane surface (Dufresne *et al*., 1997).

An increase in aeration rate, and thus cross-flow velocity (CFV), suppresses fouling and so increases permeate flux (J_c). Although most of the studies on J_c are based on sidestream (SS) operation, studies carried out with submerged MBRs (Bouhabila *et al*., 1998) or with ideal feed solutions (Madaeni, 1997; Gunder and Krauth, 1998) suggested that an increase in air flow rate at the membrane surface relieved fouling. However, it was recently reported that the higher aeration rate may not mitigate fouling in MBR with complex bulk solution. This is due to the propensity of aeration rate on the particle size distribution (Meng *et al*., 2008; Sun *et al*., 2006; Han *et al*., 2005) as well as EPS composition (Meng *et al*., 2008; Tan and Ng, 2008; Ji and zhou, 2006).

It was noted that the floc size of sludge played an influential role on the specific permeate flux rate. An increased in floc size may reduce particle penetration into the membranes pores and also enhance floc/particles back-transport from the membrane surface to the bulk solution. This hypothesis was in agreement with some other research works indicating that particle size was one of the major parameters that affected the membrane filtration performance (Chang *et al*., 1999; Rosenberger *et al*., 2002). Han *et al*. (2005) reported that the increased shear provided to control fouling could breakup biofloc as well as cause cell lysis. Moreover, the increase in aeration

intensity to keep the high MLSS levels in suspension and properly oxygenated may not be a sustainable option for the treatment process. Similarly, the work done by Meng *et al*. (2008) demonstrated that the mixed liquor supernatant would become heterogeneous as the aeration intensity increased. When operating under a high aeration intensity of 800 L/h, colloids and solutes in MBR became the major foulants. The authors also illustrated that aeration had a positive effect on cake layer removal, but pore blocking became severe as aeration intensity increased to 800 L/h. These phenomena have been similarly described in the side-stream MBR configuration in which the circulation pump is responsible for the breakup of bacterial flocs (Tardieu *et al*., 1999; Wisniewski and Grasmick, 1998). On the other hand, floc/particle sizes of pollutants in wastewater may strongly affect fouling mechanisms in a membrane filtration system. If foulants are comparable, or smaller than the membrane pores, adsorption and pore blocking may occur (Chae *et al*., 2006). However, if the floc/particle sizes are much larger than membrane pores, they tend to form cake layer on the membrane surface. In this case, the aeration rate selected will significantly affect the fouling mechanisms of membrane in terms of the particle size. Besides the flocs size, the aeration did have an effect on the EPS composition in MBR. A novel explanation for the influence of aeration on MBR fouling has been proposed by Ji and Zhou (2006). According to their results, aeration rate directly controls the quantity and composition of the polymeric compounds (EPS) in the biological flocs, and ultimately the ratio of protein/carbohydrate deposited on the membrane surface. Similar results have been reported by Meng *et al*. (2008), in which more EPS was released when the aeration intensity was increased. Based on these literatures, it is expected that a high aeration rate may damage the floc structure by reducing their size and releasing EPS in the bioreactor, which will consequently affect membrane fouling.

It has been noted that biofilm/biocake structures are altered in response to flow conditions. Biofilms grown under laminar flow were found to be patchy and consisted of rough round cell aggregates separated by interstitial voids; while biofilms grown in the turbulent flow cells were also patchy, but elongated streamers that oscillated in the bulk fluid were also observed. Scanning electron micrographs of in vitro *P. aeruginosa* showed that the streamers thin along the tail until there was only a small chain of single cells at their tips (Davey and O'Toole, 2000; Stoodley *et al.*, 2002; Hall-Stoodley *et al.*, 2004).

In addition to influencing the biofilm macro-structure, fluid shear also influences the micro-structure of the biofilm, in which the physical properties of biofilms such as density and porosity are described. Other physical properties like the strength of the biofilm are also affected by the hydrodynamic conditions. It was found that biofilms grown at higher shear were smoother and denser than those grown at a lower level of shear (Kwok *et al.*, 1998; Stoodley *et al.*, 2002).

Effect of SRT

It is well known that SRT is one of the important factors, which can change the state of biomass in an activated sludge system (Knoblock *et al.*, 1994) and the concentration of mixed liquor suspended solid (MLSS) in the bioreactor increased with SRT (Ng *et al.*, 2006). A membrane bioreactor (MBR) system can maintain a higher MLSS compared to a conventional activated sludge system through membrane separation technology, which can accomplish perfect liquid/solid separation. Therefore, one can expect that biomass properties and membrane fouling in an MBR system can be significantly influenced by SRT (Listed in Table 2.2).

SRT (and consequently the F/M ratio), which ultimately controls biomass characteristics, is probably one of the most important operating parameters that would affect fouling propensity in MBRs. Operating an MBR at a higher SRT leads inevitably to an increase in MLSS concentration, but this in itself may not necessarily lead to a greater fouling (Section 3.2.3). The propensity of different SRTs on membrane fouling in MBR have been studied from an extremely low SRT of 0.25 day (Ng and Hermanowicz, 2005) to infinite SRT (only take sludge samples for sampling purposes) (Liu *et al*., 2005; Orantes *et al*., 2004). Extremely low SRTs (down to 2 d) have been tested to assess fouling propensity (Trussell *et al*., 2006). Not surprisingly, fouling rate increased nearly 10 times when SRT was lowered from 10 to 2 d (corresponding to an increase in F/M ratio from 0.5 to 2.4 gCOD/gMLVSS/day). This phenomenon could be attributed to more SMP released in the system with shorter SRT whereby the biomass was in a growth phase (Ng *et al*., 2006). However, in the MBR operated under infinite SRT, the progressive accumulation in the MBR tank of non-biodegradable materials (like hair and lint), which are not completely removed by the MBR pre-treatment processes, inevitably led to the clogging of the membrane module (Le-Clech *et al*., 2005). At infinite SRT, most of the substrate is consumed to support the maintenance needs and the synthesis of storage products. The very low apparent net biomass generation observed could also explain the low fouling propensity observed for high SRT operation employed in this study (Orantes *et al*., 2004). These two studies showed that extended-SRT-operation could facilitate a lower fouling behavior; other operating conditions such as flux and aeration rates could also have a major influence on fouling propensity (Listed in Table 2). In contrast, the increase in MLSS concentration due to the extended SRT could also result in a higher fouling propensity. Previous experiments revealed an increase of

MLSS concentration levels from 7-18 g/L and a decrease of F/M ratio from 0.15 to 0.05 gCOD/gMLVSS/day when SRT was increased from 30 to 100 d. Even after the aeration rate was increased from 15 to 25 L/min, fouling rate was nearly twice as great for the longer SRT conditions (Han *et al*., 2005). The other difficulty with very high SRT is the raised viscosity that could attenuate the effect of bubbling. Even though these observations showed that the longer SRT might induce faster fouling, the actual effect of SRT on fouling is still unclear. As other operating conditions (like aeration rate) other than the SRT could exacerbate fouling, the fouling rate under longer SRT which was twice greater than that of shorter SRT (Han *et al*., 2005) might be due to the increase of the aeration rate, too. Other than this, the influence of the influent characteristics, on membrane performance could not be overlooked, either.

In order to rule out all the other affecting factors (influent characteristics, other operating conditions except the SRT), running MBR parallel to investigate the effect of SRT on membrane fouling is desirable. Ng *et al*. (2006) reported the influence of SRT (3, 5, 10 and 20 d) on biomass characteristics and consequently affecting the membrane fouling in four parallel MBRs. The authors demonstrated that with the increase of SRT the concentration of MLSS increased from 4.48 $\pm$ 0.97 g/L to 21.90 $\pm$ 0.95 g/L while the ratio of MLVSS/MLSS decreased from 0.70 $\pm$ 0.04 to 0.64 $\pm$ 0.02. Both concentrations of carbohydrate and protein in MBR decreased along with the increase of the SRT. Taking the 160 d as a whole, no obvious fouling has been observed in the MBR operated under 20-d SRT, which indicated that the 20-d SRT is the optimal SRT observed in this study. However, as discussed earlier SRT would not only affect the biomass characteristics but also the microbial community in the MBR (Ahmed *et al.,* 2007).

Other Operating Conditions

Besides SRT and aeration intensity, other operating conditions like HRT and flux will also affect biomass characteristics (Table 2.2), which results in different fouling characteristics in various studies. Table 2.2 listed the effects of reported operation conditions (aeration rate, SRT, HRT and flux) on the biomass characteristics, which will correspondingly affect the membrane fouling propensity. In this case, controlling the operating conditions is a vital step for a comprehensive fouling mechanisms illustration.

Table 2.2 Effect of operation conditions on membrane fouling.

Operating conditions	**Affecting mechanisms**	**Publications**
Aeration rates	EPS and SMP concentrations	(Meng *et al*., 2008; Tan and Ng, 2008; Ji and Zhou, 2006)
	Particles size distributions	(Meng *et al*., 2008; Sun *et al*., 2006)
	DO concentration	(Meng *et al*., 2008)
	Sludge morphology	(Sun *et al*., 2006)
	Biopolymer on membrane surface	(Ueda *et al*., 1997; Hong *et al*., 2002)
SRT	Sludge morphology and sludge floc size	(Meng *et al*., 2006; Ahmed *et al*., 2007)
	Microbial communities	(Ahmed *et al*., 2007)
	Sludge volume index	(Mass é2006; Al-Halbouni *et al*.,2007)
	Capillary suction time	(Al-Halbouni *et al*.,2007; Ng *et al*., 2006)
	EPS and SMP compositions and concentrations	(Ng *et al*., 2006; Al-Halbouni *et al*.,2007; Ng and Ng; 2010)
	Adherence of biomass on membrane surface	(Han *et al*., 2004)
HRT	EPS and SMP concentrations and compositions	(Chae *et al*., 2006; Ng *et al*., 2005; Rojas *et al*., 2005)
	Particle size distribution	(Chae *et al*., 2006)
	Mixed liquor concentrations	(Sun *et al*., 2006; Le-Clech *et al*., 2006a)
	Critical flux leads to faster fouling	(Le-Clech *et al*., 2003; Brookes *et al*., 2006; Wen *et al*., 2004)

2.3 Fouling Minimization

In order to widen the MBR application, most MBR studies performed aimed to identify, investigate and model membrane fouling. The approach of maintaining constant flux is always employed in the MBR system by using TMP as a fouling indicator. With the constant flux approach, the convection of foulant does not diminish and fouling phenomena self-accelerates and can eventually create a sharp increase of TMP. A detailed analysis of the mechanisms and factors involved was conducted by Zhang *et al*. (2006). As in constant TMP operation, strong interactions between the membrane surface and the EPS present in the mixed liquor are probably responsible for the initial stage of fouling during constant flux operation –called Stage 1. Ognier *et al*. (2002b) described the rapid fouling phenomena inducing irreversible resistance taking place in the early stage of MBR filtration (in frontal mode, i.e., dead-end operation). Passive adsorption of colloids and organics has been observed even with zero-flux operation, and before any deposition mechanism initiates (Zhang *et al*., 2006). The adsorption propensity (determined with the modified Freundlich isothermal adsorption equation) was also reported in relation to the filtration modes employed in submerged MBRs (Ma *et al*., 2005). As a result, colloid adsorption and initial pore blocking (Jiang *et al*., 2005) of new or cleaned membranes by organics substances were expected in MBRs. The intensity of this effect depended on membrane pore size distribution and surface chemistry (and especially hydrophobicity) (Ognier *et al*., 2002b) (Sections 2.2.2). Biomass approaching the membrane surface was then able to attach more easily to the membrane, colonizing the separation surface and contributing to Stage 2.

Even though MBRs are operated below the critical flux for the biomass, biofloc may randomly land (see above) and contribute to the second fouling stage. After Stage 1, the membrane surface is expected to be mostly covered by SMP, leading to the higher attachment propensity of biomass particles and colloids. Owing to the low critical flux for SMP species, further adsorption and deposition of organics on the membrane surface may also occur during stage 2. Since adsorption may take place not only at the membrane pores but also on the whole surface, biological flocs may initiate cake formation without directly affecting the permeability in this stage. The rate of EPS deposition, and resulting TMP rise, is expected to increase.

In Stage 3, with regions or pores of the membrane more fouled than others, flux is expected to significantly decrease in those specific locations. As a result, the overall permeate productivity redistributes to the less fouled membrane areas or pores. These phenomena have a self-accelerating nature and severe fouling, characterized by an exponential TMP increase, and are generally obtained if the filtration is maintained. The sudden rise in TMP or "jump" is a consequence of constant flux operation (Le-Clech *et al*., 2006a).

Generally, membrane fouling is attributed to the membrane pore blocking, membrane cake layer formation and membrane initial resistance. Among them, resistance from the cake layer formation is considered as the major contributor for membrane fouling. Meng *et al*. (2007) studied the membrane resistance distribution and found that cake layer formation contributed to 84% of the total hydraulic resistance by conducting 8 runs of dead-end filtration. Huang *et al*. (2008) reported that the cake layer resistance accounted for 92.3 and 66.2% in MBR and HMBR (MBR with 1% carrier dosage), respectively. In order to control the membrane fouling, a number of studies have been

conducted, including the operating condition optimization (Defrance and Jaffrin., 1999a; Liu *et al*., 2000; Bourgeous *et al*., 2001; Sofia *et al*., 2004), biomass characteristics optimization (Chang and Fane., 2002; Holbrook *et al*., 2004) and membrane surface property optimization (Chang and Fane., 2002; Holbrook *et al*., 2004; Roux *et al*., 2005). However, due to the complex compositions of the mixed liquor and different operating condition applied in different studies, it is hard to draw an optimum operating condition for specific purposes in different cases as reported in Section 2.2.3. As discussed in Section 2.2.2, the advantages of hydrophilic membrane surface might be masked by adsorption of particles and macromolecular species. Therefore, the approaches of biofilm carrier addition and in-situ backwash were conducted to mitigate membrane fouling by delaying the cake layer formation.

2.3.1 Relationship between Biofilm Carrier Addition with Fouling

Recently, adding certain carriers with specific characteristics in order to absorb biomass and small molecules became an attempt for membrane fouling alleviation. Activated carbon were mostly applied in the MBR due to its excellent capacity for adsorb dissolved organic matters (DOM) in the mixed liquor supernatant. As reported by Kim *et al*. (2005), the membrane permeability of biological activated carbon biomass was greatly enhanced due to the adsorption of DOM by activated carbon which decreased extracellular polymeric substances content inside the microbial floc. Similar results were also reported in other studies (Kim and Lee, 2003; Li *et al*., 2005). On the other hand, cake layer was found to be the main contributor to membrane fouling in MBR (Chiemchaisri and Yamamoto, 1994., Choo and Lee, 1996; Meng *et al*., 2007). Thus, fouling control by reducing the cake layer formation by scouring effect provided by suspended scrubber addition became a worthwhile idea. Yang *et al*.

(2006) reported that the addition of porous and suspended carriers enhanced the membrane performance. The similar trends were also reported by Wei *et al*. (2006) and Huang *et al*. (2008) by investigating the effect of scrubbers on biomass characteristics, indicating that scrubber dosage could be a good attempt for cake layer control. Since the cake layer were considered as the main contributor in membrane fouling, the evaluation of the cake characteristics in terms of its volatile suspended solids (VSS), colloidal, solutes and inorganic matters compositions is a meaningful step in order to elucidate the fouling control mechanisms by scrubber addition. However, it remains unclear how suspended scrubbers will affect cake layer compositions. In addition, the effect of the suspended carriers on the biomass characteristics remains conflicting due to the different membranes and biofilm carriers applied in different studies. Huang *et al*. (2008) reported that the addition of bioiflm carriers impose more shear force on large flocs and more microbial products was released in the mixed liquor supernatant that in turn lead to higher SMP and lower EPS concentration in the mixed liquor. Yang *et al*. (2006) used a different kind of porous suspended carrier did not observe the same findings, whereby the system with the biofilm carriers was able to operate longer. These differences might be due to the different origin of the biofilm carriers used. In addition, all these studies were focused on the polymeric MBR system, in which the membrane properties might be affected by the rigid suspended scrubbers. Thus far, there is limited information available regarding the effect of the biofilm carriers in the SCMBR systems. Furthermore, even much fewer literatures are available with respect to the effect of the suspended biofilm carriers on the cake layer components. A comprehensive study on the evaluation of influence of the biofilm carriers on membrane fouling in terms of changing the cake layer composition is therefore necessary.

2.3.2 Relationship between Backwash and Fouling

It was reported that in addition to operating condition optimization, system optimization and suspended carrier addition, backwash is also an alternative for relieving membrane fouling (Kuberkar *et al*., 1998; Hong *et al*., 2005). Backwash is an in-situ membrane cleaning method by reversing the transmembrane pressure periodically. Permeate liquid is forced back to the reactor through the membrane when transmembrane pressure is reversed. The pressure induced by the backwash flux dislodges some deposited particles. In the MBR with backwash system, most of the reversible fouling leading to pore blocking and cake layer was found to be removed by the backwash (Le-Clech *et al*., 2006b). This is because the backwash pressure was able to partially dislodge the loosely attached foulants on the membrane surface and loosen pore clogging near the membrane surface. As a result, the membrane filtration flux can be partially recovered through a backwash operation, and eventually the filtration period could be prolonged. Several studies have been done and confirmed the advantages of backwash introduction in cross-flow microfiltration systems. Kuberkar *et al*. (1998) found that very short backpulses (0.1–1.0 s) could increase the net flux for washed bacterial suspensions and whole bacterial fermentation broths during cross-flow microfiltration of biological suspensions. The role of backpulsing was demonstrated by the experimental data on the bench-, pilot- and large-scale filtration systems with ceramic membranes by Sondhi and Bhave (2001), and they reported that backpulsing was very effective in minimizing membrane fouling for up to five fold increase in steady-state permeate flux. Sondhi *et al*. (2000) also reported that up to five-fold permeate flux increase was observed in a cross-flow filtration system with $Cr(OH)_3$ suspension as synthetic electroplating wastewater. These studies focused on the effect of backpulsing on membrane fouling minimization. The

difference of backpusing and backwash was that the backpusing represent a higher reveral pressure (up to 10 bar) for a very short periods of time (typically less than 1 s) every few minutes, while the backwash/backflushing was related to 5-30 s flow reversal every 30 min to several hours (Sondhi and Bhave, 2001).

Recently, some studies have been done in the filtration system with backwash/backflusing. Yigit *et al*. (2008) investigated the effect of different backwash scenarios on membrane fouling and found that 9 min 55 s of filtration followed by 5 s of backwash and 9 min 45 s of filtration followed by 15 s of backwash were the optimum selection in a submerged MBR system. Hwang *et al*. (2009) investigated the effect of the backwash on membrane performance and found that backwash could effectively remove most of the cake layer. However, up to now, most of the studies have been focused on cross-flow systems (Kuberkar *et al*., 1998; Sondhi and Bhave, 2001; Sondhi *et al*. 2000) and the optimization of the backwash parameters, such as the backwash flux and backwash intervals (Xu *et al*., 1995; Kuberkar *et al*., 1998; Yigit *et al*., 2008; Hwang *et al*., 2009). Relatively, fewer efforts have been put on the evaluation of influence of backwash on cake layer structure and compositions. It was reported by Hong *et al*. (2005) that backwash efficiency is closely related to the structure of the cake layer formed on the membrane surface in terms of affecting the ironic strength. However, limited studies have been conducted in terms of the cake layer structure and compositions. In this case, in order to know the in-depth affecting mechanisms of backwash on fouling minimization, it is necessary to conduct a systematical study on the effect of backwash on the cake layer structure and compositions.

2.4 Summary for Literature Review and Research Potential

As discussed above, membrane characteristics, biomass characteristics and operating conditions affect membrane fouling. The biomass characteristics will affect the fouling by either the interaction between the membrane surface and the bulk biomass or the EPS and SMP, while the operating conditions always indirectly affect the membrane fouling by influencing the biomass characteristics (Table 2.2). Although the effects of operating conditions on biomass properties in the bulk have been studied in polymeric MBR systems, there is not much information available in the inorganic MBR counterparts. And, there is even less study being conducted regarding the effect of membrane pore size on the fouling in SCMBR system. This lack of information makes it difficult to come to a comprehensive conclusion with respect to the effects of membrane properties on inorganic membrane fouling in MBR system.

It was suggested that membrane microstructure, material and pore openings all affected MBR fouling significantly. However, how these parameters contribute to the formation of the biofilm/biocake layer developed on the membrane surfaces have not been studied. Moreover, the effect of the membrane characteristics on fouling is rarely reported, especially for ceramic membrane with a hydrophilic surface. It is expected that the pore size of ceramic membrane will affect the roughness of the membrane surface. However, how roughness difference induces different fouling characteristics has not been studied in SCMBR system.

Membrane fouling will inevitably increase the operational cost for the MBR system. Therefore, there is a need to find out an economical and effective way to relieve membrane fouling during the operation (such as biofilm carrier addition, backwash/backflush/backpulse). The lack of such information in the SCMBR system

baffles the wide application of SCMBR in wastewater treatment industries. In addition, even fewer studies have been conducted to understand the effects of these fouling minimization strategies on the biofilm/biocake structure and compositions. Thus, it is believed that a comprehensive study on the characterization of the biofilm/biocake structure and compositions will shed light into this question.

Chapter 3. Materials and Methods

3.1 Experimental Set-up and Operating Conditions for SCMBR

3.1.1 Phase 1 (Four SCMBRs in Parallel)

Four types of flat sheet ceramic membrane (ITN, German), each with 21 permeate channels (see Fig. 3.1b), with different pore sizes were used for investigation. The dimension of the flat sheet membrane is 6.5×110×330 mm. These membranes are made of a fine layer of $ZrO_2/TiO_2/\alpha\text{-}Al_2O_3$ with nominal sizes of 300, 200, 100 and 80 nm established on $\alpha\text{-}Al_2O_3$ porous support. The initial permeabilities of the new membrane were about 3,300, 1,450, 1,450 and 260 L/h·m^2·bar, respectively, based on de-ionized water tested at 20℃. The properties of the ceramic membranes are summarized in Table 3.1 and the picture of the membrane module is shown in Fig. 3.1.

Table 3.1 Properties of flat sheet membrane module (according to the manufacturer's specification)

Membrane module properties	
Nominal pore size	300/200/100/80 nm
Material of active separation layer	α- Al_2O_3/ TiO_2/ZrO_2
Material of substrate	α- Al_2O_3
Membrane permeability	3300/1450/1450/260 L/m^2 ћ ƀar
Module dimension	360.8 x 126.7 x 15.6 mm
Active membrane area	0.08 m^2
Maximum operating pressure	2 bar

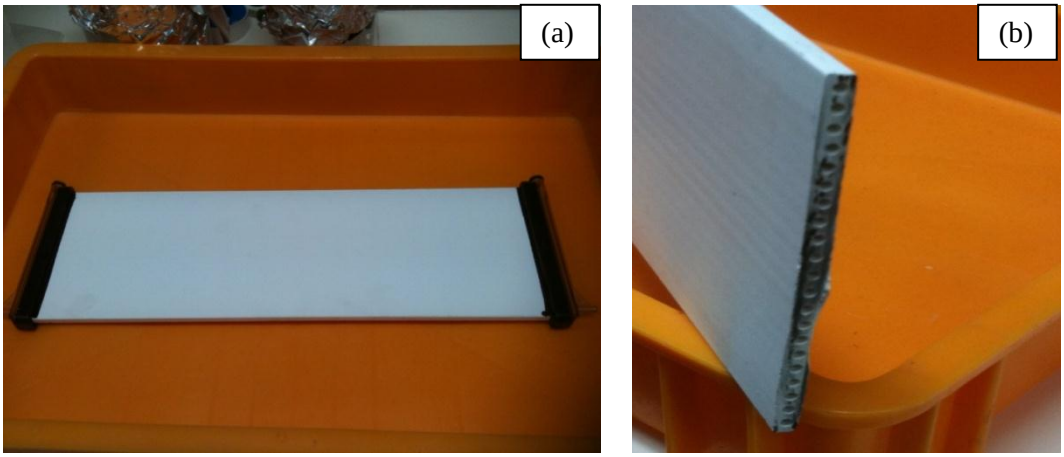

Figure 3.1 Picture of a flat sheet ceramic membrane: a). Front view of the membrane; b). Cross section of the membrane.

In study of Phase 1, four lab-scale SCMBRs (Figure 3.2a), each with a volume of 7 L were operated in parallel to investigate the fouling potential of different pore-sized ceramic membranes. The four SCMBRs are denoted as R80, R100, R200 and R300, which referred to the SCMBR equipped with 80-, 100-, 200-, and 300-nm pore-sized ceramic membranes, respectively. For each SCMBR, three flat-sheet ceramic membrane modules were mounted between two baffles. Each module was allocated above a diffuser with an effective aeration rate of 2 L of air per minute per module. Each SCMBR was kept at a constant membrane permeate flux of 6.09 LMH by following a suction cycle of 8-min on and 2-min off. The SCMBRs were operated under room temperature ranging from 25 - 30˚C during the entire experimental period of one year. pH of the system was controlled at 7.0 ± 0.2 with $NaHCO_3$ as pH buffer.

To facilitate a meaningful comparison of performance between each system, all SCMBRs were started with identical seeding activated sludge, fed continuously with identical domestic wastewater and run under the same operating conditions (see Table 3.2). Typical HRT of 6 h for MBR was selected in this study. By considering the different initial membrane permeability of the four pore-sized membranes and making sure that all membranes are run under sub-critical condition, the permeate flux of membrane was selected as 6.08 LMH. Seed biomass and the raw domestic wastewater were collected from a local water reclamation plant in Singapore. The collected wastewater was sieved with a 1- mm pore-sized sieve and added into a common feed tank, which was equipped with a stirrer to keep its contents homogenous.

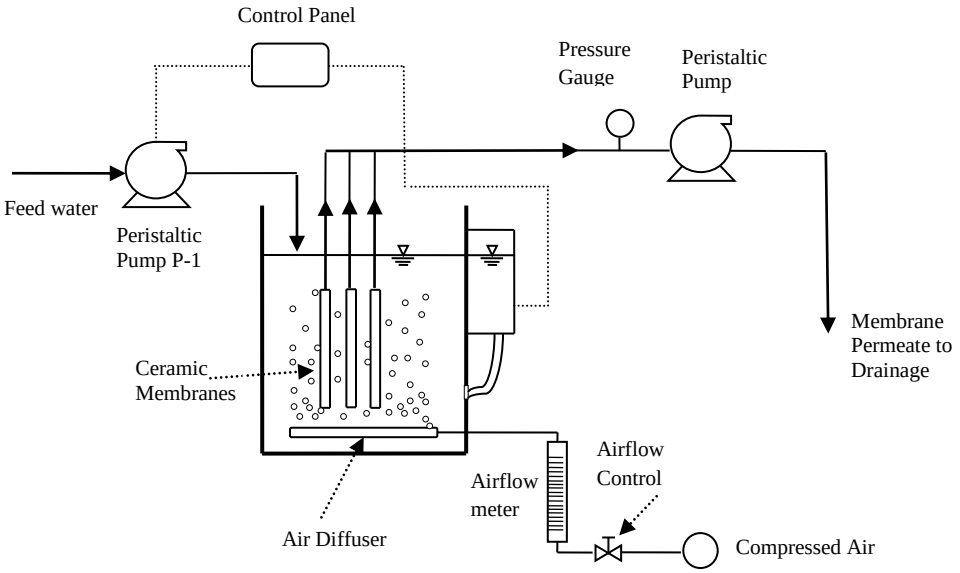

(a) Schematic Diagram

(b) Picture

Figure 3.2 (a) Schematic diagram of a lab-scale SCMBR; (b) Picture of the lab-scale SCMBR.

Table 3.2 Operating conditions of SCMBR (Phase 1 and Phase 2).

Phase 1 (Four SCMBRs in parallel)	
Parameters	Value
HRT (h)	6
SRT (d)	10
Working volume (L)	7
Flux (LMH)	6.08
Aeration rate (L air/min)	2 per membrane module
pH	7.0 ±0 .2
Phase 2 (One SCMBR with four different pore-sized membranes)	
Parameters	Value
HRT (h)	6
SRT (d)	20
Working volume (L)	14
Flux (LMH)	9.11
Aeration rate (L air/min)	1.5 per membrane module
pH	7.0 ±0 .2

3.1.2 Phase 2 (One SCMBR with Different Pore-sized Membranes)

In order to rule out the effect of sludge characteristics on membrane fouling, in Phase 2 four ceramic membranes with different pore size were mounted in one SCMBR to evaluate the sole effect of membrane surface properties on fouling. The membrane permeate from each membrane was suctioned by an individual peristaltic pump which was kept at a constant membrane permeate flux of 9.11 LMH by following a suction cycle of 8-min on and 2-min off. TMP was obtained using a digital pressure switch (ZSE50F-02-22L, SMC, Japan) with 0.1 kPa precision. Each module was allocated above an individual diffuser with an effective aeration rate of 1.5 L of air per minute per diffusor. The schematic diagram was shown in Fig. 3.3. This reactor was operated for over one year under the condition of 20 d SRT and 6 h HRT (see Table 3.2).

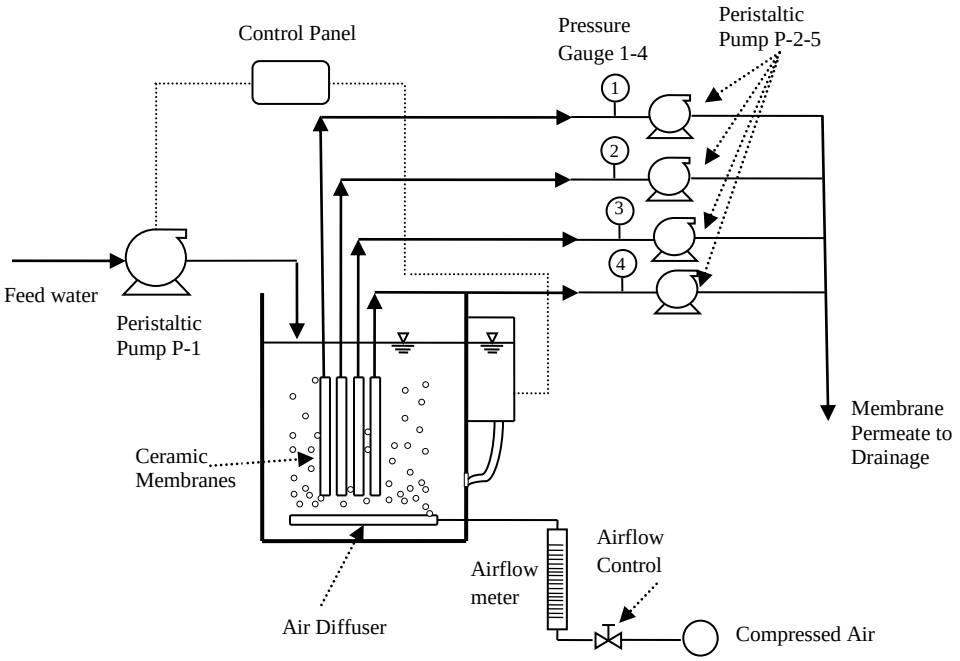

Figure 3.3 Schematic Diagram for SCMBR (four different membranes in one SCMBR).

3.1.3 Phase 3 (Biofilm Carrier Addition)

The porous and suspended scrubber/ biofilm carrier used in this study has a dimension of 12 mm in length, 10 mm in width and 7mm in thickness (see Fig. 3.4). It was made of polypropylene with a true density of 573.3 kg/m^3. The scrubber characteristics allow them to be easily circulated throughout the whole reactor and get in contact with membrane surfaces through aeration. The biofilm carrier dose was calculated as total biofilm carrier volume versus total effective volume of wastewater in bioreactor.

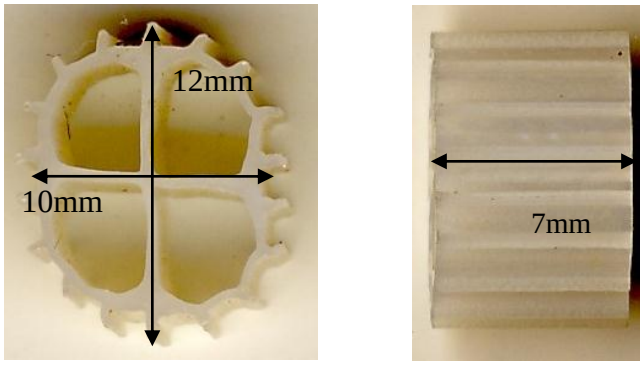

Figure 3.4 Picture of a biofilm carrier.

In Run 1, two identical lab-scale SCMBRs were operated in parallel to investigate the fouling controlled mechanisms by biofilm carriers by simultaneously conducting tests in SCMBRs with (R1) or without scrubbers (R2). A dosage of 5.70% suspended biofilm carrier was conducted in R1. For each SCMBR, two flat sheet ceramic membrane modules with the nominal pore size of 300 nm were mounted with each module allocated above a diffuser with an effective aeration rate of 2 L of air per minute per diffusor. The membrane flux of each SCMBR was kept constant at 9.13 LMH by following a suction cycle of 8-min on and 2-min off, and the TMP was recorded to evaluate membrane fouling. To facilitate a meaningful comparison of performance between each system, both SCMBRs were started with identical seeding activated sludge, fed continuously with identical wastewater and run under the same operating conditions of 10 d SRT and 6 h HRT. In order to investigate the optimum scrubber dosage, in Run 2 another two SCMBRs were set up by reseeding the systems with 2.85% (R3) and 5.70% (R4) carrier dosage, respectively. The operating conditions were controlled the same as that in Run 1. Fig. 3.5 shows the reactor with carrier addition during the process (Run 2).

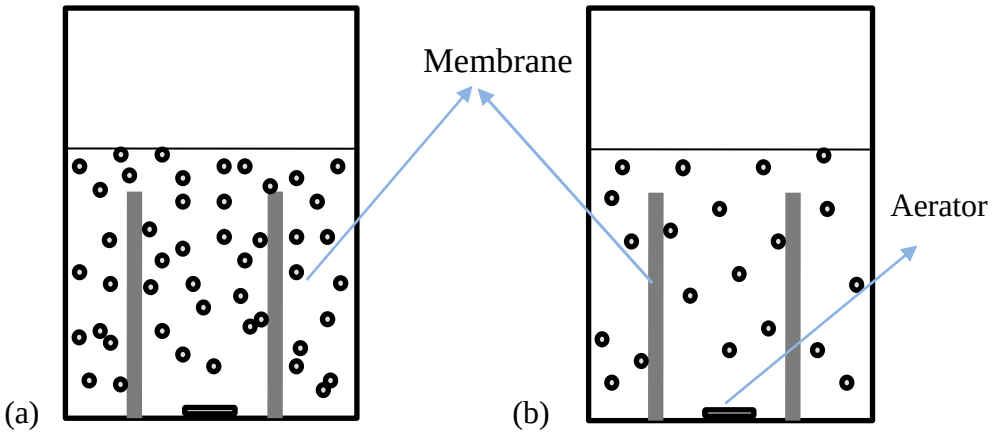

Figure 3.5 (a) Reactor with 1,400 pieces of biofilm carriers), and (b) Reactor with 700 pieces of biofilm carriers.

3.1.4 Phase 3 (Membrane Backwash)

Membrane in-situ backwash was operated in this phase to investigate the effect of backwash on membrane fouling mitigation. Two SCMBRs (one with backwash and one without backwash) were operated simultaneously under the same HRT and SRT (see Table 3.3). The membrane permeate pump and backwash pump was monitored by a PLC control panel. Fig. 3.4 shows the schematic diagram of the backwash system.

Table. 3.3 Operating conditions of Phase 3 (backwash).

	w/o Backwash	**w/ Backwash**
Working volume (L)	8.8	8
Permeate flux (LMH)	11.89	11.89
Backwash flux (LMH)	-	35.67
Run cycle	8’ on; 2’off	8’ on; 1’45” off; 15” backwash
HRT (h)	5.8	5.8
SRT (d)	12	12

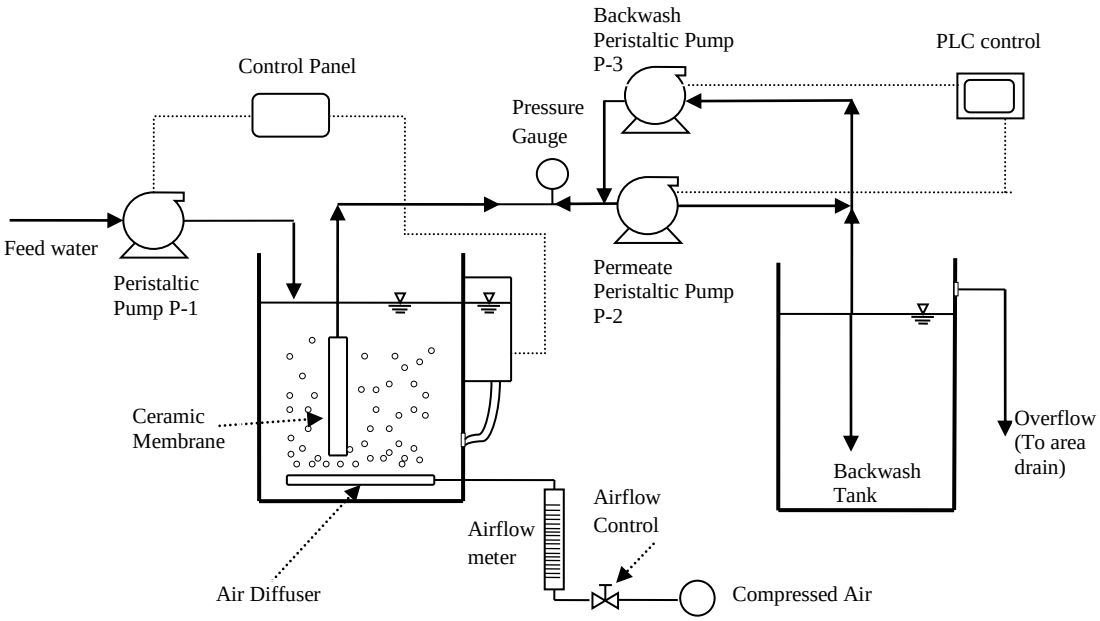

Figure 3.6 Schematic diagram of the in-situ backwash SCMBR system.

3.2 Sampling Methods

3.2.1 Liquid Samples

Feed wastewater and membrane permeate were collected regularly for water quality analysis. Influent and effluent were collected from inlet and outlet, respectively, following the sequence of effluent, mixed liquor and influent. This sequence from downstream to upstream aimed to alleviate the effects of sampling on the SCMBR processing. Mixed liquor was sampled from three desludge ports located near the mid-height of the SCMBR. Mixed liquor supernatant (also treated as SMP in this study) was obtained by centrifuging the samples at 9,000 rpm for 10 min at 4℃ before filtering by a 0.45 μm membrane filter (PALL, USA).

3.2.2 EPS Extraction

The extraction of EPS was carried out by the heating method. The mixed liquor precipitated after centrifuging by 9,000 rpm for 10 min was re-suspended to original volume by using ultra-pure water. After completely mixing the biomass, the sample was incubated in an 80 ℃ water bath for 10 min. The warm sample was taken out of water bath and centrifuged by 9,000 rpm for 10 min at 4℃, and the supernatant of the centrifuged sample was collected after filtration by a 0.45 μm membrane filter for subsequent analysis.

3.2.3 Foulants Extraction

In Part 1 of Phase 3, membranes were taken out from both reactors once the TMP of either SCMBR reached 30 kPa and cake layers were removed by a sponge with foulants dissolved in 500 ml of ultrapure water (foulant liquid). In Part 2 of Phase 3,

cake layer sample was collected when each SCMBR reached TMP of 30 kPa. About 50 ml of foulant liquid were centrifuged for 10 min at 9,000 rpm and the precipitates were placed in incubator at 55˚C for 48 h to obtain dry foulants for FTIR analysis of the biomass in cake layers. The suspended solids and volatile suspended solids of the cake layer liquid were measured in accordance with Standard Methods (APHA *et al*., 2005). The supernatant of the liquid were characterized by determining the soluble TOC ($_s$TOC) and colloidal TOC ($_c$TOC). The supernatant TOC was determined after centrifuging by 3,500 rpm for 2 min, and $_s$TOC was determined by filtering the liquid by a 0.45-μm membrane filter. The difference of supernatant and $_s$TOC was considered as $_c$TOC. Ion Chromatography (Dionex, DX-500) machine was used to determine ion contents in the cake layer.

3.2.4 DNA Extraction

Phenol-Chloroform Method was applied to extract the genomic DNA of biofilms on the membrane surface in Phase 2. Mixed liquor samples were collected in an empty 1.5 mL tube, and biofilm samples were collected in a 1.5 mL tube with 0.1 mL of ultrapure water. The supernatant of the mixed liquor was disposed after centrifuging at 12,000 rpm for 5 min. 600-uL of Extraction Buffer composed of 100-mM *Tris*-HCl, 100 mM EDTA and 0.75-M sucrose, 6-μL Lysozyme, and 6-μL achoromopeptidase were added into the tube. The addition of achoromopeptidase and lysozyme was aiming to break cell wall of Gram +ve bacteria and –ve bacteria, respectively. After 30 min of incubation at 37˚C, 3-μL of proteinase K used to deconstruct protein (i.e. Dissolve cell membrane& nucleate membrane) and 60-μL of 10% SDS used for the removal of cell membrane lipids, were added into the test tube. 2 h incubation at 37˚C in a water bath was needed after the solution addition. After that, 60-μL of 10%

CTAB and 84-µL of 5-M NaCl were added sequentially, and vertex thoroughly in order to destruct cell membrane after destruction of the cell wall. In addition to the enzymatic lysis method, a physical method that followed by three cycles of freezing at -80˚C for 15 min and then thawing at +65˚C for 10 min was conducted in order to ensure that the DNA has been extracted.

The purification of the genomic DNA followed the Phenol-Chloroform Method. Three steps PCI (Phenol: Chloroform: Isoamyl Alcohol = 25:24:1) and one step CI (Cholorform: Isoamyl Alcohol = 24:1) were applied for mixed liquor samples, while two steps PCI and one step CI were used to extract genomic DNA in biofilm. After purification process, iso-propanol was added into the tube for DNA to precipitate overnight. Finally, 70% Ethanol was used to remove salts (else may affect subsequent PCR reaction) and wash out the isopropanol. The extracted DNA sample was dried in a laminarhood and the dried pellet was re-suspend in 20-50 µL sterilized distilled water (sdH_2O) and stored in -20˚C for the subsequent tests.

3.3 Analytical Methods

3.3.1 Total Suspended Solids (TSS) and Volatile Suspended Solids (VSS)

Biomass concentration was measured as mixed liquor suspended solids (MLSS) and volatile MLSS (MLVSS) in accordance with Standard Methods (APHA *et al*., 2005). Sample was filtered by a glass fiber (GF/F, Whatman) and dried in the oven (MEMMERT ULM 6, Schmidt Scientific) at 105˚C for at least 1 h, after that the sample was placed in a desiccators for at least 1 h before weighing and ignited in a furnace (Thermolyne 48000, Omega Medical Scientific) at 550 ˚C for 30 min. The

glass fiber used was rinsed by ultra-pure water and baked in the furnace at 550˚C to remove the impurities before analysis.

3.3.2 Chemical Oxygen Demand (COD) and Total Organic Carbon (TOC)

COD analysis was done using the Closed Reflux Titrimetric Method (Electro Thermal Heater: Electromatle ME, Fisher General Scientific) according to the Standard Methods (APHA *et al*., 2005). Total organic carbon (TOC) was determined using a TOC analyzer (TOC-VCSH Shimadzu, Japan) to quantify the concentrations of the organic contents.

3.3.3 Total Nitrogen (TN), Ammonia Nitrogen (NH_4^+-N), Nitrate (NO_3^-)and Nitrite(NO_2^-)

TN was determined using a TOC/TN analyzer (TOC-VCSH Shimadzu, Japan). Nitrite and nitrate concentrations in the influent and effluent were measured by an Ion Chromatography (Dionex, DX-500) machine. In Phase 1, the Ammonia nitrogen concentration was measured using by the HACH DR/5000 spectrophotometer coupled with HACH test "N Tube" vials kit. The testing procedure followed the HACH Method 10023 for low range (0-2.5 mg N/L) and Method 10031 for high range (0-50 mg N/L). In Phase 2 and 3, Ion Chromatography (Dionex, DX-500) machine was used to measure the ammonia nitrogen.

3.3.4 Capillary Suction Time (CST)

The dewaterability of the mixed liquor was determined by a capillary suction time apparatus (Triton Electronics Ltd). 5.6 mL of mixed liquor was collected for the

measurement by a 1.8-cm diameter cylinder according to the Standard Methods (APHA *et al*., 2005).

3.3.5 Carbohydrate

The phenol-sulfuric acid was used to measure the carbohydrate using glucose as the standard (Dubois *et al*., 1956). 2 mL of sample was added into a test tube, and then 1 mL of 5% (W/V) phenol solution was added into each tube. A rapid dispenser was used to add 5 mL of concentrated sulphuric acid. The solution was mixed immediately followed by a 30 min incubation period under room temperature. Absorbance measurements were taken at the wavelength of 490 nm with a spectrophotometer (HACH, DR/5000U).

3.3.6 Protein

Protein content was measured using the Lowry method with bovine serum albumin as the standard reference (Lowry *et al*., 1951). Briefly, 1 mL of sample was added into two tubes and mixed with 5 mL of assay mix (Sample 1a+Assay Mix 1=Total; Sample 1b+Assay Mix 2=Blind) and vortexed thoroughly. After incubation of the sample in room temperature for 10 min, 0.5 mL diluted Folin Ciotalteu reagent was added into each tube and mixed by a vortex. The solution was incubated under room temperature for another 30 min before measuring by the spectrophotometer at a wavelength of 650 nm (HACH, DR/5000U). The Assay Mix 1 was composed of 25 mL of alkaline reagent (0.1-M NaOH, 2% Na_2CO_3, 0.02% sodium potassium tartrate and 1% Na Dodecylsulfate) and 1 mL copper reagent (0.5 % $CuSO_4$ $5H_2O$), while Assay Mix 2 was composed of 25 mL of alkaline reagent and 1 mL of ultra-pure water. Eq. 3.1 and Eq. 3.2 were used to calculate $A_{protein}$ of the sample.

$A_{total} = A_{protein} + A_{humic}$ (Equation 3.1)

$A_{blind} = 0.2A_{protein} + A_{humic}$ (Equation 3.2)

where A_{total} represents the total adsorption rate; $A_{protein}$ and A_{humic} represent the adsorption contributed by protein and humics, respectively.

3.3.7 Ultraviolet Absorbance at 254 nm Wavelength (UV_{254})

UV_{254} of the soluble influent, mixed liquor supernatant and membrane permeates were measured according to the Standard Methods (APHA *et al*., 2005). The absorbance of the sample was measured at a wavelength of 254 nm by a spectrophotometer (HACH, DR/5000U) using a 10-mL quartz cell to hold the sample. The specific UV_{254} was calculated by dividing UV_{254} absorbance by the TOC of the sample.

3.3.8 Molecular Weight Distribution (MWD)

In Phase 1 and 2, molecular weight distribution (MWD) analysis was conducted according to the ultrafiltration method reported by Chin *et al*. (1994). Briefly water samples were filtered through cellulose membranes having nominal molecular weight cutoffs of 1, 10 and 100 kDa (Amicon®, Millipore Corporation, USA). Filtrates were collected for TOC analysis. Normalized TOC concentration against the total TOC for each fraction was calculated. Four ranges of molecular weight distribution were calculated from this fractionation method, namely, less than 1 kDa, between 1-10 kDa, between 10-100 kDa and more than 100 kDa. In Phase 2, MWD was also obtained by using a high performance liquid chromatography (HPLC) (Shimadze, Japan) to understand the detailed MW distribution of organic compounds.

3.3.9 Particle Size Distribution (PSD)

Particle size distribution of the mixed liquor supernatant was measured using a Marlvern counter (Zetasizer Nano, UK). Particle size distribution of biomass suspensions were analyzed by a laser diffraction particle analyzer (LS230 Coulter, Beckman, Germany).

3.3.10 Polymerase Chain Reaction (PCR)

Polymerase chain reaction (PCR) was performed using primers (Table 3.4) to amplify 16S rRNA gene in 25-µL reaction mixtures with 1× PCR buffer, 200-µM deoxynucleoside triphosphate, 2.5-mM magenesium chloride, 0.2-µM of each primer (27F and 1512R), and 1U of hot *Taq* DNA polymerase (Promega, Madison, Wisc.). A thermal cycler (iCycler, Bio-Rad, Herculses, CA) was used to carry out the DNA amplicfication following the sequence of initial denaturation step (95 ℃ for 1 min), 30 cycles of denaturation (95 ℃ for 30 s), annealing (55 ℃ for 45 s), extension (72 ℃ for 1 min) and a final extension (72 ℃ for 5 min). The products of PCR were verified by a 1% agarose capillary electrophoresis in 1× TAE buffer and purified using Axygen PCR cleanup kit (Axygen, Union City, CA), according to the manufacturer's instruction.

Table 3.4 PCR primers used in16S RNA amplification

Target	Primer	Position[a]	Primer sequence (5'-3')	Reference
eubacterial 16s RNA gene	27F[b]	16S, 8-27	AGA GTT TC(C/A) TGG CTC AG	Braker et al., 2001
	1512F	16s, 1512-1527	GGC TAC CTT GTT ACG ACT T	Kane et al., 1993

[a] position of 16S gene are based on Escherichia coli.
[b] Cy 5 fluorescence dye was labeled at the 5' end.

3.3.11 Terminal Restriction Fragment Length Polymorphism (T-RFLP)

T-RFLP was performed according to a previously described protocol (Liu *et al*., 1997). The analysis was conducted by digesting the purified fluorescence-labeled PCR products with *MspI, RsaI* and *HaeIII* (New England Biolabs). All digestions were carried out according to the manufacturer's instruction for 3 h at 37 ℃ followed by 10 min at 65 ℃ for tetrametric restriction enzyme deactivation. Digested PCR products were loaded into a CEQ 8000 automated sequencer (Beckman Coulter, Fullerton, CA) and sequenced at 55 ℃ and 4.8 kV for 60 min, and the T-RF lengths were determined by comparison with internal DNA standards (60 to 640 bp) using the CEQ 8000 genetic analysis system software.

Cluster analysis of different T-RFLP fingerprints and other analyses were performed with MINITAB^{TM} Statistical Software, Release 14. Ward hierarchical clustering method was applied to compute the Hellinger distance (equals to the Euclidean distance after taking square root of the relative peak height). Relative height was computed after rejections of peaks that contributed less than 2% of the total abundance. The structural diversity between microbial communities of different samples was evaluated by Shannon-Weaver diversity index (H), which was calculated as:

$$H = -\sum (p_i)(\log p_i) \qquad \text{(Equation 3.3)}$$

Where p_i is the relative peak height abundance of T-RF *i*, Total number of the T-RFs is the sample richness (S) while the evenness (E) is calculated as H/log S.

3.3.12 Three-Dimensional Excitation Emission Matrix (EEM)

The three-dimension EEM fluorescence spectra were measured for the dissolved organic matters in the mixed liquor supernatants, membrane permeates and cake layers by a luminescence spectrophotometer (LS-55, Perkin Elmer Co.). In the measurements of fluorescence, a 3D EEM fluorescence spectra was obtained by collecting the wavelength of both excitation over a range from 230-400 nm and emission of 230-550 nm with stepwise of 5 nm. In-depth EEM fluorescence characteristics were performed by characterizing the EEM fluorescence spectra into the five excitation–emission regions. The fluorescence regional integration (FRI) method was applied in accordance with Chen *et al*. (2003).

3.3.13 Liquid Chromatography- Organic Carbon Detection (LC-OCD)

Liquid chromatography–organic carbon detection (LC–OCD) was applied to characterize the molecular weights of soluble compounds and the relative organic carbon in the mixed liquor supernatant and cake layer on the membrane. This technique has been previously applied to MBRs by S. Rosenberger *et al*. (2006). The heart of the LC–OCD (Model 8) system is the OC-detector (OCD), which is linked to a size exclusion chromatography. Apart from OC, dissolved organic nitrogen (DON) was also measured for protein content estimation.

3.3.14 Scanning Electron Microscopy- Energy Diffusive X-ray Spectroscopy (SEM-EDX)

In an SEM-EDX system, the part of EDX is the measurement of X-rays emitted during electron bombardment in order to determine the composition of the materials. The elements of the sample can be monitored by determining the energies of X-rays emitted from the area being excited by the electron beam. The dry matters of the

collected cake layer were detected by the SEM-EDX (OXFORD INCA X-act) to diagnose the chemical element in the cake layer in Phase 3.

3.3.15 Frustrated Total Internal Reflection Spectroscopy (FTIR)

A FTIR spectrometer (Varian 3000 Excalibur Series) was used to characterize the major functional groups of organic matters. KBr pellets containing 0.50% (dry powder) of the sample was prepared and examined by the FTIR spectrophotometer. The spectrum was calculated from the average of 256 scans over the wavelength ranging from 4000 to 400 cm^{-1} at a resolution of 4 cm^{-1}.

3.3.16 Scanning Electron Microscope (SEM)

Surfaces of the fresh membrane used in this study and the membranes after physical cleaning (Phase 3) were analyzed using a scanning electron microscope (SEM). The membrane samples were coated with platinum with a sputter prior to the SEM (JEOL, JSM 5600LV) observation.

3.3.17 Atomic Force Microscopy (AFM)

Membrane surface roughness was determined by an Atomic Force Microscope (AFM) (Veeco, USA) using tapping mode.

3.3.19 Resistance Analysis

The resistance-in-series model proposed by Choo and Lee (1996) was applied to analyze the fouling resistance distribution:

$$J = \frac{\Delta P}{\mu R_t} \qquad \text{(Equation 3.4)}$$

$$R_t = R_m + R_c + R_p \quad \text{(Equation 3.5)}$$

where J is the permeate flux, ΔP is the TMP, μ the viscosity of the permeate, R_t is the total membrane resistance, R_m the intrinsic membrane resistance, R_c the cake layer resistance, and R_p is the pore plugging resistance.

The filtration of ultrapure water with new membrane was conducted to calculate R_m. Once the TMP of the SCMBR reached 30kPa, the membrane was taken out from the reactor. By applying Eq. 3.4, the filtration of ultrapure water of the fouled membrane gave $R_{t.}$ Eq. 3.5 was used to measure R_m+R_p after the cake layer removing by a sponge.

3.3.20 Membrane Cleaning Procedure

In Phase 1, membrane chemical cleaning was conducted once the TMP of each SCMBR reached 30 kPa. During the membrane cleaning process, new plates of ceramic membranes were used temporarily to maintain the SCMBRs. The chemical cleaning procedure was as follows:

Step 1. The fouled ceramic membranes were soaked in 500 ppm of NaOH for 24 h.

Step 2. The membrane was flushed by tap water and soaked in 500 ppm of citric acid solution for 24 h.

Step 3. The membrane was flushed by tap water and soaked in 5% of NaClO solution for another 24 h.

Chapter 4. Phase 1 - SCMBR Treatment and Membrane Performance

This part of the study investigated the treatment performance and the membrane performance of the SCMBR with different membrane pore size. To facilitate a meaningful comparison of performance between each system, all SCMBRs were started with identical seeding activated sludge, fed continuously with identical domestic wastewater (Figure 4.1 and Table 4.1) and run under the same operating conditions as mentioned in Section 3.1.1.

Table 4.1 Influent characteristics

Parameters	Cycle 1(mg/L)	Cycle 2 (mg/L)
TCOD	394.03 ± 109.38	436.96 ±98.57
sCOD	68.91 ± 26.03	89.58 ± 23.68
SS	270.08 ± 107.13	320.38 ± 73.43
VSS	207.78 ± 76.62	272.00 ± 64.02
VSS/SS	0.81 ± 0.09	0.85 ±0.03
TN	39.96 ± 7.49	40.07 ± 5.98
Ammonia	36.47 ± 5.30	39.94 ± 3.82

Note: Number of samplings = 22 in Cycle 1; 24 in Cycle 2.

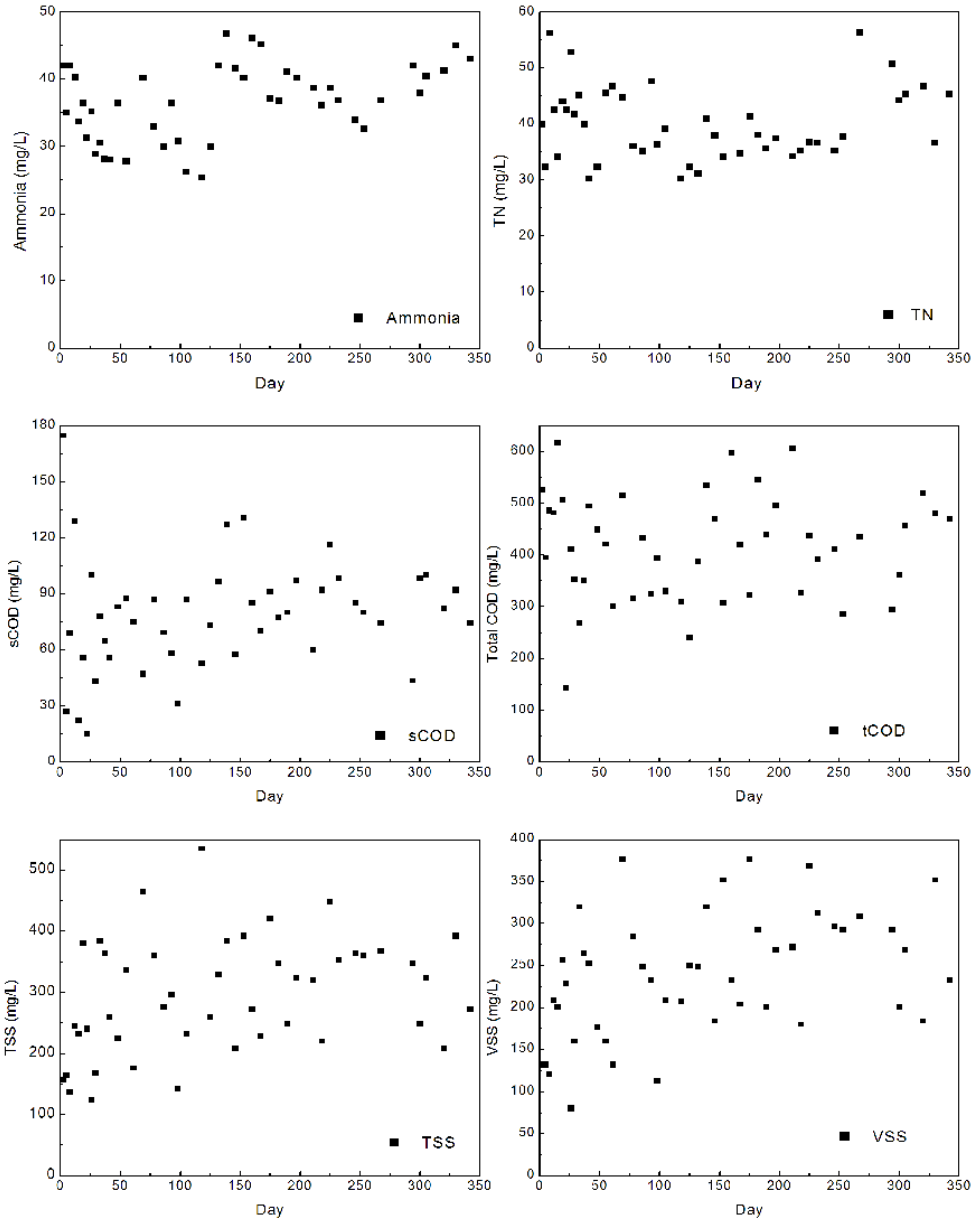

Figure 4.1 Influent characteristics (number of sampling = 46).

4.1. Treatment Performance of SCMBRs

4.1.1 Carbonaceous Removal by SCMBRs

This study revealed that all four SCMBRs could achieve an average total COD (TCOD) removal efficiency of over 94.5%, despite experiencing fluctuation in influent wastewater characteristics. R80, with the smallest membrane pore size achieved the highest total organic removal efficiency (95.0%), while the TCOD rejection rates were 94.5, 94.7 and 94.7% for R100, R200 and R300, respectively. These results indicated that the smaller pore-sized membrane had a little higher organic rejection when all the SCMBRs were operated under the same conditions in terms of the average TCOD removal efficiency, although the differences were minor. This finding is in agreement with He *et al*. (2005) who demonstrated that the effect of the MWCO within the range of 20-70 kDa on TCOD removal efficiency was insignificant. The consistently high TCOD removal regardless of membrane size could be due to the formation of a cake layer on each membrane surface which would trap colloidal particles. In the beginning of the process, R80 was able to retain more organics inside the reactor due to its smallest pore size. However, with increasing filtration time, foulants would either attach on membrane surface or trap inside the membrane pores. These foulants would form a fouling layer on the membrane surface, known as the secondary active layer which would achieve sieving of colloidal particles that contribute to COD (Evans *et al*., 2008). Hence, TCOD average removal efficiencies of all membranes were eventually rather similar.

4.1.2 Nitrogen Removal and Nitrogen Balance

Excellent nitrification was observed in all SCMBRs. Over 350-d operation, an average of over 98% NH_3-N removal efficiency could be obtained under a relatively

low SRT of 10 d. These results are in line with the results reported by Xing *et al*. (1999) that an average ammonia removal of 96.2% was obtained when operating the MBR under 5-, 10- and 30-d SRTs. The high ammonia removal efficiency obtained was mainly due to the fact that nitrifying bacteria were fully retained in the SCMBRs except those wasted during the desludge process. Thus, the slower growing autotrophic nitrifies, having long doubling times, would proliferate speedily within the system. Consequently, an almost complete nitrification could be obtained in SCMBR system.

4.2. Fouling Potential of Different Pore-sized SCMBRs

4.2.1 Relationship between Membrane Pore Size and Fouling

As shown in Fig. 4.2, the TMP of R300, R100, R200 and R80 reached 30 kPa on Day 72, 137, 142 and 151 in the first fouling cycle, respectively. Noticeable membrane fouling was first observed in R300 on Day 40, which was mounted by the largest pore size of 300-nm membrane. Subsequently, the TMP of R300 increased significantly and reached 30 kPa on the 72th day of the operation. R300, with the largest pore-sized membrane, was the system that experienced the earliest fouling phenomenon followed by the highest fouling rate among the four SCMBRs. Noticeable fouling could also be observed for R100 on Day 40, while the fouling rate was lower than that of R300. Fouling phenomenon could also be observed for R80 and R200; however, the fouling rates were much lower. The various fouling rates observed in the four SCMBRs indicated that although R300 had the lowest initial TMP of 2.3 kPa, the increase of TMP was faster than the other three SCMBRs. On the other hand, the overall TMP increase rate was the lowest for R80 since R80 had the highest initial TMP of 4.8 kPa and was the last one to reach TMP of 30kPa.

It is noted that not only the membrane pore size would affect fouling characteristics; the operation duration also played important roles. As shown in Fig.4.2, the TMP for R80 increased from 4.8 to 5.8 kPa within 24 h; which indicated that R80 had the highest initial TMP and the TMP increase in the first few hours were more apparent than the other three SCMBRs. However, over the first fouling cycle of 151 d, R80 was the last one to reach 30 kPa of TMP. These observations are in good agreement with He *et al*. (2005) who noted that the smallest MWCO membrane tested (20 kDa) experienced the largest permeability lost within the first 15 min of filtration compared with 30-, 50- and 70-kDa membranes when operated with constant TMP. However, when operated for an extended period (over 100 d), the largest MWCO membrane experienced the greatest fouling rate.

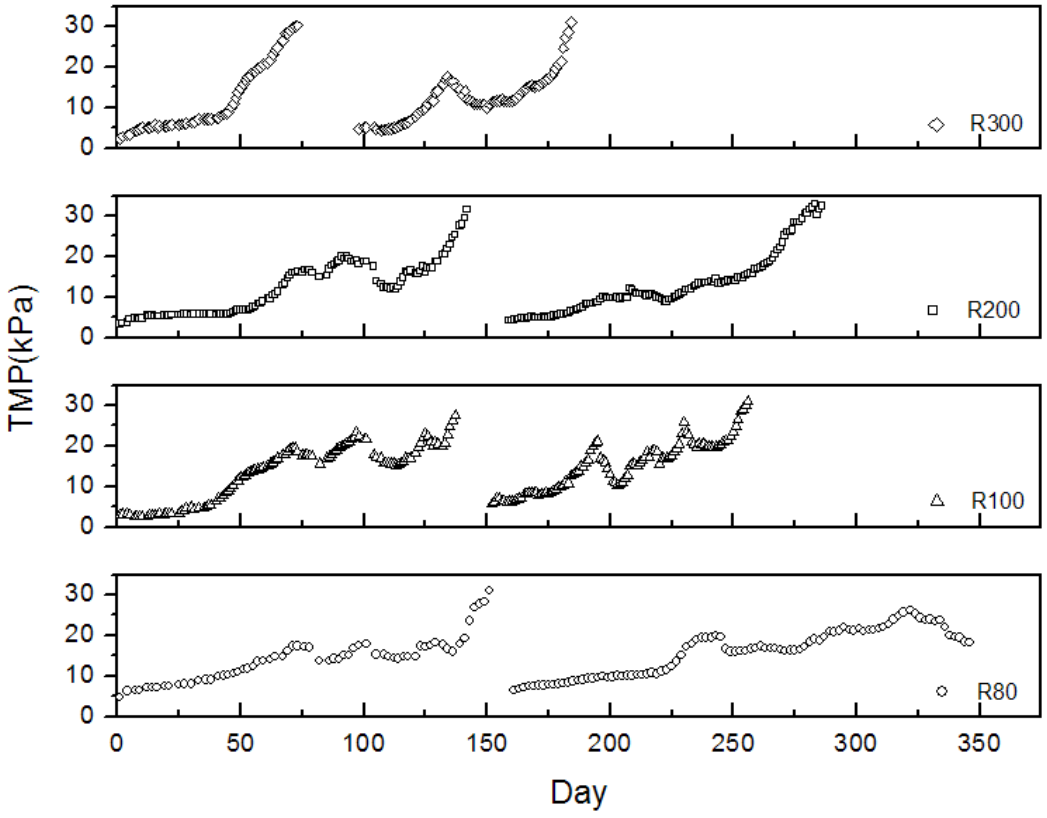

Figure 4.2 TMP profiles for four SCMBRs.

On Day 72, the 300-nm membranes were removed and chemically cleaned, results showed that chemical cleaning was very effective in recovery of the membrane permeability. As could be seen in Fig. 4.2, although chemical cleaning was effective in recovering the permeability of the fouled membranes, severe fouling was again observed on Day 115, which was the 15th Day of the second cycle of fouling test for R300. In contrast, R80, with the smallest pore size, encountered serious fouling only after two months of operation, and the TMP of R80 never reached 30 kPa after six months of operation in the second fouling cycle. This observation could be attributed to the influent which had a stable characteristics during the second fouling cycle compared to that during the first cycle during which the influent characteristics changed significantly due to the monsoon season (see Table 4. 1). These observations suggest that membrane fouling mechanisms for larger pore-sized and smaller pore-sized membranes could be different. Although the smaller pore-sized membrane was able to reject a wider range of materials, resulting in a fouling layer that featured a higher resistance compared to that created by a larger pore-sized membrane, this kind of fouling was more reversible. However, fouling found in systems with larger pore-sized membrane probably attributed to pore blocking by organic and inorganic compounds was more irreversible (Le-Clech *et al*., 2006a). Overall, it was observed that R300 fouled faster than R80 even though R80 had higher TMP values in the first few days. The fouling mechanisms discussed above could possibly explain the phenomenon observed. However, there was one exception - the fouling rate of R100 was slightly faster than that of R200 although the pore size of R100 was smaller than that of R200. This observation suggests that besides the membrane pore size, other membrane properties such as surface roughness could also affect membrane fouling, which will be discussed in Section 3.4.

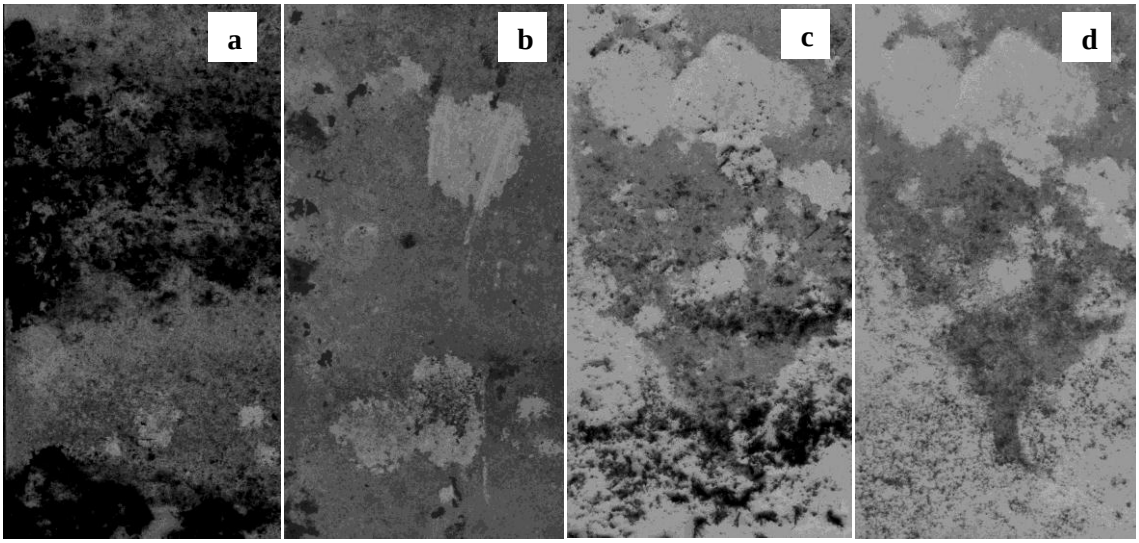

Figure 4.3 Scanned images of membrane obtained during second fouling cycle. a) R80 at Day 71; b) R80 at Day 85; c) R200 at Day 71; d) R200 at Day 85.

A strange phenomenon, which has not been reported in either ceramic MBRs or polymeric MBRs, was observed in this study. From Fig. 4.2, it could be seen that although the TMP increased gradually over time, there were a few instances whereby the TMP decreased abruptly. On Day 79, 104, 134, 249 and 338, drastic declines, namely 4-5 kPa, of TMPs were observed for R80. Similarly, the same observations happened on Day 82, 104, 127, 196 and 133 for R100 and on Day 82, 107 and 225 for R200. In contrast, no such TMP decline was observed in R300 in its first cycle of operation, which might also have led to the short operation time (i.e., rapid membrane fouling) in this cycle of operation. However, the phenomenon of TMP decrease was observed in the second cycle of its operation – the TMP of R300 increased gradually from Day 115 to 134, dropped from Day 134 to 161 and started increased again subsequently. Eventually, the TMP in R300 reached 30 kPa on Day 184, which was the 86th day in the second cycle of operation. Compared to the first fouling cycle, the TMP decrease occurring from Day 134 to 161 during the second fouling cycle had lengthened the membrane operation period by 14 d before reaching 30 kPa of TMP. As reported by some researchers (Dufresne *et al*., 1997; Wang *et al*., 2008), aeration

used in MBR systems would mitigate fouling by constant scouring of the membrane surface. Therefore, one hypothesis that may explain the TMP reduction observed is that the foulants on the ceramic membrane surface are partially sheared off by shear force provided by the aeration when the thickness of the cake layer had reached a certain degree.

In order to explain this surprising phenomenon, regular membrane scanning was conducted during the second fouling cycle using a scanner with high resolution. Fig. 4.3 shows some pictures of the scanned membrane surfaces. It could be seen that there were less biomass attached on the membrane surface on Day 85 (Fig. 4.3b, 4.3d) (second cycle) compared to that of Day 71 (Fig. 4.3a, 4.3c) in both SCMBRs (R80 and R200), indicating that the cake layer on the membrane surface might be partially sheared off by aeration. This observation coincided with the TMP reduction observed, namely 4 kPa for R80 on Day 83 and 3.3 kPa for R200 on Day 81 in the second fouling cycle. These results clearly indicated that the TMP reduction was attributed to the effect of the aeration shearing the cake layer from the membrane surface – a phenomenon observed in all the SCMBRs in this study.

4.2.2 Effect of Biomass Concentrations, Zeta Potential and Capillary Suction Time on Fouling

Several researchers have reported that high MLSS concentration would increase the membrane fouling rate (Cicek *et al*., 1999; Chang and Kim, 2005). In this particular study, however, the relationship between the MLSS and the fouling propensity could not be observed. The discrepancy might be due to the different operating conditions employed in the different studies. For example, in Chang and Kim's study (2005), different sources of MLSS with different concentrations ranging from 0.09 to 3.7 g/L

were applied in a dead-end filtration system. However, the findings observed in this study was in agreement with the observation reported by Le-Clech *et al*. (2003), wherein no impact of MLSS on fouling could be observed for MLSS concentration ranging from 4-8 g/L. The average MLSS concentrations, ranging from 4.86 to 5.13 g/L, observed in this study are summarized in Table 4.2. Ng *et al*. (2006) reported that normalized capillary suction time (CST) was also an indicator for the membrane fouling. However, although the mixed liquor of R80 and R200 had a lower normalized CST (0.0037 s•L/g), the relationship between membrane fouling potential and normalized CST was insignificant (Table 4.2). The mixed liquor of R100, which had a higher normalized CST (0.0042 s•L/g), possessed a lower fouling rate than that of R300 (0.0040 s•L/g). Although the normalized CST has been reported to be an indicator for membrane fouling in Ng *et al*.'s (2006) study with different operating conditions, it is noted in this study that the difference in normalized CST values was negligible and it was not a suitable indicator for membrane fouling when different pore-sized membranes are used under similar operating conditions. The zeta potential of the biomass was monitored regularly. It was observed that the zeta potential of microbial flocs among the reactors were not significantly different. Both observations infer that when all the SCMBRs were operated under similar conditions simultaneously, the properties of the mixed liquor were rather similar and the negligible differences were not the main cause of the various fouling rates observed. Thus, the mixed liquor properties were not the dominant contributors for the difference in membrane fouling observed in this study.

Table 4.2 Biomass concentration, CST and zeta potential for different pore-sized SCMBRs.

Pore size (nm)	MLSS (g/L)	MLVSS/MLSS	Normalized CST (s·L/g)	Zeta potential (mV)
80	4.96 ± 0.96	0.75 ± 0.04	0.0037 ± 0.0010	-22.58 ± 3.30
100	4.87 ± 0.91	0.75 ± 0.05	0.0042 ± 0.0011	-23.95 ± 3.34
200	5.13 ± 1.02	0.75 ± 0.04	0.0037 ± 0.0012	-22.25 ± 4.55
300	4.86 ± 0.94	0.75 ± 0.03	0.0040 ± 0.0013	-21.94 ± 3.25
Note: Number of samplings = 46				

4.2.3 Effect of EPS and SMP Components on Fouling

EPS and SMP are currently considered as the most important factors which influence membrane fouling in MBR. However, it might be difficult to draw similar conclusion from this study. Table 4.3 shows that the concentrations of the protein and carbohydrate in EPS were irregularly related to the membrane pore size or the fouling propensity according to the TMP profile (Fig. 4.2) in SCMBRs. The TMP of R300, R100, R200 and R80 reached 30 kPa on Day 72, 137, 142 and 151 in the first fouling cycle, respectively. However, based on the samples collected for regular analysis, no dramatic increase of protein and carbohydrate (results are not shown here) were observed in the entire process for all SCMBRs. This finding is not in agreement with the results reported by Lee *et al*. (2003) and Chang and Lee (1998) wherein EPS was found to have relationship with membrane fouling in MBR. As reported, the components of the EPS are largely affected by the operating conditions, such as HRT (Ng *et al*., 2005), SRT (Ng *et al*., 2006; Al-Halbouni *et al*., 2008) and aeration rate (Tan and Ng, 2008). Therefore, the different SRTs employed in previous research (Ng *et al*., 2006) might have contributed to the differences. It has been reported that shorter SRT will cause more EPS release, which to some extent lead to higher fouling rate in an MBR with 3-d SRT. In contrast, all the SCMBRs investigated in this study were operated under similar operating conditions. As a result, the differences between

the concentration of carbohydrate and protein, and protein/carbohydrate ratio among four SCMBRs were negligible. In addition, the influent characteristics would also contribute to the membrane fouling. The fact that synthetic wastewater was employed in previous studies conducted by Lee *et al*. (2003) and Chang and Lee (1998), might account for the differences. Yamato *et al*. (2006) used real wastewater and concluded that no relationship between the EPS concentrations and membrane fouling was obtained in an MBR. This again indicated that the difference in membrane fouling observed in this study, when all the SCMBRs were operated under the similar conditions and were fed with real wastewater, could not be attributed directly to the EPS or SMP concentrations. Other affecting mechanisms, such as membrane nominal pore size, pore openings and surface morphology, could be accountable for the various fouling propensity observed.

Table 4.3 EPS composition and P/C ratio of biomass in different pore-sized SCMBRs.

Pore size (nm)	**TOC (mg/L)**	**Carbohydrate (mg/gMLVSS)**	**Protein (mg/gMLVSS)**	**Protein/carbohydrate**
80	6.25 ± 3.23	11.66 ± 4.6	35.19 ± 9.19	3.53 ± 0.84
100	6.16 ± 3.00	10.91 ± 4.24	34.19 ± 8.21	3.34 ± 0.79
200	5.94 ± 3.29	10.28 ± 3.2	33.81 ± 9.19	3.49 ± 0.88
300	5.69 ± 3.19	10.98 ± 3.6	34.99 ± 9.13	3.86 ± 0.88

Note: Number of samplings = 46

4.2.4 MWD of the Biomass Supernatant in Four SCMBRs and Correlation with Membrane Fouling

Figure 4.4 shows the apparent MWD of dissolved organic matters (DOM) in supernatants and effluents of different pore-sized SCMBRs. It could be seen that the DOM in SCMBR supernatant had a broad spectrum of MW. The majority of the DOM, accounting for around 50%, had MW less than 1 kDa. Nevertheless, the second largest MW fraction was in the range of 1-10 kDa, consisting 15-22% of DOM. The

two fractions with MW larger than 10 kDa accounted for around 20-30% of DOM. The results obtained indicated that organics in supernatants with small MW (<1 kDa) accounted for a larger fraction. Although the distribution differences between the four SCMBRs were not apparent, R80 had the highest faction (55%) of smaller MW organics (<1 kDa) in the supernatant of mixed liquor compared to that of R300, which was 46%. This phenomenon again indicated that R80 with the smallest pore-sized membrane has a stronger ability to reject small MW organics.

(a)

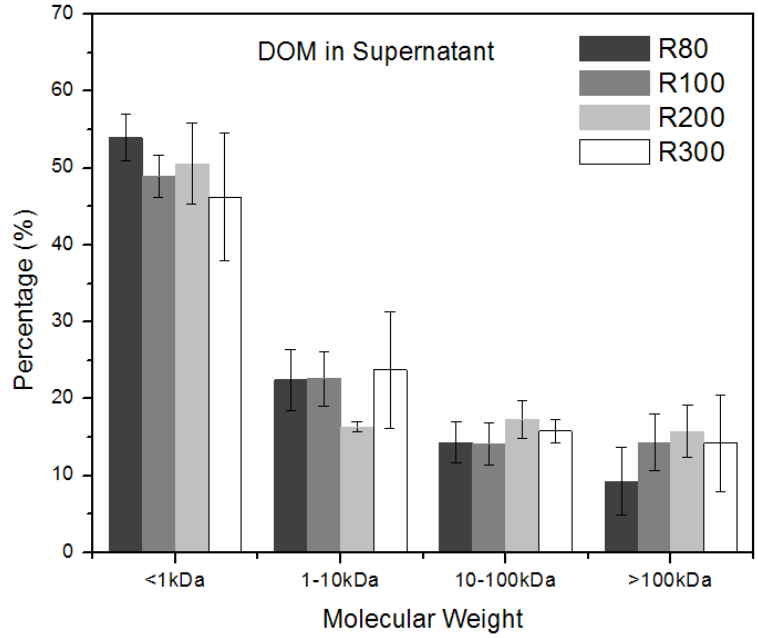

(b)

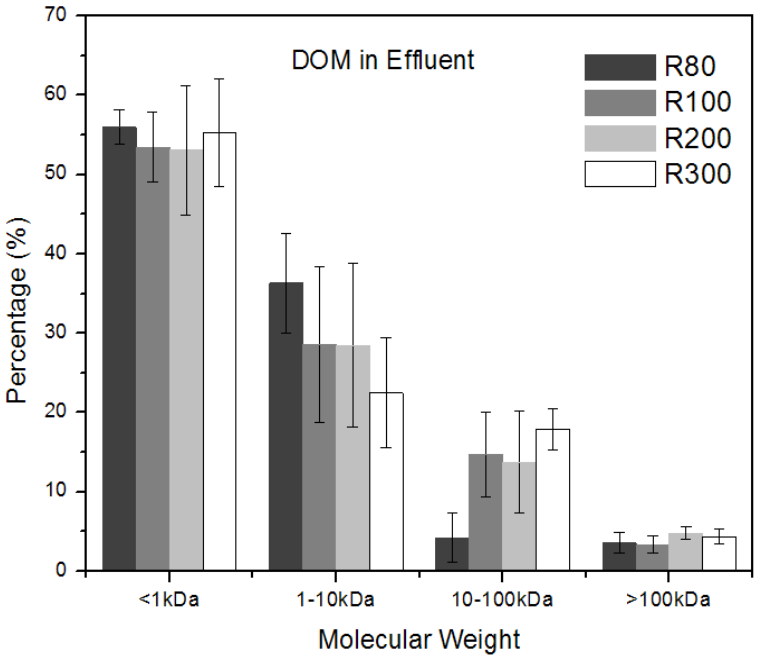

Figure 4.4 Molecular weight distributions of a) supernatants and b) effluents. (Note: number of samplings = 15).

It was noted that the MWD of the DOM in the supernatants and effluents were slightly different. The majority of the DOM in the effluents, accounting for over 50%, had MW less than 1 kDa, whereas the largest MW organics (> 100 kDa) constituted the smallest fraction, which only represented 5% of DOM. This observation was different from those observed by Liang *et al*. (2007) who reported that membrane sieving would not work for most DOM. One possibility is that synthetic wastewater was applied in their studies, and the compositions of the DOM were not comparable with that of the system associated with sewage. This inconsistency could also be attributed to the different membranes, in terms of materials and pore sizes, used in different studies. The smaller pore-sized membrane used in this study might have resulted in fewer fractions of organics with higher MWs in the effluent. The smaller MW fractions, namely less than 10 kDa, accounted for over 90% of the DOM in the R80's effluent also indicated that the smaller the membrane pore size, the higher the rejection rate of DOM in SCMBR. It could also be seen that even though the smaller MW fraction (< 1 kDa) in permeate were somewhat similar for the four SCMBRs, R200 and R300 had higher variability. Again, a hypothesis that the secondary active layer formed by the cake/foulant layer on membrane surface contributed to the DOM rejection might explain this observation. In the early stage of the process, when the active layer had not been formed yet, both R200 and R300 with larger membrane pore sizes might not be able to reject a wider range of particles. Nevertheless, once the active layer established, smaller particles/DOM could be retained within the bioreactors. The standard deviations of MWD of the small MW oragnics (< 1kDa) for the R200 and R300 were 8.2 and 7.1%, respectively. In contrast, it was relatively low for R80, which was 2.2%. Based on the samples collected for analysis, it was noted

that R80 was able to reject more small MW organics constantly. Detailed PSD information will be discussed in the next two paragraphs.

4.2.5 Particle Size Distribution of Mixed Liquor Supernatant and Correlation with Membrane Fouling

The filtered supernatants of mixed liquors were collected for PSD measurement. Figure 4.5 shows the PSD for the different SCMBRs mixed liquor supernatant. It could be seen that for all SCMBRs the general trends were not significantly different with a peak number at around 100 nm. However, the size range and the consistency of the results were slightly different. The filtered supernatant of R80 had a wider range of particle sizes ranging from 58.8 to 255.0 nm, while a narrow particle size range ranging from 68.1 to 164.2 nm were observed for those of the other three SCMBRs. This observed phenomenon could be due to the possibility that the smaller pore-sized membrane in R80 could reject a wider range of particles in the mixed liquor. The good agreement in the trends of PSD and MWD of organics in the supernatant confirmed that a secondary membrane layer possibly formed as discussed earlier and also as reported by He *et al*. (2005). For R80, the smallest pore-sized membrane was able to readily reject particles with larger size. Based on the sieving mechanisms, for R200 and R300, particles with 100-nm size should easily penetrate through the membrane if there were no other rejection mechanisms present. Due to the pore size distribution of the ceramic membrane, as shown in Fig. 4.6 (SEM images), some particles with smaller pore size might be retained inside the reactors since in some areas the membrane pores are smaller than the membrane nominal pore size. Another possibility might be attributed to the cake/foulant layer formation on the membrane

surface, which would act as a secondary active layer to reject smaller particles with sizes smaller than the membrane pore sizes.

In addition, the hypothesis, which a formation of secondary layer on the membrane surface increase large particles rejection, might also account for the lower consistency of the results for three sets of tests associated with R100, R200 and R300. As shown in Fig. 4.5, the three curves (results obtained from three different sampling) did not fit perfectly for R100, R200 and R300. This was possibly due to the different rejection rate of the smaller particles by the ceramic membranes along with different amount of particles accumulating either inside the membrane pores or on the membrane surfaces. In the early stage of the operation (blue curve), smaller particles could penetrate easily through the membranes. Therefore, the size of dominant particles in R300 was over 150 nm. However, as the filtration process went on, the size of the dominant particles appeared to be 100 nm, which suggested that more particles with size around 100 nm were retained inside R300 due to the formation of cake/foulant layer.

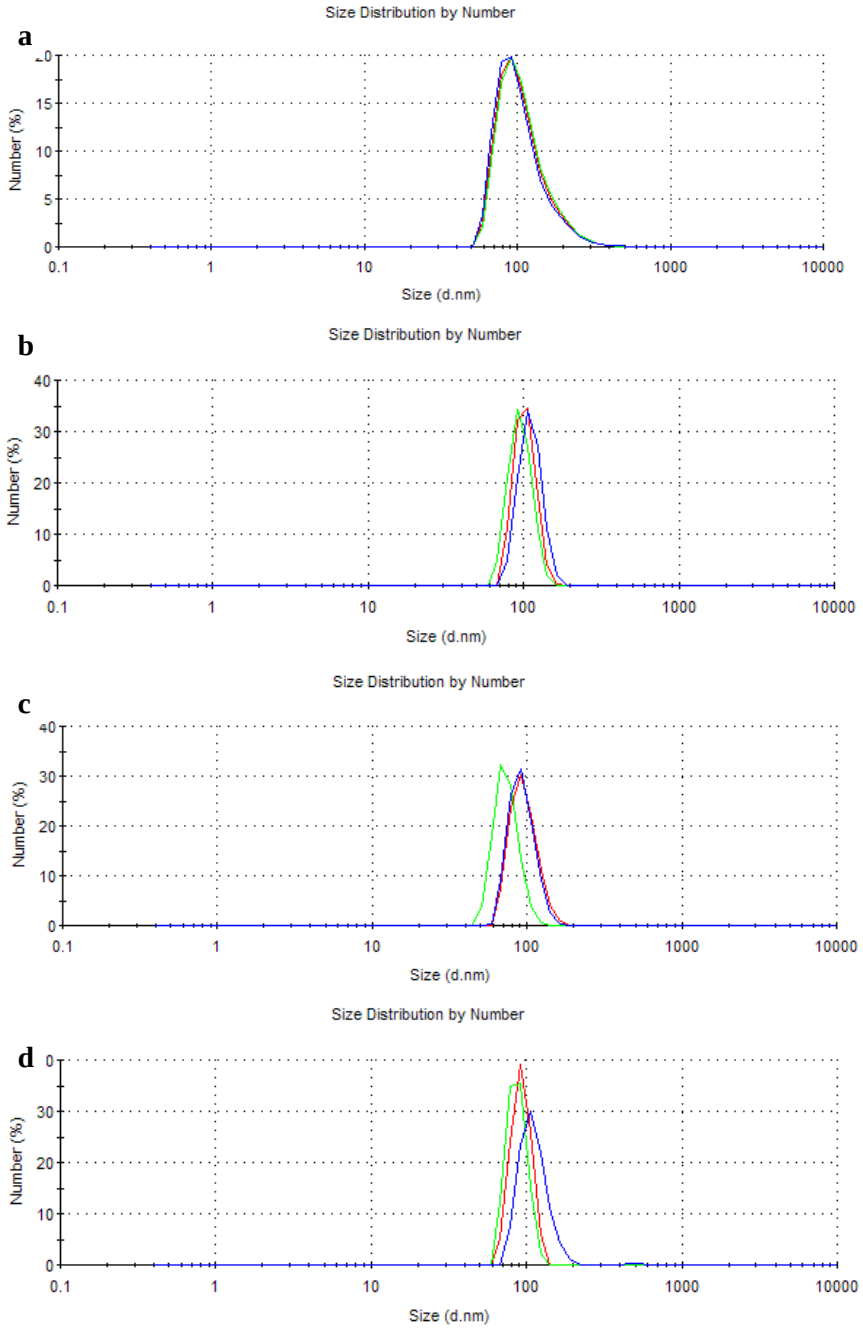

Figure 4.5 PSD of mixed liquor supernatants. a) R80; b) R100; c) R200; d) R300. (Note: Blue curve: sampling on Day 7. Red curve: sampling on Day 30. Green curve: sampling on Day 50.).

4.2.6 SEM Images of Ceramic Membrane Surface

Figs. 4.6a-d show the SEM images of the surfaces of the four different pore-sized fresh ceramic membranes at similar magnification (5000x). As could be deduced from the figures, the 80-nm membrane (Fig. 4.6a) has a dense and smooth structure with small pores. In contrast, the other three membranes had an interwoven and sponge-like microstructure. Based on the micrographs, it was noted that although 200-nm (Fig. 4.6c) membrane had a bigger nominal pore size than that of 100-nm membrane (Fig. 4.6b), its surface structure was much smoother. The 300-nm (Fig. 4.6d) membrane, however, appeared to have the roughest surface and biggest pore openings. As mentioned in Section 3.2, R300 with the biggest membrane pores had the highest membrane fouling rate, while R80 with smallest membrane pores had the lowest fouling rate. R200 and R100 with the same initial membrane permeability had similar fouling rates. Combining the SEM images and the fouling rates results discussed in previous section, it could be concluded that ceramic membrane with denser (i.e., smaller pore size) and smoother membrane microstructures were less prone to fouling.

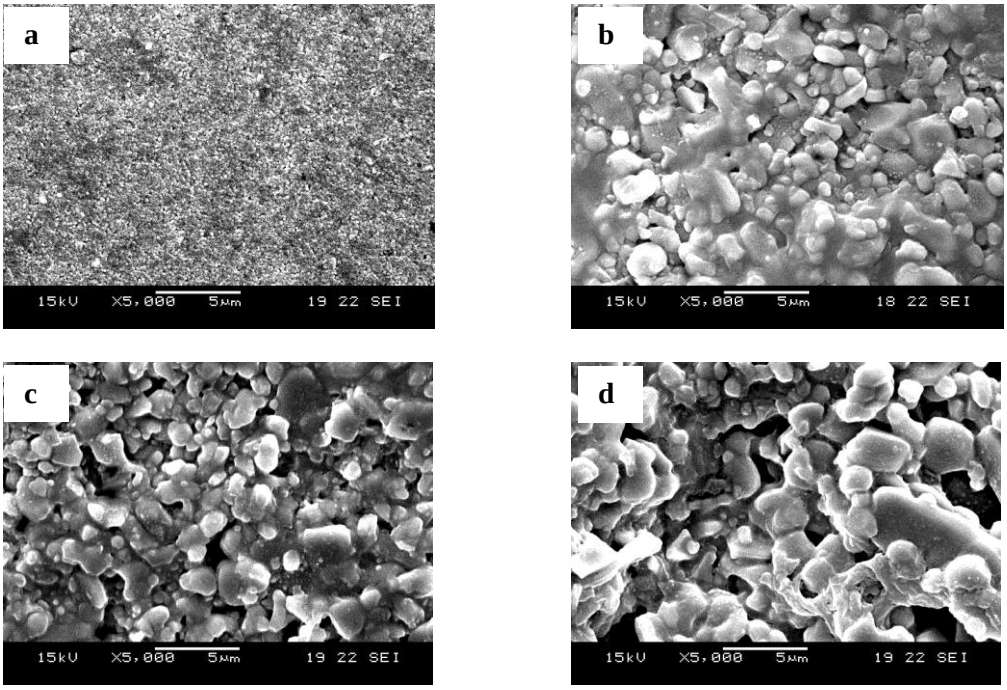

Figure 4.6 SEM images of the surfaces of different pore-sized fresh ceramic membranes. a) 80 nm; b) 100 nm; c) 200 nm; d) 300 nm.

4.2.7 AFM Images of Ceramic Membrane Surface

Several researchers have reported that a rougher membrane surface would induce a higher membrane fouling potential (Evans *et al*., 2008; Fang and Shi, 2005, He *et al*., 2005) since a rougher membrane would trap more deposits. This study demonstrated a similar trend whereby membrane fouling rate corresponded well to the membrane roughness sequence: R80 < R200 < R100 < R300. Figs. 4.7a-d show the AFM images of the surfaces of the four different pore-sized fresh ceramic membranes. It could be seen that the surfaces of membranes were not smooth, but consisted of a mass of peaks (bright regions) and vales (dark regions). The 80-nm membrane was found to have lower peaks and shallower vales, suggesting a smoother membrane surface. The deeper the "valley" and the higher the "peaks" on a rougher membrane surface, the greater the amount of filling-in points will be available for building up a fouling layer.

This in turn would lead to a faster TMP increase (as observed for bigger pore-sized ceramic membranes).

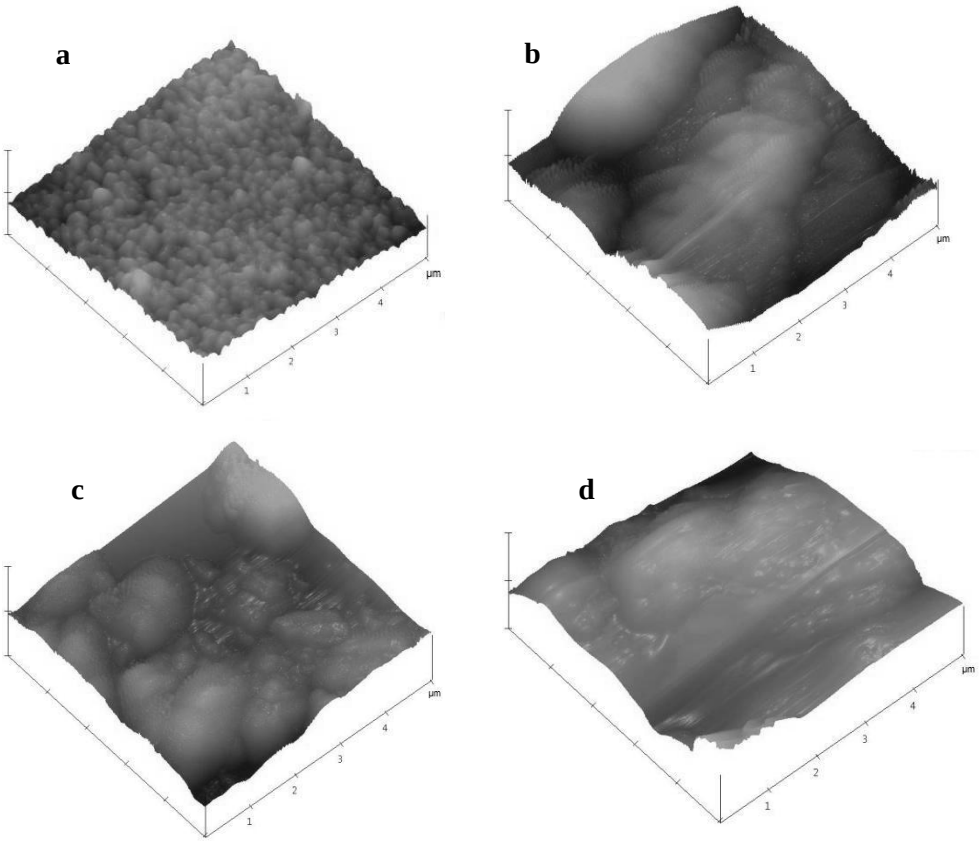

Figure 4.7 AFM images of the surfaces of different pore-sized fresh ceramic membranes. a) 80 nm; b) 100 nm; c) 200 nm; d) 300 nm.

Table 4.4 summarizes the analyzed results of the AFM images. As could be seen from the table, the 80-nm membrane not only had a much lower R_{ms}, it also had lower R_a, Z range and max height. R_{ms} and R_a are the root mean square of roughness and roughness mean of the membrane surface, respectively. The higher the values of the R_{ms} and R_a, the rougher the membrane surface would be. Z range and Max height are another two parameters indicating surface roughness. However, R_{ms} and R_a are normally used to represent the surface roughness. The R_{ms} and the R_a values of the 300-nm membrane were almost 6 times higher than those of the 80-nm membrane. It

could also be seen from Table 4.4 that the Z range and the max height of the 100-nm and 200-nm membranes were similar, whereas the roughness of the 100-nm membrane, either R_{ms} or R_a, was higher than those of the 200-nm membrane. As discussed above, the fouling rate of the R100 was a bit higher than that of R200. These observations suggested that instead of the Z range and max height, R_{ms} or R_a, which indicates membrane roughness, correlated well with the fouling propensity of the membrane.

Table 4.4 Analyzed results of AFM images of fresh membranes.

Pore size(nm)	**R_{ms}(nm)**	**R_a(nm)**	**Z range(nm)**	**Max Height(nm)**
80	43.48	33.74	359.24	362.26
100	172.73	141.90	886.11	877.80
200	126.70	98.54	899.81	841.52
300	251.95	198.95	1702.00	1489.00

R_{ms}: Root mean square of roughness; R_a: Roughness mean

4.3 Summary of Phase 1 Research and Recommendation

This study investigated the treatment performance and the different fouling characteristics of the different pore-sized SCMBRs by operating four SCMBRs in parallel. The results are summarized as below:

(1) Ceramic membrane with the smallest pore size of 80 nm and smoothest membrane surface was found to foul the slowest, whereas the 300-nm ceramic membrane with the largest pore size and roughest membrane surfaces fouled the fastest.

(2) Biomass on the cake layer was partially removed by the shear force provided by the aeration during the operation, resulting in the TMP reduction observed in all SCMBRs.

(3) The profiles of MWD and PSD were slightly different in the early stage of the operation and appeared to be similar for SCMBRs with different pore sizes. These results suggested that an active layer might have developed on the membrane surface, which would achieve sieving of colloidal particles that contribute to COD, resulting in similar PSD and MWD profiles.

(4) Results on the effect of mixed liquors characteristics (MLSS, CST, Zeta Potential, EPS and SMP) on fouling showed that mixed liquor properties were not the key factors leading to various fouling behaviors with different pore-sized SCMBRs operated under similar conditions observed in this study. The experimental results also suggested that both membrane pore sizes and membrane surface properties affected membrane fouling significantly, and membrane fouling potential was in good

accordance with the sequence of membrane surface roughness: R80 < R200 < R100 < R300.

Based on the results obtained in this phase, minor difference of the mixed liquor properties could be observed in the four SCMBRs with different pore sizes. However, due to the usage of raw domestic wastewater, slight fluctuations of the SMP/EPS concentration were inevitable in the four reactors. In order to rule out all the possible causes of different membrane fouling behaviors of different pore-sized SCMBRs, mounting the four membranes in one SCMBR will be a meaningful process. In this phase of the study, the morphologies of the biofilm/biocake on the membrane surface were not taken into account to explain the different fouling behaviors. It was suggested that membrane microstructure, material and pore openings all affected MBR fouling significantly. However, how these parameters contributed to the formation of the biofouling layer developed on the membranes have not been studied. It is expected that the pore size of ceramic membrane will affect the roughness of the membrane surface. However, how roughness difference induces different fouling characteristics has not been studied in SCMBR systems. Therefore, it is believed that a complete characterization of the biofilm structure will shed light into these questions.

Chapter 5. Phase 2- Application of Four Different Pore-sized Membranes in One SCMBR

This phase of study focused on in-depth evaluation of fouling characteristics of different pore-sized ceramic membranes in one SCMBR. Samples were collected at 0 h, 1 h, 6 h, 24 h, 72 h, 7 d, 14 d, 21 d, 28 d, 35 d, 42 d and 49 d throughout the whole process in order to analyze the biofilm/biocake development taking place on the membrane surface. Some non-traditional analytical methods like EEM, HPLC and LC-OCD were also applied to investigate the influence of biofilm/biocake on the organic rejection and membrane fouling for different pore-sized membranes. The four membranes with pore sizes of 80, 100, 200 and 300 nm used in this study were related to as M80, M100, M200 and M300, respectively.

5.1 Fouling Behavior and Mixed Liquor Suspended Solids Characteristics

5.1.1 Fouling behavior of One SCMBR

The TMPs of the four different pore-sized membranes were recorded at 0, 1, and 6 h after the start-up and the corresponding readings were recorded once a day thereafter.

The results are shown in Fig. 5.1. From this figure, it can be seen that overall under the membrane permeate flux of 9.11 LMH, the conditional fouling was not obvious whereby the membrane pore blocking occurred yet no obvious TMP increase was observed. Zhang *et al*., (2006) reported that under a constant flux condition, there existed an initial fouling stage where no significant TMP increase could be observed. However, in this study all the membrane has significant TMP increase from the beginning of the process. This observation indicated that under a permeate flux of 9.11 LMH, the biofilm/biocake layer formed immediately once the process started, and the effect of the pore blocking observed in an MBR operating at sub-critical condition could not be observed clearly in this current study. The detailed discussion regarding this phenomenon will be presented in Section 5.3.1.

M80, with the smallest pore size, had the highest TMP increase rate within the first 7 d operation period. It was noted that TMP increase of the four pore-sized ceramic membranes was in good accordance with the pore size increase within the first 7 d as can be clearly seen in Fig. 5.2. The smaller the membrane pore size, the faster the increase rate. M80 had the smallest membrane pore size increased TMP fastest in the first 7 d. This finding might be due to the significant differences of membrane resistance between M80 and the other three membranes. Membrane fouling resistance is a sum of membrane resistance, resistance contributed by pore blocking and resistance contributed by cake layer. In the early stage of the operation, operating under the same mixed liquor, the difference of the resistance contributed by cake layer and pore blocking were similar and was relatively low for the four membranes. Thus, the membrane internal resistance was the dominant fouling resistance at this phase. Fouling resistance consisted of the resistance contributed by cake formation, pore blocking and membrane internal resistance. In the beginning stage, contribution

difference from pore blocking and cake layer was not significant. Therefore, the higher internal membrane resistance of M80, which was 7 times higher than that of the other three, led to the fastest TMP increase rate.

From Fig. 5.1, we could also observe that from Day 10 to 20, a significant TMP increment could be observed for all membranes. From the TMP data collected daily, it is expected that a linear relationship between the time course and TMP might exist. Looking into the TMP datasets from Day 10 to Day 20, a linear relationship between the time course and TMP was found for each membrane with a good regression rate (R^2 >0.92). The TMP increase rates (dp/dt) were found to be 0.96 for M80, 1.72 for M100, 1.79 for M200 and 2.31 for M300. The TMP increase rate (dp/dt) seemed to be in a good accordance with the membrane pore size. However, M100 reached a TMP of 30 kPa earlier than M200. This was because, on Day 22, a significant TMP reduction was observed in M200. Although, TMP reduction was also found for M100, the decrease was not that significant compared to that of M200. Overall, the membrane performance of M100 and M200 were very similar, which might be due to the similar membrane resistance as well as the membrane configuration. As discussed in Section 4.2.7, not only the membrane pore size, the membrane surface roughness also contributed to the different fouling propensities in SCMBR.

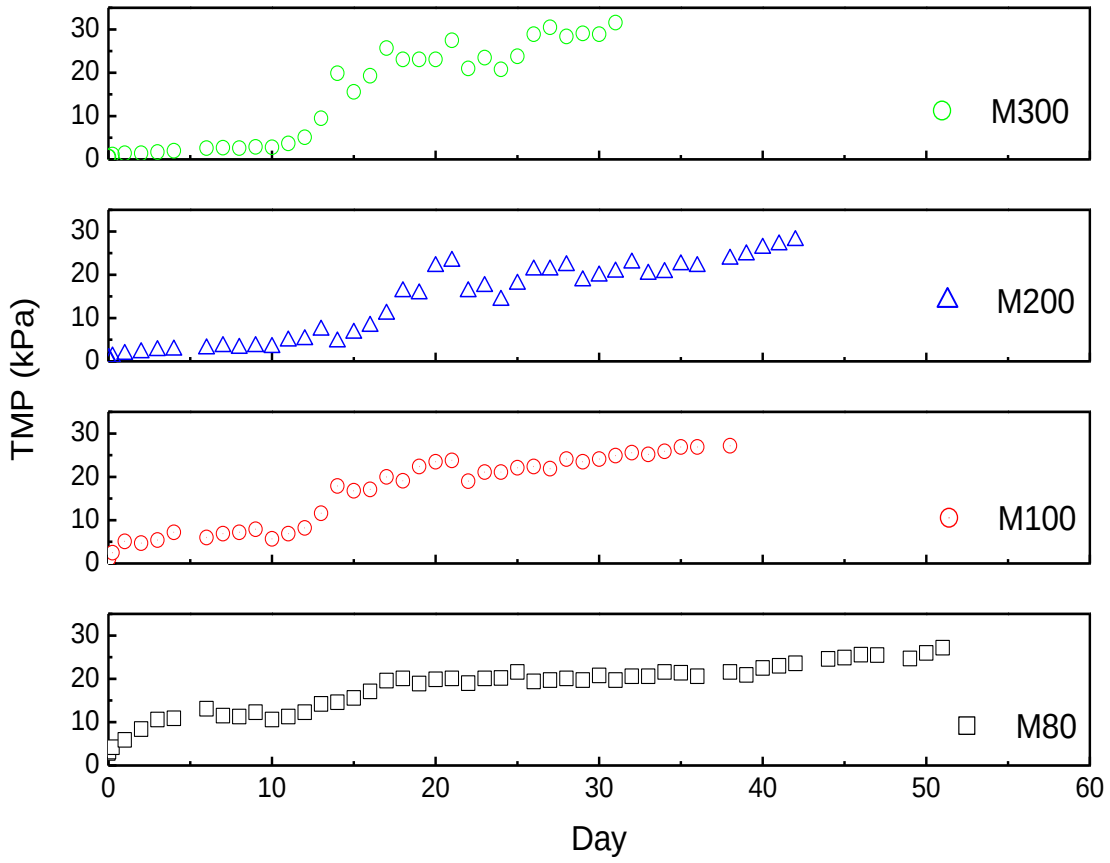

Figure 5.1 TMP profiles of the four membranes with different pore sizes in one SCMBR.

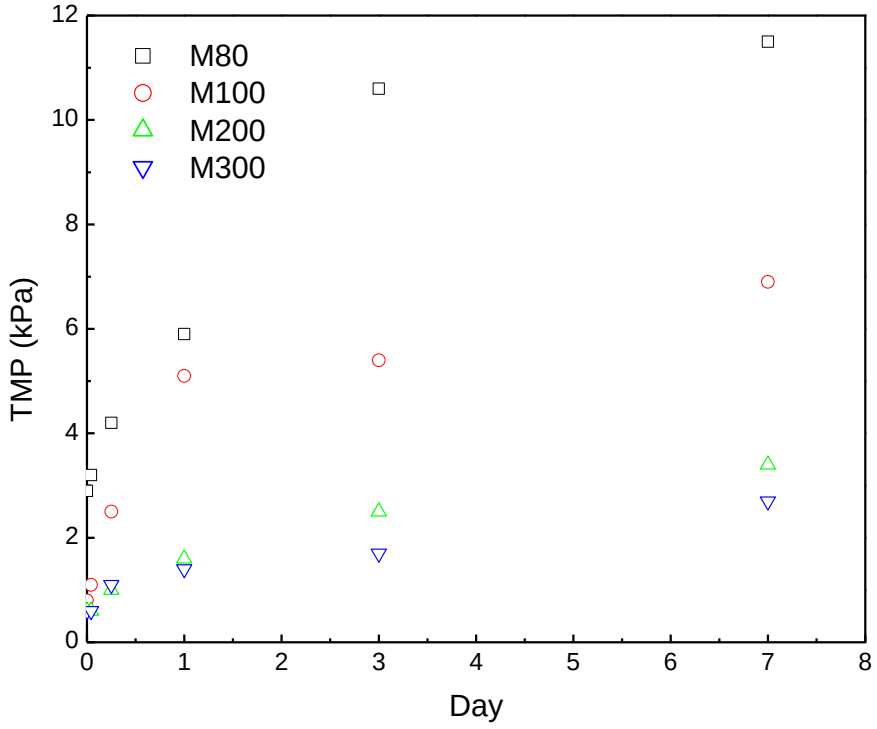

Figure 5.2 Membrane fouling propensity within the first 7d of the operation

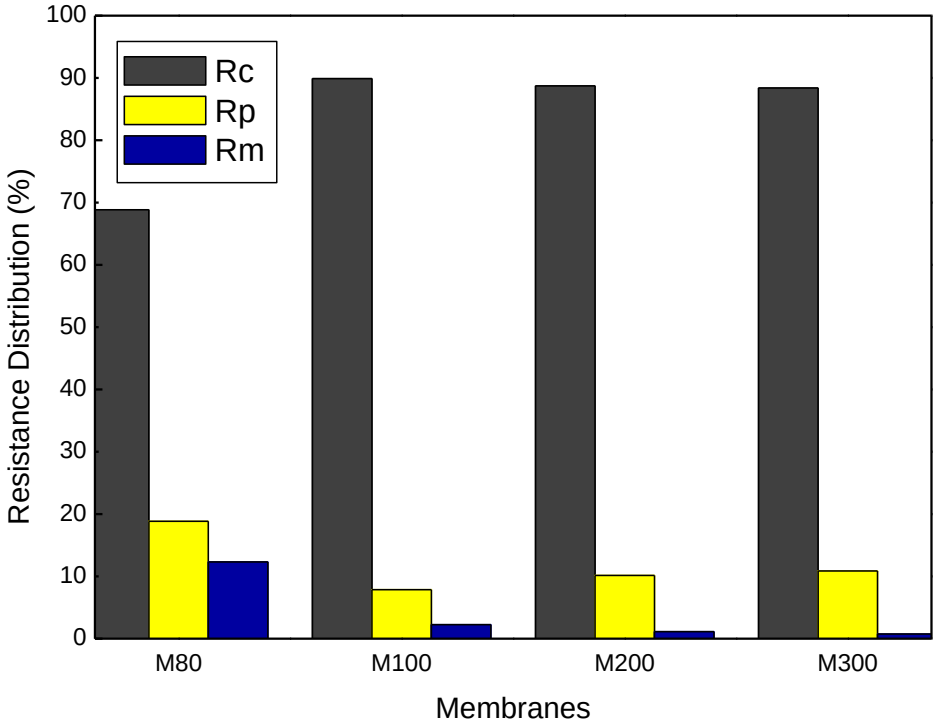

Figure 5.3 Fouling resistance distributions in the four ceramic membranes when they were fouled.

Membrane fouling resistance distributions were also investigated and the results are summarized in Fig. 5.3. From this figure it could be concluded that cake layer was the main contributor to membrane fouling. This observation was supported by various studies (Lee *et al*., 2001; Le-Clech *et al*., 2006; Meng *et al*., 2007; Huang *et al*., 2008). The contribution from membrane resistance (R_m) was almost negligible for M100, 200 and 300, while it contributed 12.3% of the total resistance to the fouling of M80. This finding, again, indicated that for a membrane with smaller pore size like M80, the fouling resistance due to the membrane internal resistance was not negligible. In addition, M80 also had the highest R_p, while M300 had the second highest R_p of 10.9% after 31 days of operation. This finding seemed contradictory with our previous finding that it was easier for the ceramic membrane with bigger pore size to induce membrane pore blocking, while the membrane with the smaller pore size was prone to

induce cake layer. However, other than the fouling mechanism, the operation duration would also contribute to fouling resistance distribution. The longer operation course of M80, which was 51 d might cause more pore clogging because the membrane pore clogging is a process of particulates or solutes accumulation into the membrane pores and is always irreversible. The longer operation duration of M80 would inevitably give more chance for solutes to block the pores, and eventually the membrane pore blocking would be more severe when membrane fouled after 51 d of operation.

5.1.2 Mixed Liquor Concentrations, EPS and SMP

The characteristics of the biomass properties, such as the MLSS, MLVSS, EPS and SMP, were monitored during the whole process in order to evaluate the good working condition of the SCMBR, and finally to draw a better understanding of the fouling characteristics. Table 5.1 shows the components of SMP and EPS in the mixed liquor. It can be seen that the MLSS concentration was controlled at around 4,500 mg/L with a reasonable variation due to the employment of the raw wastewater. Figs. 5.4a and 5.4b show the total EPS and SMP concentrations during the biomass acclimization period and the steady period, respectively. As shown in Fig. 5.4a, the total EPS was not stable during the biomass acclimation period, which decreased from 100 mg/gMLVSS to 18 mg/gMLVSS. However, once the biomass reached a steady state, the average total EPS was around 39 mg/gMLVSS. Compared to EPS, total SMP were more stable at around 14 mg/gMLVSS throughout the 4 months of operation, which indicated that steady state was achieved in the SCMBR.

Table 5.1 MLSS, TOC, SMP and EPS in mixed liquor.

MLSS (mg/L)	**TOC (mg/L)**	**Protein (mg/g MLVSS)**		**Carbohydrate(mg/g MLVSS)**		**Total SMP (mg/gMLVSS)**	**Total EPS (mg/gMLVSS)**
		SMP	**EPS**	**SMP**	**EPS**		
4,560 ±713	16.5 ±6.5	5.2 ±1.7	28.9 ±7.4	8.5 ±3.0	9.9 ±1.6	13.7 ± 4.2	38.9 ± 8.2
Number of sampling =13							

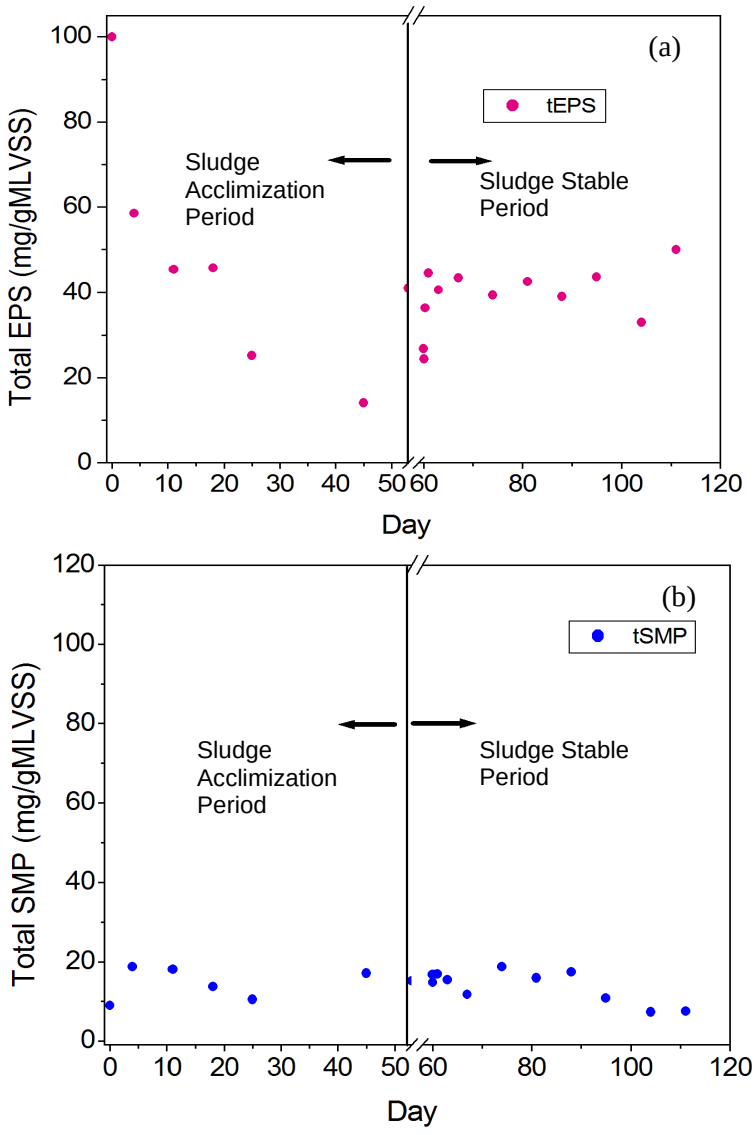

Figure 5.4 a) Total EPS concentration in SCMBR; b). Total SMP concentration in SCMBR.

5.2 Organic Rejection by Different Pore-sized Ceramic Membranes

5.2.1 Molecular Weight Distribution and High Performance Liquid Chromatography (HPLC)

Figs. 5.5a and 5.5b illustrate the apparent molecular weight distribution of DOM in all the membrane permeates and supernatant. As shown in Fig. 5.5a, DOM in the supernatant had a broad spectrum of molecular weight. Majority of the organics, accounting for 50%, have a molecular weight of more than 100 kDa. However, the distribution for the effluents showed different results. It could be observed from Fig. 5.5b that the DOM in all effluents had less than 10% large molecules (>100 kDa). These observations indicated that ceramic membranes with pore sizes ranging from 80 to 300 nm have an ability to partially remove DOM in the mixed liquor supernatant, and these rejected organics could play an important role in leading to membrane fouling by either blocking the membrane pore or adhering onto the membrane surface. In addition, it could also be observed that the membrane with the smallest pore size of 80 nm was able to reject more large molecules, and over 70% of the particles in effluent have a molecular weight of less than 1 kDa. On the contrary, the portion of small organics (<1 kDa) accounted for less than 50% for the effluents from the other three pore-sized membranes. These observations suggested that membrane pore size would affect the DOM rejection during the operation.

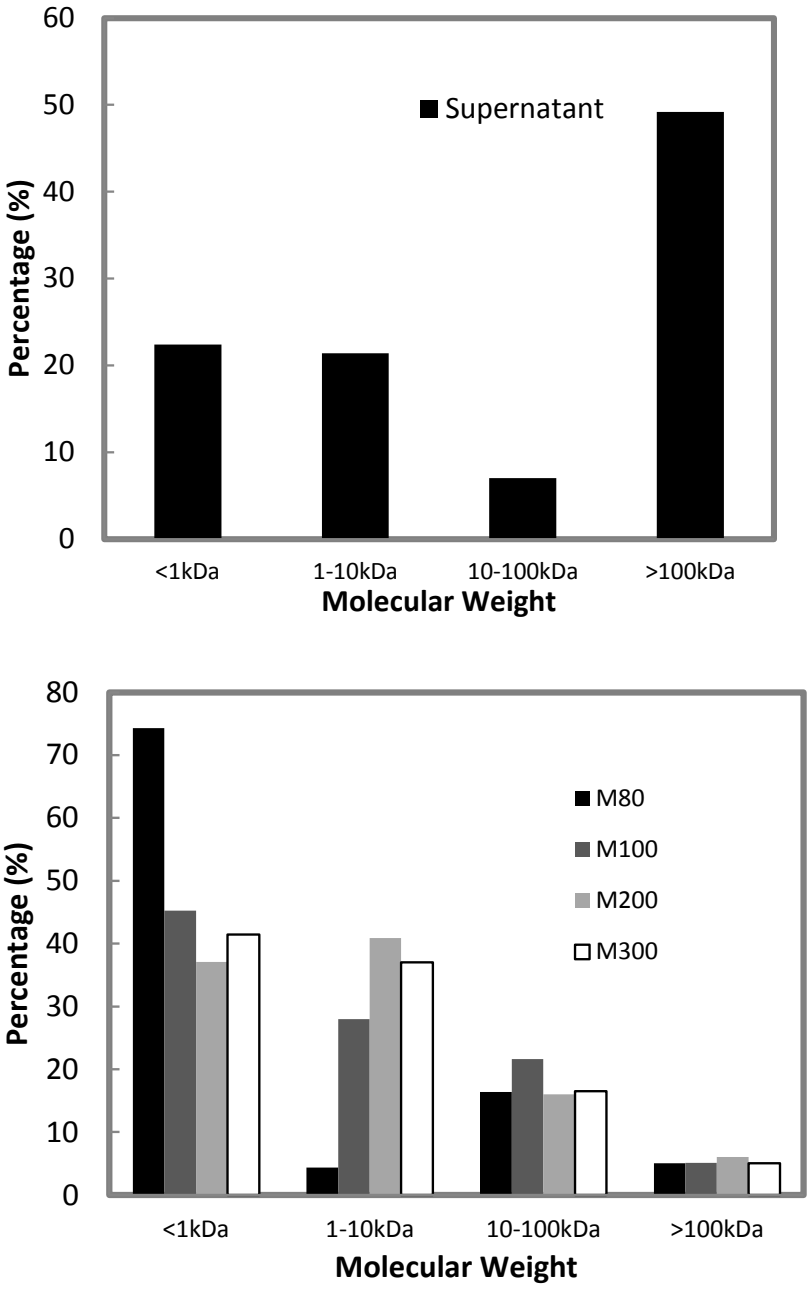

Figure 5.5 Molecular weight distributions for mixed liquor supernatant and permeates a). supernatant; b). membrane permeates.

However, the information provided by the MWD was unable to provide the detailed molecular weight distribution and information regarding the formation of biofilm/biocake layer throughout the process. In order to give more detailed profile of the molecular weight distribution and the change of the MWD profile during the operation, the mixed liquor supernatant and membrane permeate were analyzed by HPLC at each sampling point. The results of HPLC at 1 h and 14 d sampling are summarized in Figs. 5.6 and 5.7. From Figs 5.6a-e, it could be seen that there are five obvious peaks for all the samples, which corresponded to the molecular weights of 246.1, 347.1, 487.6, 10,155.1 and 32,985.8. Compared to the HPLC profile for the supernatant and the membrane permeate at 1 h sampling, it could be observed that the intensity of all fives peaks were higher in supernatant profile than those of the membrane permeates, especially for the peak at the molecular weights of 10,155.1 and 32,985.8. This finding was in accordance with the MWD results obtained by the filtration methods which showed that the ceramic membranes with the pore size ranging from 80 to 300 nm were able to reject part of the large molecules. Although the intensities for the peaks of the smaller molecules in the supernatant were also higher than those of the membrane permeates, the differences were minor. Comparing Figs. 5.6a, 5.6b, 5.6c and 5.6d, we could observe that the effluent from M80 had the lowest intensity of the bigger molecules, and the rejection for the peaks at MW of 10,155.1 and 32,985.8 was almost complete.

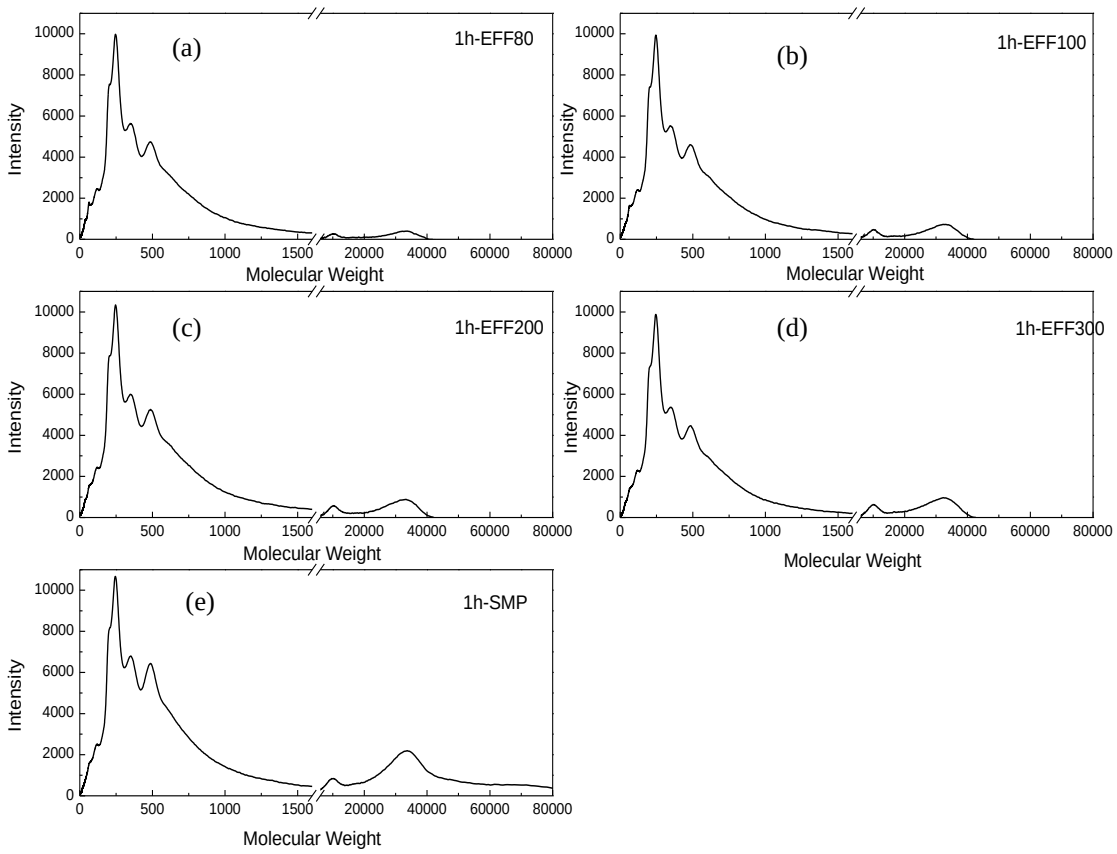

Figure 5.6 HPLC profiles of molecular weight distribution at 1-h sampling: a), b), c), d) Effluent from M80, M100, M200 and M300, respectively; e) Supernatant (SMP)

In order to look into the effect of foulants layer development on the membrane surface, sequence sampling of HPLC measurement was conducted. The results showed that from Day 14 onwards, the HPLC profile differences between permeates of four membranes could not be distinguished. The HPLC profiles of the samples on Day 14 were shown in Fig. 5.7. From this figure, it could be observed that the five peaks of the dominants MW were clearly seen in all the samples. However, the intensities of these peaks slightly changed compared to the results of 1 h samples. All HPLC profiles for membrane permeates were identical with each peak having the similar intensity. This phenomenon might be due to the formation of a gel layer or biofilm/biocake layer on the membrane surface, which contributed to the rejection of bigger organics. Eventually, the differences of the higher MW organics presence in

the membrane permeate from the four pore-sized ceramic membranes were obscured. In addition, it could be observed from Figs. 5.7a-e that unlike the HPLC profile for the 1 h sample where mixed liquor supernatant had higher intensity of all the five peaks, not all the intensities of five peaks were higher in supernatant than that of the permeate after 14 d operation. The HPLC profile for mixed liquor supernatant had similar profile of smallest MW molecules to all permeates at peak 246.1. However, lower intensity of small MW molecules at peak 347.1 and 487.6 and higher intensity of bigger MW molecules at peak 10,155.1 and 32,985.8 were observed in supernatant than that of membrane permeates. These observations are in agreement with Meng *et al*. (2010) that the hydrolysis is able to hydrolyze the organics with high MW into low MW ones. This finding, again, confirmed the presence of the biofilm/biocake layer, which not only functioned as a barrier for the organic solutes, but also induced the biological reactions on the membrane surface.

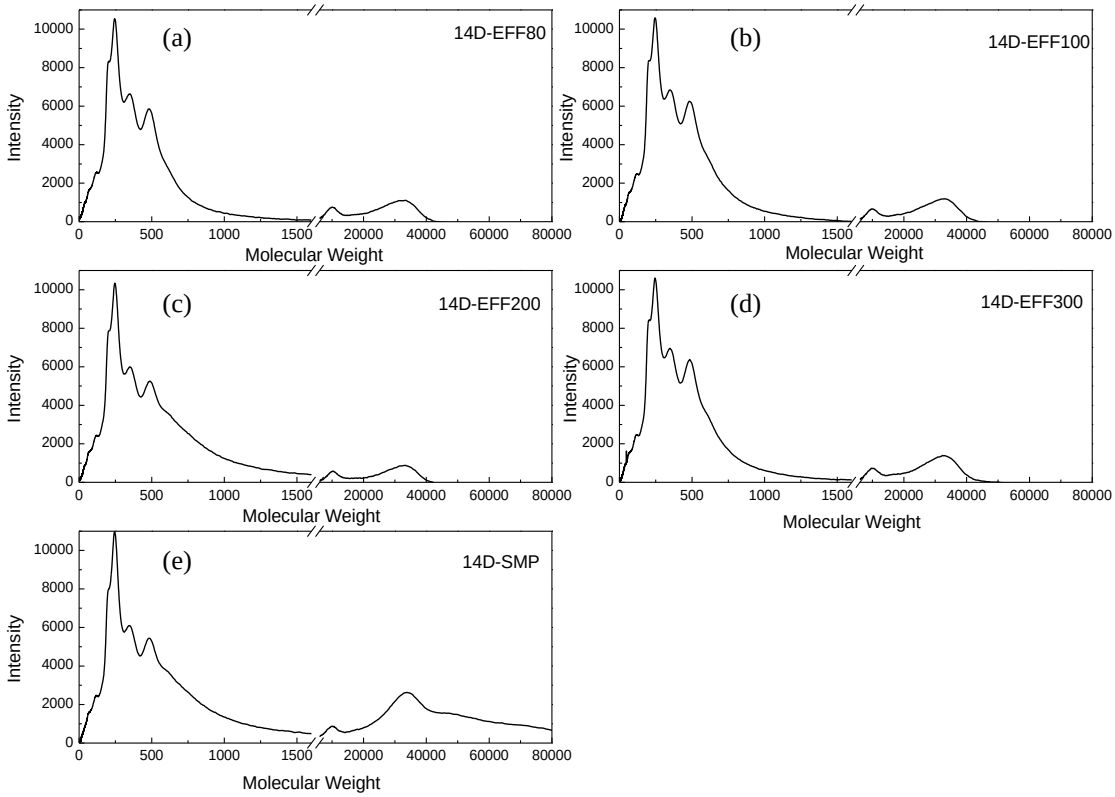

Figure 5.7 HPLC profile of molecular weight distribution on Day 14 sampling: a), b), c), d) Effluent from M80, M100, M200 and M300; e) Supernatant (SMP)

5.2.2 Excitation Emission Matrix (EEM) Fluorescence Spectra

Figures 5.8 and 5.9 show the excitation emission matrix (EEM) fluorescence spectra of all permeates and supernatant after 1 h operation and 14 d operation. As observed in Fig. 5.8e, three major peaks with wavelength of Ex/Em of 270/370 (Peak A); 260-275/380-390 (Peak B) and 250/420-430 (Peak C) are very obvious. Peak A was reported to be aromatic protein-like substances (Baker, 2001). Compared to the recent study done by An *et al*. (2009) who reported that the Ex/ Em ratio of 230-240/335-350 indicated the presence of aromatic protein-like substances and Wang *et al*., (2009) who described the peak of 235–240/340–355 as aromatic protein-like substances, the location of the Peak A observed in this SCMBR showed a shift both in terms of the excitation (red shift) and emission wavelength (blue shift). The shift in terms of the

emission wavelength is named as blue shift, which is related to a decomposition of condensed aromatic moieties and the break-up of the large molecules into smaller fragment. A reduction in the degree of the π-electron system, a decrease in the number of the aromatic rings, a reduction of conjugated bonds in the chain structure, a conversion of linear ring system to a non-linear system or an elimination of particulate functional groups including carbonyl, hydroxyl and amine would all contribute to the blue shift (Coble, 1996; Korshin *et al*., 1999; Swietlik *et al*., 2004; Wang *et al*., 2009). While a shift in terms of excitation wavelength is called red shift, which is associated with the presence of carbonyl containing substituents, hydroxyl, alkoxyl, amino groups and carboxyl constituents (Chen *et al*., 2002; Senesi, 1990). The blue and red shifts observed in Peak A in this current study and previous study might be due to the different source of wastewater used in difference studies. Peak B, at the wavelength of the 260-275/380-390, was described as protein-like substances such as tryptophan with a blue shift as reported by An *et al*., (2009) and Wang *et al*., (2009). Peak C was also reported as protein-like substances (Chen *et al*., 2003; Yamashita and Tanoue, 2003).

Other than the EEM spectra of the mixed liquor supernatant, the permeates from different pore-sized membranes were also measured by fluorescence spectrophotometer after 1 h operation, and the EEM spectra matrix were listed in Figs. 5.8a-d. By comparing the EEM spectra of effluents and mixed liquor supernatant, we could observe that higher intensity for both peaks was found in the supernatant spectra than those of effluents (Table 5.2). In addition, there was one peak observed in the supernatant EEM spectra but not observed in permeates from M80, M100 and M200, which was at the wavelength of Ex/Em at 270/370 nm. This finding indicated that this peak might be produced by the microbial activities, and this portion was

removed by the membrane with smaller pore size during the process. These results were in accordance with MWD and HPLC measurements that the ceramic membrane was able to reject part of the DOM present in the mixed liquor supernatant. All these observations suggested that the DOM contributed a lot to membrane fouling in SCMBR. We could also observe that the membrane with the biggest pore size of 300 nm was not able to reject many organics within the first one hour, since the intensity of these two peaks (Ex/Em (260-270/390nm) and Ex/Em (240-250/420-430nm)) were quite high compared to the other three. The presence of peak A also indicate that, after 1 h of operation the differences of EEM fluorescence spectra of the DOM in the membrane permeate from M300 and mixed liquor supernatant were minor.

Table 5.2 Fluorescence spectral parameters of DOM in the mixed liquor supernatant and membrane permeates.(Peak:Ex/Em nm)

		Peaks			Intensity		
		Peak A	**Peak B**	**Peak C**	**Peak A**	**Peak B**	**Peak C**
1h sample	M80	ND	240-250/390	240-250/420-430	-	241.3	241.3
	M100	ND	240-250/390	240-250/420-430	-	210.7	237.1
	M200	ND	240-250/390	240-250/420-430	-	235.7	255.7
	M300	270/360	260-270/390	240-250/420-430	366.6	440.0	440.0
	Supernatant	270/370	260-275/380-390	250/420-430	442.8	498.9	442.8
14D sample	M80	ND	240-250/390	240-250/420-430	-	210.3	233.8
	M100	ND	240-250/390	240-250/420-430	-	189.4	189.4
	M200	ND	250/390-400	230-240/420-430	-	186.4	186.4
	M300	260/370	240-250/390	230-240/420-430	168.6	192.7	192.7
	Supernatant	270/370	250-270/390	240-250/420-430	345.8	369.0	322.8

In order to analyze the membrane fouling layer development, all permeates and supernatant were collected regularly for EEM measurements. The results of the samples collected on Day 14 were shown in Fig. 5.9. Compared to the EEM fluorescence spectra of all permeates and supernatant after 1 h operation, the two protein-like substance peaks remained low for membranes with pore size of 80, 100 and 200 nm. However, unlike the EEM of the sample collected after 1 h operation, the three protein-like substance peaks in M300 permeate decreased significantly from 442.8 to 186.6 (Peak A); from 440.0 to 192.7 (Peak B) and from 440.0 to 192.7 (Peak C), while the supernatant intensity remained high. These observations, again, indicated that a formation of a biofilm layer on the membrane surface contributed to the increment of organic removal in SCMBR system, which functioned as the second layer for organic rejection.

In Fig. 5.9e, three peaks of the protein-like substances could be observed which were at Ex/Em ratio of 270/370, 250-270/390 and 240-250/420-430. Compared to Fig 5.7e, the Peak B shifted a bit from Ex/Em of 260-275/390 to 250-270/390, which indicated that red shift occurred after 14 d operation. The slight difference could be due to the slight difference environmental stress the microbes faced at the difference phase of the operation. In addition, comparing Figs. 5.8a-d, it is observed that after 14 d operation, Peak B and Peak C were slightly different in permeates from the four different pore- sized ceramic membranes. For permeates from M 80 and 100, Peak B remained at Ex/Em of 240-250/390. However, it shifted to 250/390-400 for permeate from M200. For permeates from M200 and M300, Peak C shifted to 230-240/420-430, which was different from Peak B associated with mixed liquor supernatant. The biodegradation and hydrolysis process happened on the membrane surface by the biofilm/biocake formation might explain this finding. During the membrane filtration,

a number of particles, solutes and biomass accumulated onto the membrane surface or into the membrane pores, forming a biofilm/biocake layer. This layer would eventually contribute to the occurrence of biodegradation process and change the form of these protein-like substances.

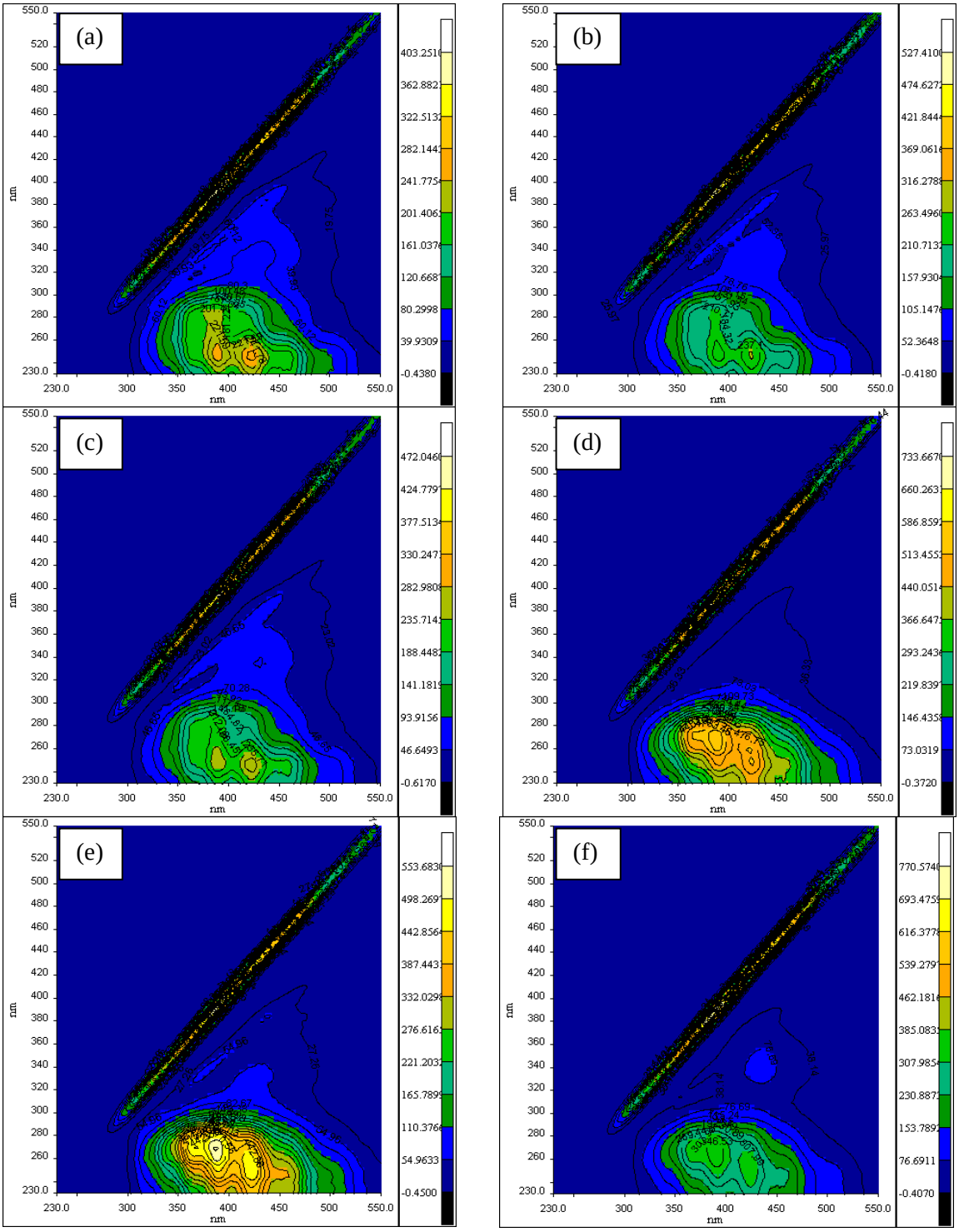

Figure 5.8 EEM spectra profile of permeates, mixed liquor supernatant and EPS at 1 h. a), b), c), d) Permeate from M80, M100, M200 and M300; e) SMP; f) EPS.

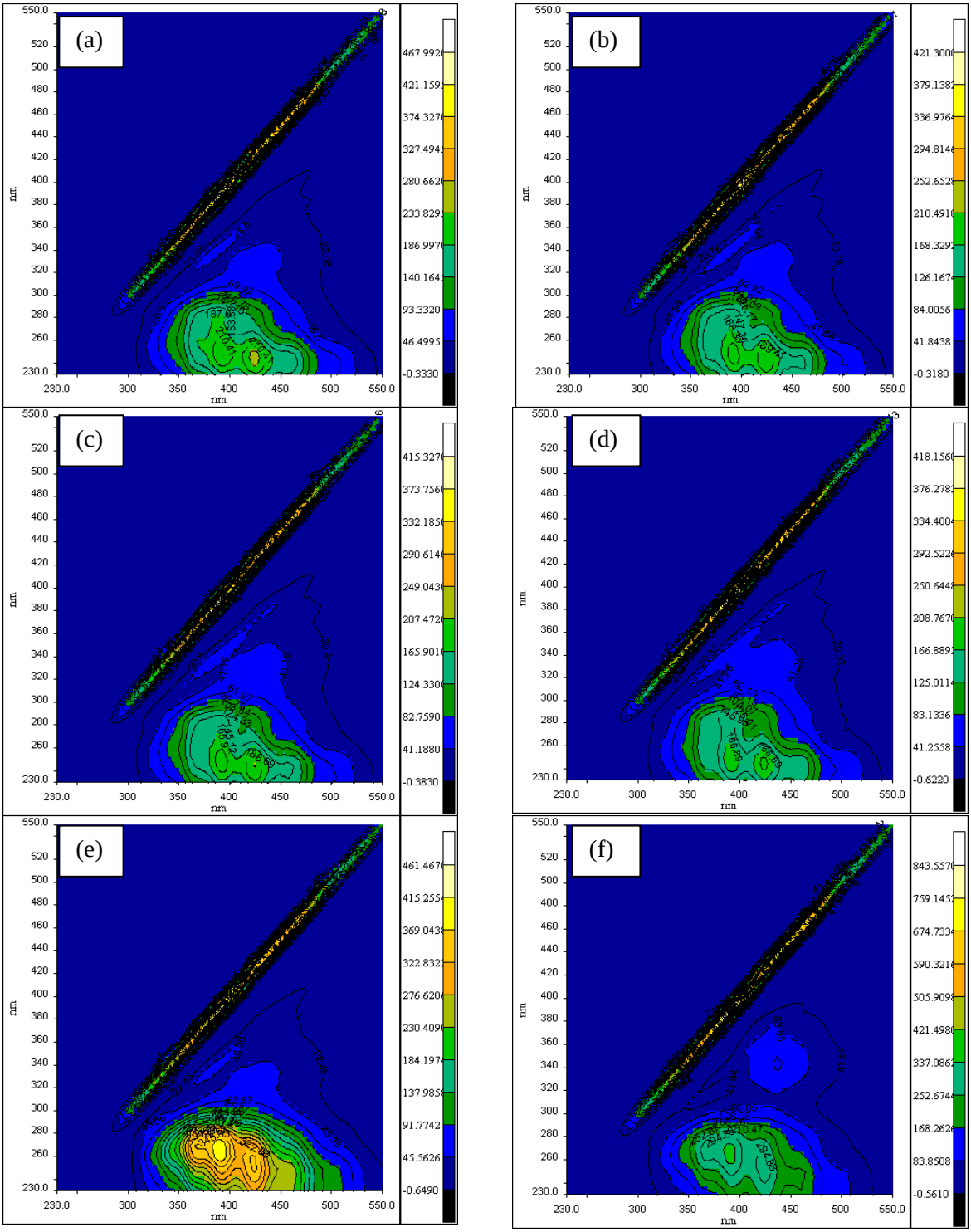

Figure 5.9 EEM spectra profile of permeates, mixed liquor supernatant and EPS on Day 14. a), b), c), d) Permeate from M80, M100, M200 and M300; e) SMP; f) EPS.

5.2.3 Liquid Chromatography –Organic Carbon Detector (LC-OCD)

In order to look into the detailed size distribution and organic characteristics of the DOM present in permeates and mixed liquor supernatant, LC-OCD measurement was conducted at each sampling point. Again, the results of the DOM LC-OCD profile were selected and the detailed results are summarized in Table 5.3 (1 h operation) and Table 5.4 (14 d operation). From the LC-OCD chromatography, the typical components of SCMBR supernatant were: 1) biopolymers (i.e., macromolecular proteins and polysaccharides with high molecular weight (HMW); $t_{elution}$=25-35 min); 2) Smaller size proteins and humic substances with low molecular weight (LMW) ($t_{elution}$=45-55 min); 3) LMW acids and neutrals ($t_{elution}$>55 min).

As shown in Table 5.4 after 1 h operation, most of the biopolymers could be removed by the ceramic membranes. However, the rejection rate differed from each membrane with M80 having the highest rejection rate of over 90%, while only 60% biopolymer was rejected by M300. The differences of rejection rate between M100 and M200 were not obvious after 1 h operation. Compared to the biopolymer rejection, the rejection rates for humics were quite low for all membranes, with M80 having 28.2% removal and about 16% removal for the other three membranes. These observations suggested that ceramic membranes ranging from pore size of 80-300 nm were capable of removing most of the biopolymers and partly removed some LMW substances like humics. It also suggested that biopolymers were the major foulants in MBR system, and LMW substances contributed less in membrane fouling. This conclusion is supported by various studies. Lyko *et al*. (2007) found that significant macromolecular component retention occurred in the full scale MBR system. Zhang *et al*., (2009) also reported that LC-OCD chromatography of the influent and effluent

differed significantly in terms of biopolymer fraction using a UF membrane to treat wastewater. In addition, results obtained indicated that in the early stage of the SCMBR operation, membrane pore size affected biopolymer rejection significantly. According to the fouling analysis, more biopolymer retention by M80 should induce a faster membrane fouling. However, M80 had overall lower fouling rate compared to the other three membranes. The finding in this study seemed contradictory to those published observations (Al-Habouni *et al*., 2008; Zheng *et al*., 2009; Meng *et al*., 2009). However, when looking into the early stage of the TMP profile shown in Fig. 5.2, it could be found that the TMP increase was in accordance with the biopolymer rejection observed in the early stage of the process. In order to demonstrate the fouling development and to further explain the lower overall fouling rate by M80, all permeates and the supernatant samples were collected at each sampling point during the process and more discussions regarding the biopolymers on the membrane surface will be presented in Section 5.3.2.

Table 5.4 summarizes the components of the supernatant permeates on Day 14 of the operation. From the table, it is noted that no significant difference of the biopolymer rejection is observed after 14 d operation. This finding, again, might be attributed to the formation of biocake/biofilm on the membrane surface during the operation, and the results were in good agreement with EEM and HPLC results. The difference of humic substances rejection rates among the four different pore-sized membranes also became negligible. These observations indicated that the formation of biofilm contributed to the increase of organic rejection rate and biopolymers were the main foulants.

Table 5.3 LC-OCD results of membrane permeates and mixed liquor supernatant at 1 h.

								approximate molecular weights (g/mol):						
				>>20.000				*~1000*				*300-500*	*<350*	*<350*
	DOC	HOC	CDOC	BIO-polymers	DON	N/C	% Proteins	Humic Subst. (HS)	DON	N/C	Mol-Weight	Building	LMW	LMW
	Dissolved	Hydrophobic	Hydrophilic		*(Norg)*		in BIOpol.*		*(Norg)*		*(Mn)*	Blocks	Neutrals	Acids
	ppb-C	*ppb-C*	*ppb-C*	*ppb-C*	*ppb-N*	*µg/µg*	*% BIOpol.*	*ppb-C*	*ppb-N*	*µg/µg*	*g/mol*	*ppb-C*	*ppb-C*	*ppb-C*
M80	15217 (100)	4026 (26.5)	11191 (73.5)	142 (0.9)	21	0.15	45	4362 (28.7)	194	0.04	490	2482 (16.3)	4204 (27.6)	1
M100	15217 (100)	3031 (19.9)	12186 (80.1)	1035 (6.8)	142	0.14	41	5053 (33.2)	232	0.05	500	2527 (16.6)	3571 (23.5)	n.q.
M200	15217 (100)	3393 (22.3)	11824 (77.7)	924 (6.1)	100	0.11	32	5057 (33.4)	260	0.05	503	2544 (16.7)	3282 (21.6)	n.q.
M300	15217 (100)	2828 (18.6)	12389 (81.4)	1365 (9.0)	191	0.14	42	5096 (33.5)	237	0.05	508	2541 (16.7)	3386 (22.2)	1
SMP	22664 (100)	5503 (24.3)	17162 (75.7)	5052 (22.3)	649	0.13	39	6082 (26.8)	281	0.05	546	2293 (10.1)	3733 (16.5)	2

Table 5.4 LC-OCD results of membrane permeates and mixed liquor supernatant at 14 d.

				approximate molecular weights (g/mol):										
				>>20.000				*~1000*				*300-500*	*<350*	*<350*
	DOC			BIO-polymers				Humic Subst. (HS)				Building	LMW	LMW
		HOC	CDOC		DON	N/C	% Proteins		DON	N/C	Mol-Weight	Blocks	Neutrals	Acids
	Dissolved	Hydrophobic	Hydrophilic		(Norg)		in BIOpol.*		(Norg)		(Mn)			
	ppb-C	*ppb-C*	*ppb-C*	*ppb-C*	*ppb-N*	*µg/µg*	*% BIOpol.*	*ppb-C*	*ppb-N*	*µg/µg*	*g/mol*	*ppb-C*	*ppb-C*	*ppb-C*
M80	21658 (100)	10396 (48.0)	11262 (52.0)	614 (2.8)	n.q.	-	-	4274 (19.7)	156	0.04	464	2160 (10.0)	4215 (19.5)	1
M100	21658 (100)	8281(38.2)	13377 (61.8)	906 (4.2)	96	0.11	32	4482(20.7)	253	0.06	468	2233 (10.3)	5766 (26.6)	n.q.
M200	21658 (100)	9929 (45.8)	11729 (54.2)	813(3.8)	48	0.06	18	4558 (21.0)	252	0.06	468	2177 (10.1)	4181 (19.3)	n.q.
M300	18063 (100)	5722 (31.7)	12340 (68.3)	826 (4.6)	52	0.06	19	4650 (25.7)	288	0.06	463	2261 (12.5)	4606 (25.5)	1
SMP	18063 (100)	5003 (27.7)	13060 (72.3)	2763 (15.3)	286	0.10	31	4979 (27.6)	282	0.06	494	2171 (12.0)	3147 (17.4)	2

5.3 Foulants on Membrane Surface

5.3.1 Biofilm Development

It is noted that the membrane surface properties would affect the biofilm/biocake development on the membrane surface, leading to different fouling propensities of different membranes. In order to investigate the effects of membrane pore size and roughness on the fouling in terms of the foulant layer development, the four membranes were taken out for scanning at each sampling point. The obtained images were analyzed by ISA-2 software ((Beyenal *et al*., 2004)) to determine the coverage ratio of the biofilm/biocake and the results are shown in Fig. 5.10.

It was observed that all the membrane fouled (i.e., reached TMP at 30kPa) when biocake/biofilm coverage ratio reached around 0.60. The biofilm/biocake development initiated once the operation started, especially for M80 and M100. This observation indicated that, M80 having the smallest pore size was able to reject more organics at early phase. However, taking the 51 d operation as a whole, M80 was the last one to encounter serious fouling. The results of the biofilm/biocake coverage ratio (BCR) were in accordance with the TMP profiles discussed in Section 5.1.1. M80 had the highest biofilm/biocake coverage ratio increase rate within the 24 hours; consequently, TMP increase rate was the fastest within the first 24 h, too. After 7 d operation, a significant BCR increase could be observed in M100, M200 and M300. This observation, again, was in agreement with the significant TMP increase observed from Days 10 to 20 presented in Section 5.1.1. These findings suggested that within the first 24 h, the membrane properties did not affect the initiation of biofilm/biocake significantly. It was the physical rejection by the membrane pore size that triggered the biofilm initiation. The smaller the pore size, the easier the biofilm initiation. This

observation was in agreement with He *et al*., (2005) who reported that a significant flux decreased was observed in the system with small membrane pore size in the initial stage of operation. After 1 week of operation, the membrane surface roughness was the dominant factor that affected the BCR increase rate. The rougher the membrane surface, the easier the biocake formation. Based on this 51 d investigation, BCR was a good indicator for membrane fouling in SCMBR. The increase trend of the BCR corresponded well with the TMP increment for all membranes. Overall, the BCR increase rate was in good accordance to the membrane surface roughness, which was M80<M200<M100<M300. M80, with the smallest pore size and smoothest membrane surface, was the one with the lowest BCR after 7 d of operation.

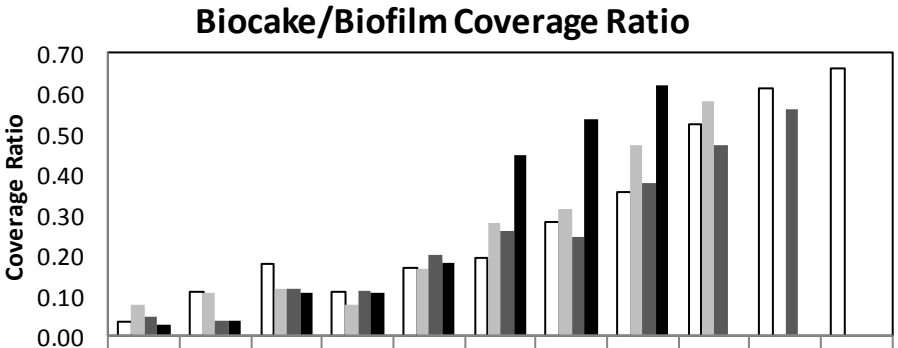

	0.04	0.25	1	3	7	14	21	28	35	42	51
M80	0.03	0.11	0.18	0.11	0.17	0.19	0.28	0.36	0.52	0.61	0.66
M100	0.07	0.11	0.12	0.08	0.16	0.28	0.31	0.47	0.58		
M200	0.05	0.04	0.12	0.11	0.20	0.26	0.24	0.38	0.47	0.56	
M300	0.03	0.04	0.11	0.11	0.18	0.45	0.54	0.62			

Figure 5.10 Biocake/Biofilm coverage ratio development in the SCMBR (X axis: Duration of study/Day)

In analysis for all the scanned membranes, some minor fluctuations of the BCR could be observed, and the TMPs did not increase consistently, especially for R80 and R200. The theory of membrane fouling mechanisms under constant permeate flux operation established by Zhang *et al*. (2006) might, to some extent, be able to explain these phenomena. Based on this theory, fouling might be attributed to the reversible

foulants formed on the membrane surface in fouling Stage 1, which was called conditioning fouling (Section 2.3). In this stage, strong interactions between the membrane surface and the EPS present in the mixed liquor are probably responsible for the initial stage of fouling during constant flux operation. These foulants might have contributed to the initial membrane pore clogging; and some foulants might be sheared off by the aeration during this period. However, this process did not significantly affect the absolute TMP value. Consequently, although the TMP increase was not that significant in some sampling points, the BCR decreases could be observed.

5.3.2 Cake Layer Analysis

To investigate the actual membrane foulants, the cake layer on each membrane surface was collected and the organic contents of the layer were analyzed by traditional methods such as TOC, carbohydrate and protein analysis, and non-traditional method such as LC-OCD chromatography was also applied. The results are summarized in Table 5.5.

Table 5.5 Organic components on the membrane surface.

Pore size (nm)	TOC (mg/L)[a]	Carbohydrate (mg/gVSS)		Protein (mg/gVSS)		Biopolymer (mg/L)[a]
		Non-filtered	Filtered	Non-filtered	Filtered	
80	13.91	66.65	27.72	69.52	18.54	9.09
100	39.04	77.86	42.86	81.22	35.26	12.70
200	13.57	56.02	25.12	64.10	18.36	8.33
300	36.16	170.82	58.34	103.41	49.74	12.09

Note: Non filtered means the total organic concentration in cake layer.
Filtered means the organic concentration after filtering by 0.45µm membrane.
[a]analysis based on solution obtained after foulants dissolved in 500ml ultrapure water.

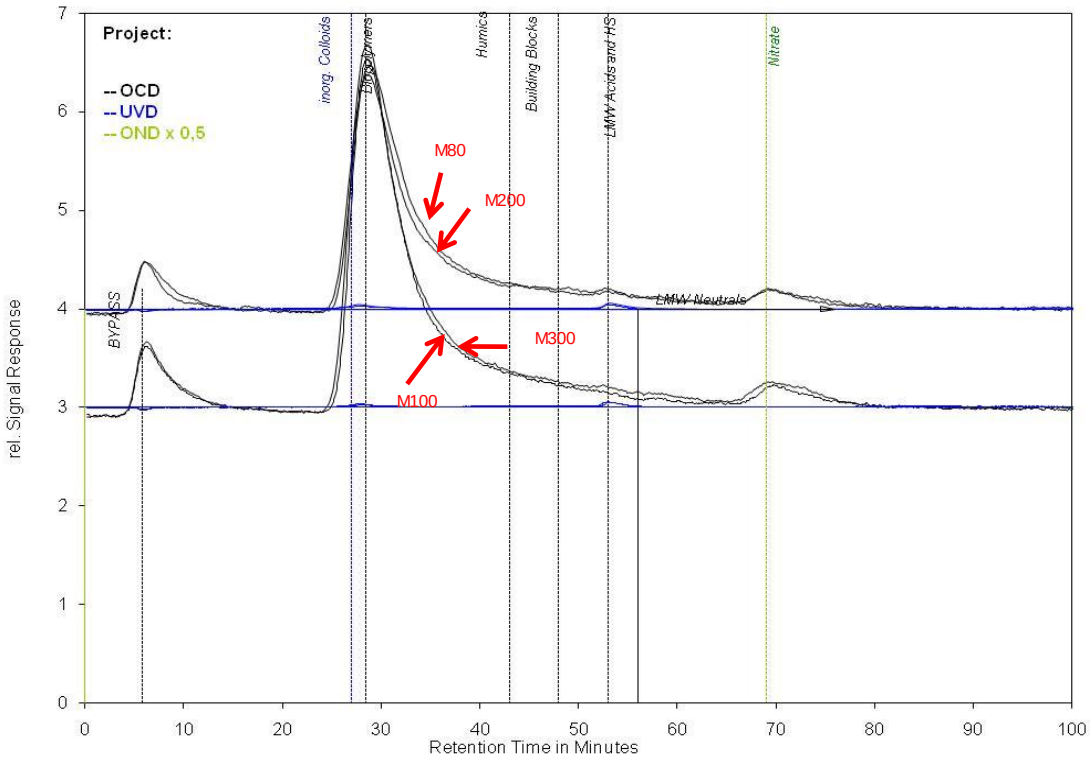

Figure 5.11 LC-OCD chromatography of cake layer compounds from four membranes.

Generally, the components of cake layer formed on M80 and M200 had lower TOC than those of M100 and M300, implying that more organic contents were retained on the membrane surface of M100 and M300. The origin of the organic compounds on the membrane surface was partly due to the accumulation of the SMP and EPS from the mixed liquor, and partly due to the microbial activities on the membrane surface (i.e. biomass metabolism attributed by the environmental stress). The more organic contents on M100 and M300 could be accounted for the rougher membrane surface (discussed in section 4.2.7) which was easier to induce biofilm formation. The biofilm/biocake formation not only caused more organic attachment onto membrane surface, it also provided a good environment for microbe growth. When looking into the detailed composition of the organic compounds, it could be seen that carbohydrate and protein were the major foulants. The concentration of carbohydrate present in the non-filtered sample and filtered from M300 was almost three times higher and two

times higher than that of M80 and M200, respectively. This finding suggested that macromolecular compounds contributed more to membrane fouling than those small molecular compounds. The same trends were also observed in the protein concentration. These results were in accordance with observations reported in published literatures (Meng *et al*., 2007; Lyko *et al*., 2007; Zheng *et al*., 2009; Zheng *et al*., 2010) that the major foulants in membrane filtration were protein and carbohydrate with macromolecular compounds of greater importance. The LC-OCD chromatography (Fig. 5.11) also confirmed the conclusion that biopolymer was the major foulants on the membrane surface. The role of the LMW compounds was of little importance as the fraction of humics and other LMW compounds were undetectable. These results also suggested that the rougher membrane surface was able to induce much more severe membrane fouling due to the tendency of more organic attachment onto the rougher membrane surface, contributing to biofilm/biocake formation and eventually leading to faster membrane fouling.

5.4 Microbial Communities

5.4.1 Microbial Communities in the Biocake/Biofilm throughout the Operation

Biomass from the fouling layer was analyzed by means of PCR followed by t-RFLP for their microbial ecology differences. In this study, 16S rRNA gene was used to target the microbial communities in each fouling layer on the basis of the DNA templates extracted from the fouling layers. In order to investigate the difference of bacterial communities at different operation time, the DNA templates of the fouling layer were extracted in sequence at the operation time of 1 h, 6 h, 1 d, 3 d, 7 d, 14 d, 21 d, 28 d, 35 d and 42 d. The extraction of DNA template was ceased once the TMP of each membrane reached 30 kPa. The t-RFLP fingerprints of fouling layer after

operation time of 1 d, 14 d and 35 d (28 d for M300) were showed in Figs. 5.12, 5.13 and 5.14, respectively. Results showed that after 1 d operation, distinct difference could be clearly seen for the t-RFLP fingerprints on ceramic membrane with different pore sizes, especially for M80 and M200. Two dominant T-RF fragments at the size of around 60 bp and 280 bp could be observed in fouling layer on M80 surface. One dominant T-RF fragment at the size of around 120 bp was observed in fouling layer on M200 surface. Compared to M80 and M200, no significant dominant T-RF fragment was seen in term of the t-RFLP fingerprints. Four different pore-sized ceramic membranes were put in the same SCMBR, with the same mixed liquor, and were operated under the same operating flux. The shift in the microbial communities after 1 d of operation could be attributed to the difference membrane pore size and the surface properties, as the membrane pore size was the only varying factor. This observation indicated that one or two bacterial species preferentially adhered onto membrane surface with those smooth surfaces. As discussed in the previous chapter, M80 and M200 had relatively smoother membrane surface than that of the other two. However, compared to M80 which has the smoothest membrane surface, M200 had a more significant T-RF fragment dominance. The formation of the fouling layer and the microbial communities of the fouling layer was a very complex process which could be affected by various factors, including the operating conditions (Falk *et al*., 2009) and the hydrodynamic conditions (Stoodley *et al*., 2002). Although the four membranes were operated under the same operating flux, the initial membrane permeability was different (see Fig. 5.15). The flux applied in this study performed as different stress to different pore-sized initially until the formation of an obvious fouling layer. Under the higher suction pressure, most of the bacterial were forcibly

adhere onto the membrane surface. This might explained the different T-RF fingerprints of M80 and M200.

The t-RFLP fingerprints of four fouling layers formed after 14 d of operation (Fig. 5.13) showed that after two weeks operation the bacterial species dominance in all fouling layers diminished with similar relative abundances of all bacterial species. It could be seen that the t-RFLP fingerprints distributed similarly for all fouling layers. This observation indicated that after a period of operation, the membrane pore size did not significantly affect the formation of the fouling layer, which reinforced the conclusions drawn in the previous section. The differences of the treatment behaviors of ceramic membranes with difference pore sizes became insignificant after 14 d operation.

Figure 5.14 showed the t-RFLP fingerprints of fouling layer in M80, M100 and M200 on Day 35 and in M300 on Day 28. On Day 28, the TMP of M300 reached 30 kPa and fouling layer was collected for the DNA extraction. After that a new piece of membrane with the same pore size were mounted in the SCMBR to maintain the mixed liquor. The same thing happened on Day 35 for M100, and same action was taken to maintain the SCMBR. It could be clearly seen from the figure that one dominant species with small T-RF fingerprints with the size of 80-100 bp was found on M100 and M300 membrane surface. These observations indicated that over time the microbial ecology in fouling layer changed, with very significant dominance by one or two species, especially when the TMP of that membrane approached 30kPa. This process suggested that after a certain operation period, some bacterial species preferentially adhered onto the membrane surface, becoming competitors to the other bacteria species, although this phenomenon was not found initially after 1 d operation.

The bacterial community diversities of each fouling layer were analyzed using Shannon Weaver diversity index H, computed from data generated by t-RFLP fingerprints analyses. Table 5.6 summarized the microbial community diversity index (H), richness (S) and evenness (E) of each fouling layer sample. It can be found from the table that distinct difference was found for M200 in terms of diversity, richness and evenness of fouling layer after 1 d operation. E value shows the distribution of the species detected, the results proved that dominance of certain bacteria were found in the fouling layer on M200. All three values of diversity index (H), richness (S) and evenness (E) did not showed significant different after 14 d operation, and such results were also evident from the t-RFLP fingerprints shown in Fig. 5.13. The results deduced from H, E and S values from fouling layer after 35 d (28 d for M300) operation further supported the findings from the t-RFLP fingerprints that when the membrane approached fouling, dominance of certain bacteria with relative abundance could be found.

Table 5.6 Shannon Weaver diversity index (H), richness (S) and evenness (E) values of fouling layer, based on the *Msp* I digestion of 16S rRNA genes.

	24 h				**14 d**				**35 d (28 d for M300)**			
	M80	**M100**	**M200**	**M300**	**M80**	**M100**	**M200**	**M300**	**M80**	**M100**	**M200**	**M300**
H	1.23	1.17	1.05	1.31	1.26	1.26	1.31	1.30	1.72	1.13	1.32	1.15
S	20	19	18	21	21	20	22	22	26	19	21	17
E	0.95	0.96	0.84	0.99	0.95	0.97	0.98	0.98	1.44	0.88	1.00	0.89

Results obtained from this study showed that the fouling layer development on surface of membrane with different pore size membranes were significantly different initially; however, after a period of operation this difference became insignificant until the membrane was approaching fouling. In the initial stage, the membrane pore size, the surface roughness, and suction pressure jointly affected the fouling layer development. Results showed that the smoother membrane surface, the higher

possibility to induce microbial ecology dominance. A higher suction pressure to the membrane would forcibly cause most of the bacterial species to adhere onto the membrane surface. Both t-RFLP fingerprints and the Shannon Weaver diversity index (H), richness (S) and evenness (E) values of the fouling layer over time supported this conclusion.

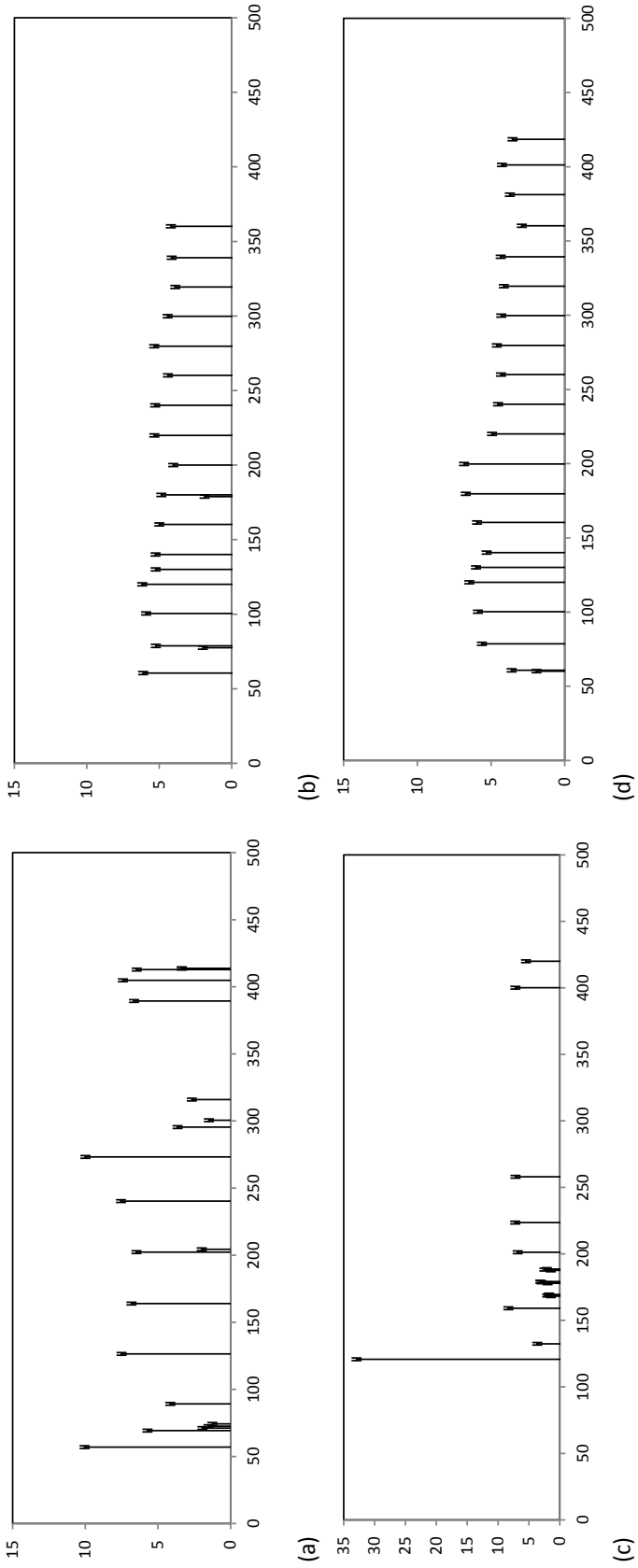

Figure 5.12 Comparison of the relative abundances of T-RFs in the fouling layer of difference pore-sized ceramic membranes (a) M80; (b) M100; (c) M200; and (d) M300 in SCMBR at operation time of 24 h, based on *MspI* digestion of 16S rRNA genes.

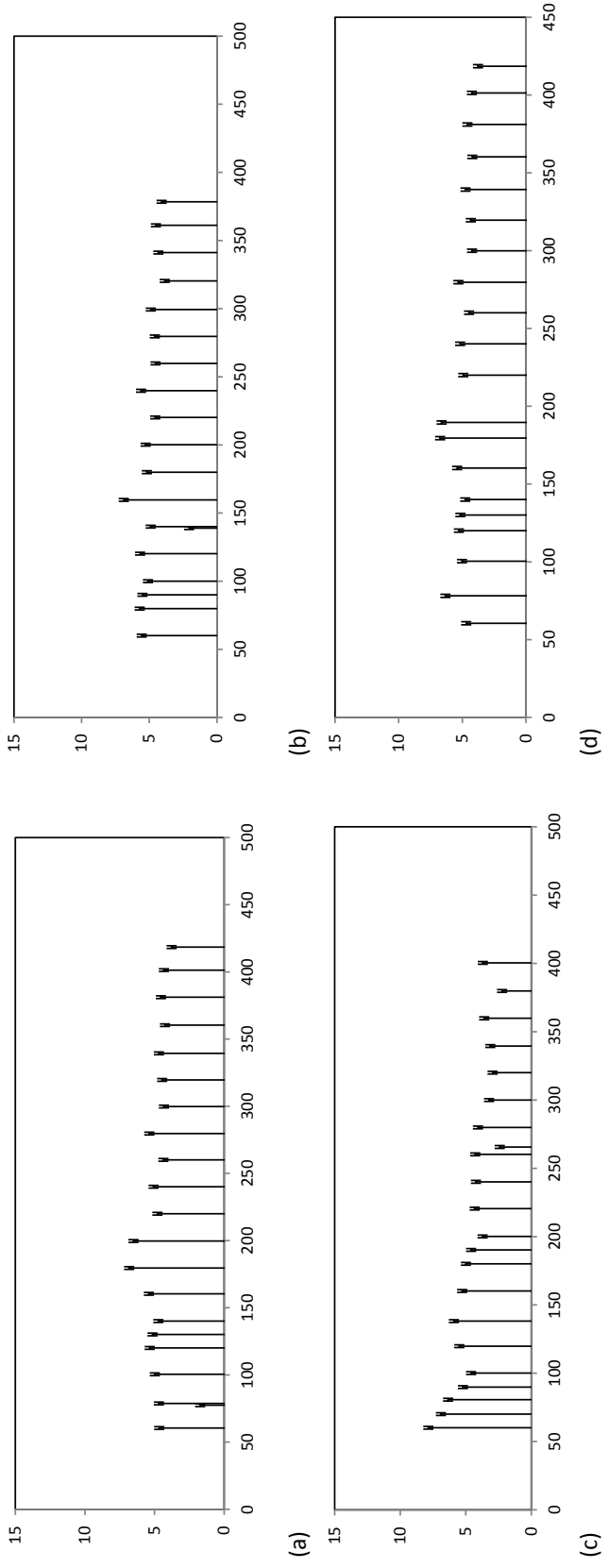

Figure 5.13 Comparison of the relative abundances of T-RFs in the fouling layer of difference pore-sized ceramic membranes (a) M80; (b) M100; (c) M200; and (d) M300 in SCMBR at operation time of 14 d, , based on M*spI* digestion of 16S rRNA genes.

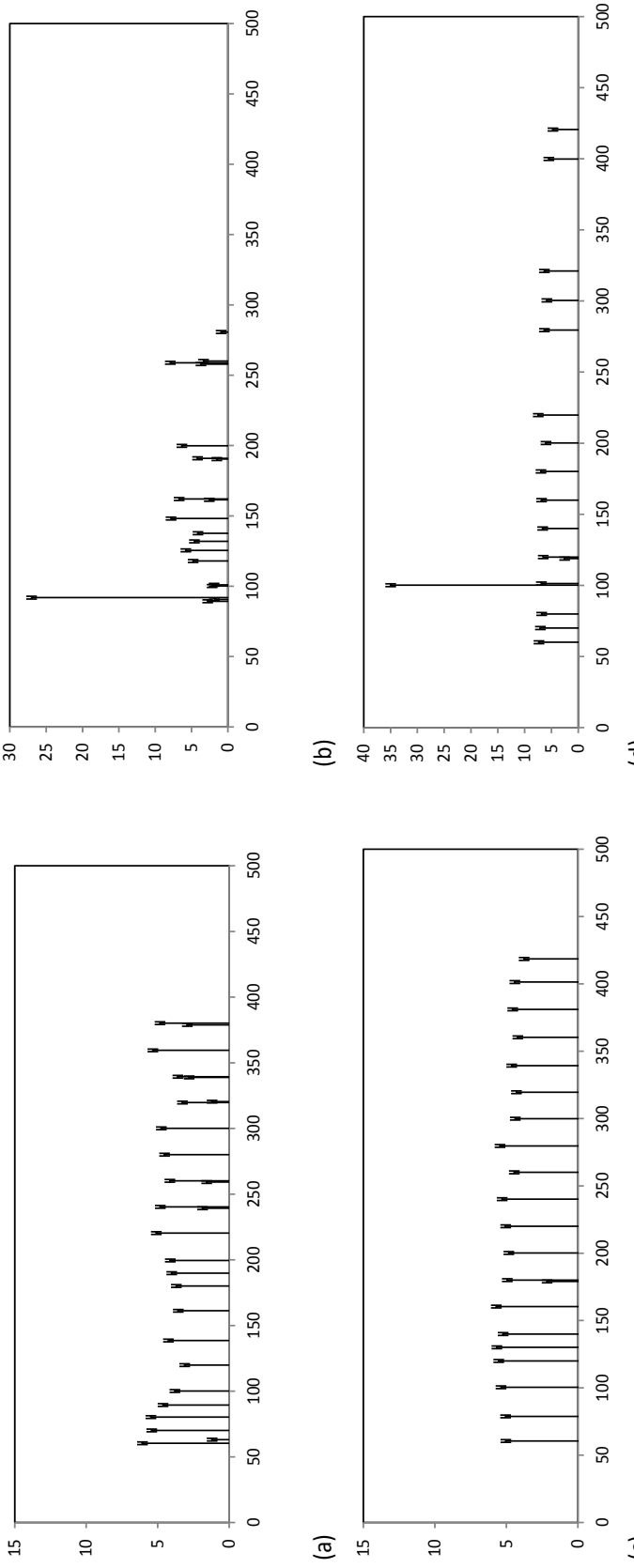

Figure 5.14 Comparison of the relative abundances of T-RFs in the fouling layer of difference pore-sized ceramic membranes (a) M80; (b) M100; (c) M200; and (d) M300 in SCMBR at operation time of 35 d (28 d for M300) , based on *Msp*I digestion of 16S rRNA genes.

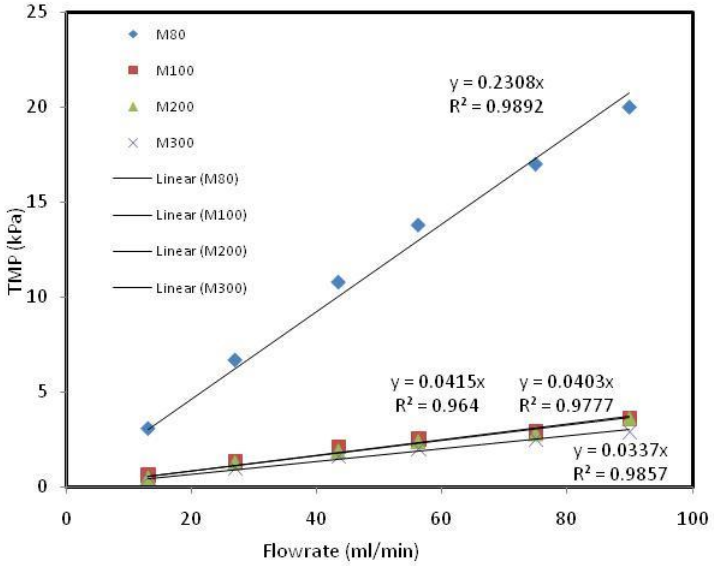

Figure 5.15 Clean membrane TMP test of four different pore-sized ceramic membranes.

5.5 Summary of Phase 2 Research and Membrane Fouling Mechanism Elucidation

In this phase, four ceramic membranes with pore sizes ranging from 80 to 300 nm were mounted in one SCMBR in order to investigate the effect of membrane pore size on organic rejection, biofilm/biocake structure as well as the microbial communities present in the biofilm/biocake. Results showed that the initial organic rejection was in good accordance with the membrane pore size, where M80 has the highest organic rejection after 1 h operation (supported by EEM, HPLC and LC-OCD tests). The formation of biofim/biocake layer was clearly observed after 7 d operation, from which the dramatic increase of BCR was observed for M300 (membrane with roughest surface and biggest pore size). This formation of biofilm/biocake layer also masked the effect membrane pore size on organic rejection, and contributed to the increased organic rejection for M300 after 14 d operation. The investigation of the bioflm/biocake compositions demonstrated that polysaccharides and proteins were the major foulants in SCMBR, while detection of the humics in the biofilm/biocake was negligible.

t-RFLP results obtained from this study showed that in the initial stage, membrane pore size, surface roughness, and suction pressure jointly affected the microbial communities. The smoother the membrane surface, the higher the possibility to induce microbial ecology dominance. A higher suction pressure to the membrane would forcibly cause most of the bacterial species to adhere onto the membrane surface. Both t-RFLP fingerprints and the Shannon Weaver diversity index (H), richness (S) and evenness (E) values of the fouling layer observed over time supported this conclusion.

Chapter 6. Phase 3 - Fouling minimization

6.1 Addition of Biofilm Carriers

In Part I of this phase, a comparative study was conducted in two SCMBRs – one with and the other without suspended biofilm carriers under the same operating conditions. Characteristics of the cake layer were investigated once when either SCMBR was fouled. The major components of biomass in cake layer were estimated by FTIR. The soluble organic contents on the membrane surface were characterized by LC-OCD and EEM fluorescence spectra. The inorganic contents in the cake layer were also evaluated to estimate the role of inorganics on membrane fouling processes. Based on Part I study, different dosage of suspended carriers was conducted in different SCMBRs to evaluate the dosage of biofilm carriers on fouling in Part II.

6.1.1 Membrane Fouling Behavior

In both Part I and Part II, the SCMBR systems were operated at a constant flux with TMP increment profile as a fouling indicator. Fig. 6.1a depicts the time course of TMP increase until the TMP of R2 (without carriers) reached 30 kPa. It could be seen that the TMP increment profile were very similar within the first 15 d with negligible TMP increase. However, from Day 15 onwards, a significant TMP increase was

observed in R2, while the TMP increase rate of R1 (with carriers) was always less than that of R2. This observation indicated that the carriers were capable of delaying the SCMBR fouling; however, it is still unclear how these carriers affect membrane fouling. To elucidate the affecting mechanisms, the membrane was taken out on Day 58 and scanned by a high resolution scanner. Fig. 6.2 shows the scanned membrane images of R1 (Fig. 6.2a) and R2 (Fig. 6.2b). It could be seen that obvious cake layer was formed on membrane surface of R2. This observation indicated that addition of carriers affects positively by shearing off the cake during the operation, and this hypothesis was supported by some previous studies (Yang *et al*., 2006; Huang *et al*., 2008). In the early stage of operation (before Day 15), the carriers did not help in slowing down the fouling rate because the cake formation in the initial stage could be negligible; therefore, the effect of scouring was not observed. Once the cake started to form the scouring effect by carrier was very significant, and eventually lowered the overall fouling rate observed in R1.

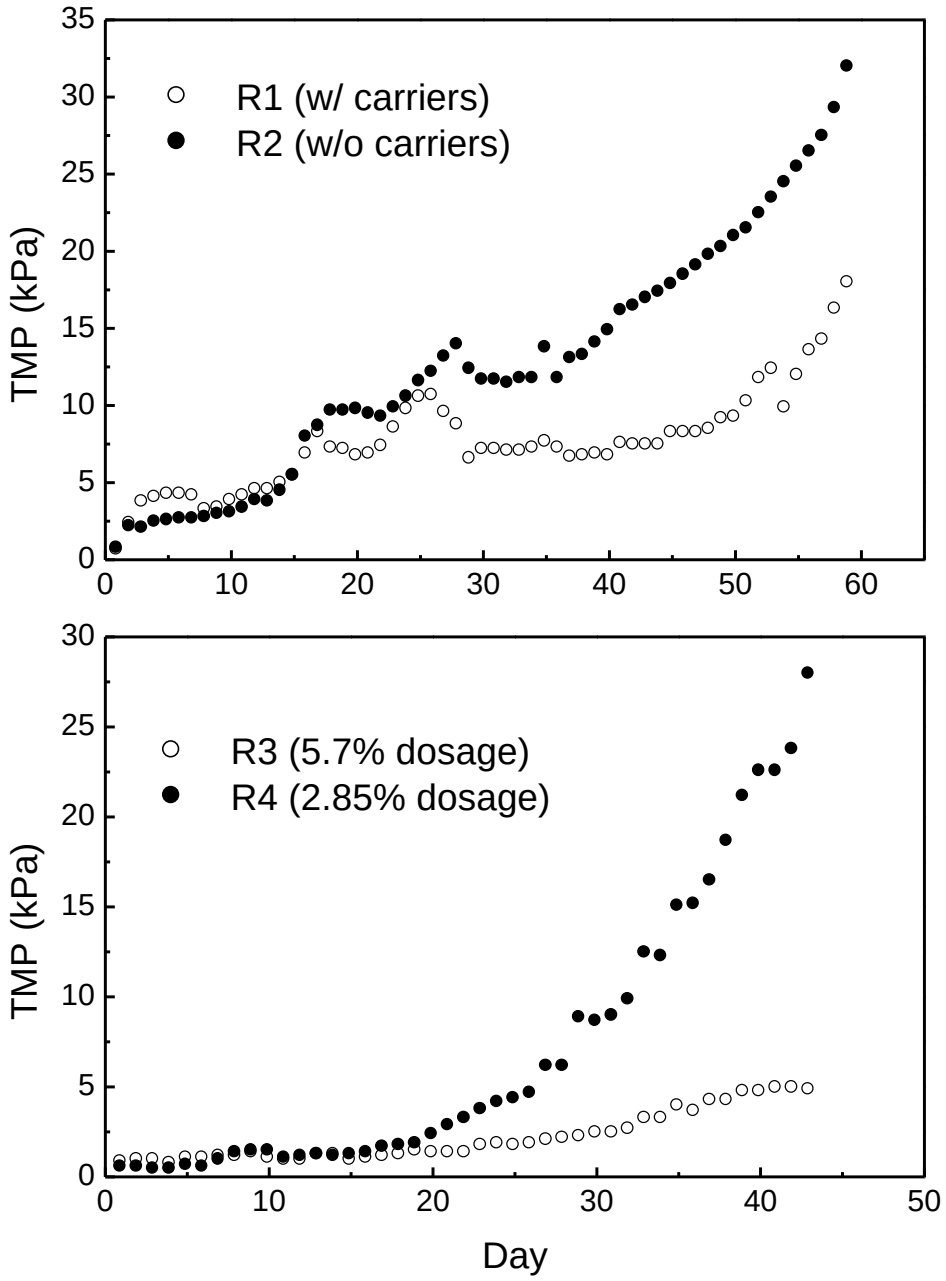

Figure 6.1 (a) Membrane fouling behavior in Part I; (b) Membrane fouling behavior in Part II.

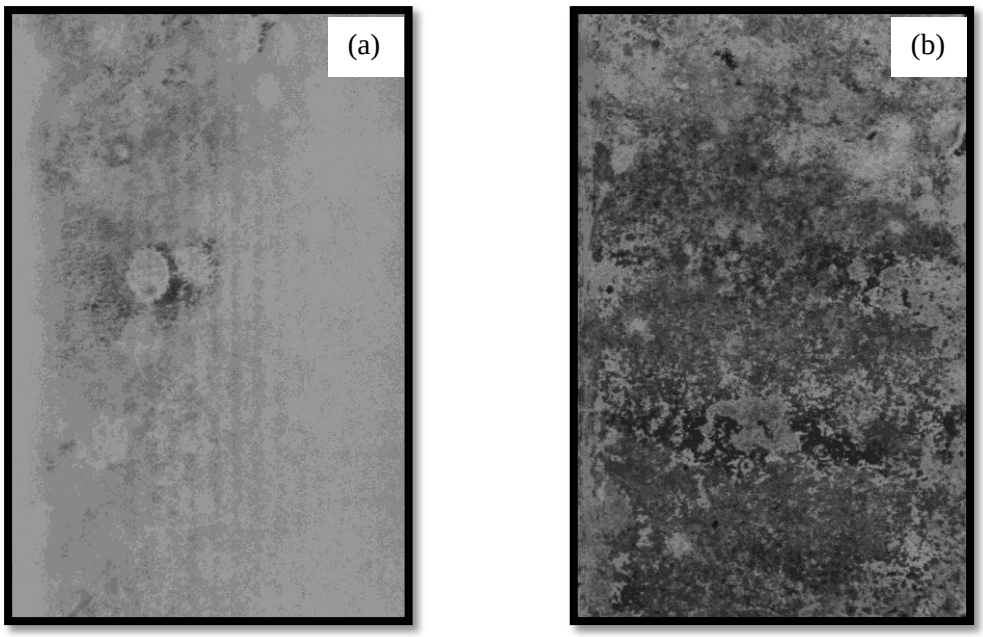

Figure 6.2 Scanned membrane images on Day 58 in Part 1: (a) R1 (b) R2.

Membrane resistance distribution was measured through specific flux with ultrapure water conducted at the end of Part I (see Table 6.1). It could be seen that the reactor with carriers (R2) had a higher total resistance, which was almost 2.5 times more than that of R1 after a period of 58-day operation. Furthermore, the cake layer fouling was even more significant. Throughout this 58-d operation, the cake layer resistance was five times higher than that of R2, indicating that the addition of carriers in the SCMBR decreased the cake resistance by 72.7%. These observations indicated that the biofilm carriers were able to mitigate fouling by controlling the cake formation. The dominant fouling factor in R2 was cake layer fouling, accounting for 82.59%; while both cake layer (56.72%) and pore clogging (41.10%) played important role in fouling in R1 after the same period of operation. This might be due to the cake layer formation taking place from Day 15 onwards in R2, leading to faster fouling. Under the drag force provided by the permeate suction and the scouring provided by aeration and carriers, the formation of a cake layer is a dynamic process. The addition of carriers in SCMBR could reduce the cake formation on membrane surface. Hence, the

biofilm carrier addition is proposed to be an effective approach to mitigate fouling by scouring effect. On the other hand, the porous carriers buoying in the reactor adsorbed smaller flocs, colloidal, solutes and suspended solids, which were reported to be main contributors to membrane fouling (Defrance *et al*., 2000; Bouhabila *et al*., 2001). The co-effect of the cake layer scouring and biomass adsorption contributed to a better performance in terms of TMP profile in R1 (with carriers).

Table 6.1 Analysis results of fouling resistance distribution (resistance/$10^{11}m^{-1}$ (percentage/ %)).

	R_m	R_p	R_c	R_t
R1	1.28 (1.81)[a]	29.30 (41.47)	40.10 (56.72)	70.68 (100)
R2	1.28 (0.72)	29.70 (82.59)	147.00 (16.69)	177.98 (100)

R_m—membrane resistance; R_p — pore-clogging resistance; R_c — cake resistance; R_t — total resistance.
[a] percentage of each resistance contributor (unit:%)

Table 6.2 Analysis results of the components of fouling cake on membrane surface.

		Foulants (%)				
		biomass (g/m^2)	**TOC_c(g/m^2)**	**TOC_s(g/m^2)**	**Inorganic matter(g/m^2)**	**Total cake (g/m^2)**
Part I	**R1**	6.94 (81.22)	0.33 (3.82)	0.14 (1.67)	1.14 (13.29)	8.54
	R2	21.50 (81.19)	0.75 (5.70)	0.23 (1.76)	1.50 (11.36)	13.24
Part II	**R3**	9.38 (72.70)	0.13 (1.03)	0.09 (0.69)	3.30 (25.59)	12.90
	R4	15.00 (73.24)	0.67 (3.25)	0.24 (1.17)	4.58 (22.34)	20.48

Note: value (percentage)

Since the biofilm/cake formation plays an important role in SCMBR, it is necessary to characterize the biofilm/cake layer. Foulants on the membrane surface were extracted and the compositions of cake layer, including biomass, colloidal particles, solutes and inorganic matters, were analyzed. From Table 6.2 (Part I) it could be seen that SCMBR without carriers (R2) not only had more total cake layer (13.24 g/m^2) than R1 (8.54 g/m^2), but also had more biomass, colloidal, solutes and inorganic matters. The biomass was the main components, accounting 81.22% for R1 and 81.19% for R2. Although the concentrations of colloidal and solutes were low, they had strong impacts on membrane fouling as their deposition and precipitation on membrane

surface would cause severe membrane pore clogging during the course of operation. The second contributor to biofim/cake layer was inorganic matter in both reactors. This finding was supported by Meng *et al*. (2007) who demonstrated that the main components of cake layer were biomass (62.4%) and inorganic matters (23.08%). To investigate the inorganic contents of biofilm/cake layer, the ion chromatography was conducted to detect the ion concentrations (PO_4^{3-} , $SO4^{2-}$, NH_4^{+}, Mg^{2+} and Ca^{2+}) (see Table 6.3). Although compared to biomass, the relative fractions of these ions were small; these ions played important roles in membrane fouling. Choo and Lee (1996) investigated the membrane-fouling mechanisms in the membrane-coupled anaerobic bioreactor for alcohol-distillery wastewater treatment and found that the major composition of inorganic foulant identified was $MgNH_4PO_4 \bullet 6H_2O$ (struvite). Kang *et al*. (2001) have investigated the filtration characteristics of organic and inorganic membranes in a membrane-coupled anaerobic bioreactor. In their study, it was found that a thick cake layer composed of biomass and struvite formed on the membrane surface, thus causing a major hydraulic resistance.

Table 6.3 Inorganic contents in cake layer (g/m^2).

	PO_4^{3-}	**SO_4^{2-}**	**NH_4^{+}**	**Mg^{2+}**	**Ca^{2+}**
R1	0.22	0.56	0.06	0.04	0.26
R2	0.45	0.58	0.08	0.17	0.24

In this study, the major inorganic ions were PO_4^{3-} SO_4^{2-} NH_4^{+} Mg^{2+} and Ca^{2+} as listed in Table 6.3. In addition, R2 has relatively higher concentrations of PO_4^{3-}, SO_4^{2-}, NH_4^{+} as well as Mg^{2+}, which led to the faster fouling. These findings indicated that both the higher concentration of biomass and inorganic matters in cake layer in R2 contribute to faster TMP increment due to the interaction of biomass, biopolymers and inorganic matters. The bridging effect between the biopolymers and the inorganic matters contributed to the cake layer tightening. Overall, the foulants, mainly

composed of inorganic matters (probably struvite) and microbial cells played an important role in the formation of strongly attached cake layer, reducing the cake layer porosity, thus enhancing the membrane fouling along the run.

6.1.2 Particle Size Distribution of Biomass Suspensions

Biomass suspension particle size was measured by a laser diffraction particle analyzer (see Fig. 6.3). The results showed differences in the particle size distribution (PSD) of biological flocs in reactor with carriers (R1) and without carriers (R2).

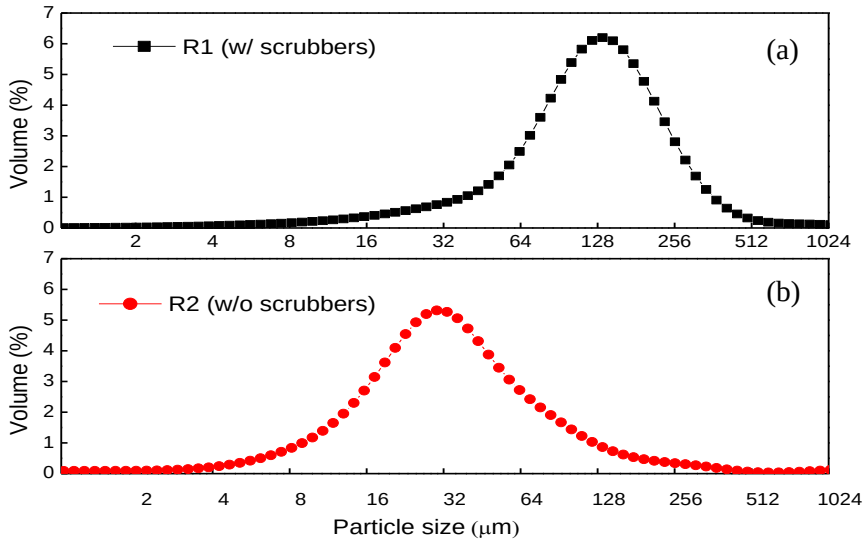

Figure 6.3 Particle size distribution for biomass suspensions: (a) R1; (b) R2.

Statistical results of PSD are summarized in Table 6.4. It could be seen that R1 had a bigger and broader range of biomass particles ranging from 1-400 μm with median biomass particle size of 129 μm. However, the reactor without the carrier (R2) had smaller particles ranging from 1-200 μm with median of biomass particle size of 33 μm. It has been reported that the biomass particles with a size smaller than 50 μm would affect membrane permeation performance significantly (Bai and Leow, 2002). Meng *et al*. (2007) also demonstrated that the biomass particles that had a size smaller than 50 μm could easily deposit on the membrane surface and eventually worsen the

membrane permeability. The observations obtained in this study were in agreement with what have been reported by Bai and Leow (2002) and Meng *et al*. (2007). R2 contained more small biomass particles (<52.6 μm), accounting for 72.51%, and it fouled faster than R1 where only 12.92% biomass particles had a size smaller than 52.6μm. These results indicated that the addition of carriers would cause the biomass flocs to become bigger. However, this finding was different from that observed by Huang *et al*. (2008) who investigated the effect of biofilm carriers on sludge particle size distribution. Huang *et al*. (2008) claimed in their study that the addition of carriers broke up the flocs due to the circulation of biofilm carriers in the reactor. However, the same phenomenon was not observed in this study, since different carriers were applied. In their study, a heavier carrier with density of 978 kg/m^3 and smaller suspended carriers with a diameter of 3 mm was used. Therefore, the suspended carriers were able to circulate easily and the smaller carrier was capable of breaking up biomass flocs. In addition, the biofilm carriers adopted by them were made of modified polypropylene without adsorption capability. In this study, carriers with a density of 573 kg/m^3 and a diameter of 12 mm were used. With this bigger and lighter carriers suspended in the mixed liquor, the movement of carrier was slower and the biomass flocs were not easily broken up. In addition, the hydrophobic characteristic of the carriers adopted in this study allowed small flocs to attach themselves easily on the carriers than to stay freely in the reactor. The addition of the biofilm carriers, on the other hand, would lower the actual aeration intensity, enhancing the flocs aggregation and finally contributing to bigger floc size observed in R1. This trend was in good agreement with Meng *et al*. (2008) who demonstrated that the higher aeration intensity will lead to the breaking up of flocs, resulting in smaller biomass size.

Table 6.4 Statistical results of biomass particle size distributions in R1 and R2

	particle size (μm)		**Particle size distributions (%)**				
	mean	**peak**	**<10.8 μm**	**10.8-52.6 μm**	**52.6-101.1μm**	**101.1-213.2 μm**	**>213.2μm**
R1	129	157	1.96	10.96	27.31	40.16	19.61
R2	33	56	8.41	64.10	18.83	5.48	3.18

6.1.3 EPS Components in Mixed Liquor and Biofilm/Cake Layer

EPS and SMP are considered as the most important factors which induce membrane fouling in MBR (Rosenberger *et al*., 2006; Ng *et al*., 2006). The total concentration of EPS (including the bound EPS and soluble EPS) in the mixed liquor and cake layer of the two SCMBRs were analyzed and the results are summarized in Table 6.5. It could be noted from the table that the concentrations of protein in mixed liquor were similar, while the concentrations of carbohydrate differed with R2 having higher mean concentration (24.5 mg/L) compared to R1 (15.66 mg/L). The different fouling propensities of the two reactors (with or without carriers) were thought to be originated from the different dissolved organic matter characteristics produced by the addition of carriers. Huang *et al*. (2008) studied the effect of suspended carrier addition on membrane fouling and found that EPS decreased but SMP increased with the addition of carriers, resulting faster fouling in the reactor with carriers. However, in this study both EPS and SMP concentration (individual results are not shown) of R2 were found to be higher than those of R1. This conflict observation could again be attributed to the fact that operating conditions applied in Huang *et al*. (2008) were different from this study and the suspended carriers were of different characteristics, in terms of density, size and material. The heavier and smaller-sized suspended carriers they used enhanced the breaking up of formed flocs in the reactor, which released a higher SMP content, while in this study, the phenomenon of breakage of formed flocs was less significant (as discussed in the previous section) as the biofilm

carriers used were bigger in size and of lower density. The higher aeration rate would induce higher shear stress and more SMP was thought to be released out (Ji and Zhou 2006; Meng *et al*., 2008). Therefore, the lower effective aeration intensity caused by the biofilm carrier addition might have contributed to the less SMP release due to the lower aeration intensity.

Table 6.5 Analysis results of EPS components in mixed liquors and biofilm/cake layers.

		EPS in Mixed liquor (mg/L)		**EPS in cake layer (g/m^2)**	
		Protein	**Carbohydrate**	**Protein**	**Carbohydrate**
Part 1[a]	**R1**	38.28±9.2	15.66 ±4.05	0.30	0.12
	R2	35.31±10.1	24.50±4.87	0.40	0.17
Part 2[b]	**R3**	29.30±4.88	20.48±7.53	0.22	0.09
	R4	37.93±8.33	52.79±8.06	0.48	0.29

n^a = 12; n^b=9.

The concentrations of the extracted EPS on the biofilm/cake layer were also investigated, and the results showed that more protein and carbohydrate were found on the membrane surface. The formation of biofilm/cake layer on the membrane surface was thought to result in more microbial activities on the membrane surface so that more organic matters were released during the process. In addition, the biofilm/cake formation also enhanced the adsorption of organic matters onto membrane surface and precipitation of inorganic matters (such as $CaCO_3$ and $MgCO_3$) (Seidel and Elimelech, 2002; Meng *et al*., 2003). Consequently, after a same operation period of 58 d, more protein and carbohydrate were detected in the biofilm/cake layer of R2, resulting in faster fouling. However, these results did not provide detailed characteristics of these organic matters in the biofilm/cake layer. Therefore, a further study should be conducted to identify the characteristics of cake layer in the SCMBR with or without biofilm carriers.

6.1.4 FTIR Analysis

FTIR was used to investigate the functional group of biomass dry powder derived from the cake layers. As shown in Fig. 6.4, a broad region of adsorption spectrum was found at wavelength of 3,400 cm^{-1} (C-H bond) and 2,945 cm^{-1} (O-H bond) (Kumar *et al*., 2006). Three peaks at the wavelength of 1,385, 1,550 and 1,650 cm^{-1} corresponded to the presence of Amide III, II and I, respectively, which are unique to the protein secondary structure (Cho *et al*., 1998; Zhou *et al*., 2007). Hence, these results indicated that there were proteins in the membrane foulants. In addition, there were another obvious peaks in the spectrum (1,100 cm^{-1}), indicating the presence of polysaccharides. By estimation from the FTIR spectra, the major components of the foulants were identified as proteins and polysaccharides which suggested a significant organic fouling which mainly resulted from EPS. Compared the two spectrums shown in Fig. 6.4, it could also be seen that the absorption spectrums of R1 and R2 were similar in their profiles but significantly differing in their adsorption intensities at the wavelength of 1100 cm^{-1}. These results indicated that more polysaccharides are detected in the biomass (Cho *et al*., 1998), while the peaks for protein or protein-like substances were similar. The biomass in the cake was presumed to be originated from the suspended solids in the reactor. As discussed in Section 6.1.3, minor difference of protein concentrations was detected in the mixed liquor in two SCMBRs, while R2 had higher carbohydrate concentration than that of R1. The results obtained in the FTIR spectrum agreed well with the EPS contents, confirming that majority of the biomass in the biofilm/cake were resulted from the EPS. In the previous section, it was reported that the significant difference of fouling propensity was due to the different soluble organic fraction concentration present in the biofilm/cake layer. FTIR results only characterize the functional groups in organics in the biomass, but

did not give detail organic information in the solutes. Therefore, further investigation of organic fraction were conducted (to be discussed in next sections) to elucidate the fouling control mechanism by carriers.

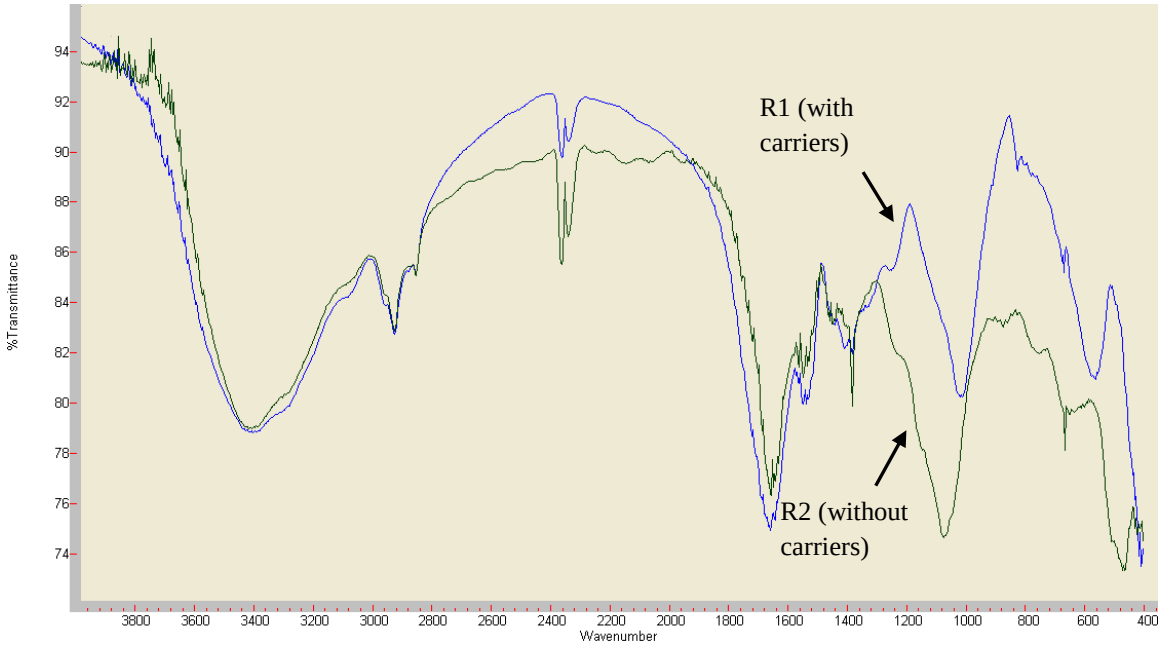

Figure 6.4 FTIR analysis of dry biomass in cake layer.

6.1.5 LC-OCD Analysis of Permeates, Mixed Liquor Supernatants and Biofilm/Cake Layers

In order to investigate the affecting mechanisms of biofilm carriers on membrane fouling, the detailed organic fraction was analyzed by the LC-OCD method. Table 6.6 shows the compositions of the solutes in the effluents, mixed liquor supernatants and biofilm/cake layers, which included biopolymers, humic substance, building blocks and LMW acids. The chromatogram in Fig. 6.5 shows the detailed molecular weight distribution of the organic solutes in cake layer. Table 6.6 gives the concentration of different fraction of organics in the supernatants, permeate and biofilm/cake layer solutes (derived from the chromatograms in Fig. 6.5) in R1 and R2.

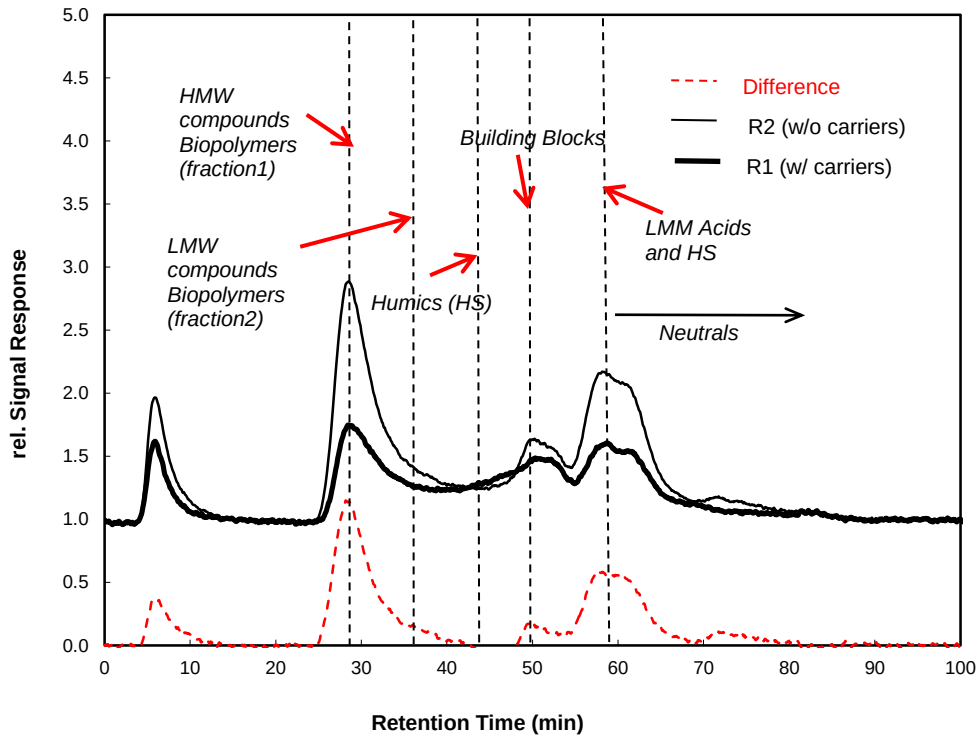

Figure 6.5 LC-OCD analysis of organics in biofilm/cake layers.

Table 6.6 LC-OCD analysis of solutes in the effluents, mixed liquor supernatants and biofilm/cake layers in R1 and R2

		Total CDOC Hydrophilic TOC (ppb)	Approx. MW g/mol				
			Biopolymer (>>20k (fr.1); 1k-20k (fr.2))			<1000 (LMW compounds)	
			TOC (ppb)	TOC (%)	DON (ppb)	TOC (ppb)	TOC (%)
Effluent[a]	**R1**	6030	625	10.4	45	5405	89.6
	R2	7655	725	9.5	95	6930	90.5
Supernatant[a]	**R1**	9730	2870	29.5	370	6860	70.5
	R2	14865	5510	37.1	790	9355	62.9
Cake layer[b]	**R1**	22020	5480	25.0	1280	16540	75.0
	R2	37480	11900	31.8	2240	25580	68.2

[a] concentration of samples in the effluent or mixed liquor supernatant.
[b] concentration of samples in 500ml cake suspensions.

Chromatographic dissolved organic carbon (CDOC) refers to the OC values obtained by the area integration of the total chromatogram. From Fig. 6.5, the peak in the fraction 1, which was high molecular weight (HMW) compounds with MW higher than 20k, accounted for 20-30% of the total CDOC (see Table 6.6). Majority of

molecules had a LMW of less than 1000, which accounted for 70% of the total CDOC (see Table 6.6). These observations indicated that although the proportion of organic solutes in biofilm/cake layer was small, the LMW compounds still played an important role in membrane fouling. This was because the LMW compound would deposit or adsorb on the membrane surface, enhancing the membrane pore blocking by the impact of suction drag force. From Table 6.6, it could be deduced that some LWM compounds with a MW of less than 1000 (bigger than membrane pore size) was also rejected, with retention rate of 21.2% in R1 and 25.9% in R2, respectively. The observation of the high LMW compounds concentrations in the biofilm/cake layer indicated that the impacts of LMW compounds adhesions on the membrane surface were significant. This conclusion was in accordance with Zhang *et al*. (2006) who claimed that the cake formation on the surface of MF could cause MF behave like a relatively tight UF along with the penalty of steady TMP increase.

A comparison between the organic fractions in mixed liquor supernatant, membrane permeates and biofilm/cake layers was conducted and the results are summarized in Table 6.6. Compared to R1, more organic compounds were detected in R2 for the supernatant and biofilm/cake layer. This finding indicated that more protein and carbohydrate were released into the mixed liquor supernatant in R2 (biopolymer=5,510 ppb, LMW compounds=9,355 ppb), and consequently more organic were deposited or adsorbed on the membrane surface (biopolymer=11,900ppb, LMW compounds=5,480ppb). This result confirmed that the addition of biofilm carriers helped to lower the organic concentrations in the mixed liquor. Membrane fouling and membrane foulants were noted to be closely related to the dissolved organic matters present in bulk mixed liquor (Rosenberger *et al*., 2006). The biopolymer/LMW ratio was similar to those in supernatant (R1=0.42; R2=0.59) and

cake layer (R1=0.33; R2=0.47), indicating that the fouling contribution of solutes in the mixed liquor was not negligible. Compared to the HMW fraction in supernatants (R1=2,870 ppb; R2=5,510 ppb), the concentrations of HMW in membrane permeates were much lower (R1=625 ppb; R2=725 ppb). In addition, it could be seen that although R2 had a two times higher concentration of biopolymers than that of R1, the concentration differences in permeates were minor. Hence, ceramic membrane was able to reject most of the biopolymers present in the mixed liquor. However, the solutes concentration in permeates was not solely controlled by the solute concentration in the supernatant. The mechanisms of organic rejection was a complex process, which was combined by the cake formation, pore blocking and membrane physically rejection.

6.1.6 EEM Fluorescence Spectra Analysis

The EEM fluorescence spectra of DOM in the cake layer were also investigated. Figs. 6.6a and 6.6b show the EEM fluorescence spectra for the biofilm/cake layer in R1 and R2, respectively. In both EEM fluorescence spectra for the biofilm/cake layer, two major peaks with wavelength of Ex/Em (250-270/380-390nm) and Ex/Em (250-260/420-430) were very obvious, which were reported to be protein-like substances (Chen *et al*., 2003; Yamashita and Tanoue, 2003). Wang *et al*., (2009) investigated the EEM fluorescence spectra of membrane foulants in an MBR with anoxic zone for pretreatment and found that three peaks with the wavelength of Ex/Em (235/335nm), Ex/Em (285/325nm) and Ex/Em (315/420nm). Kimura *et al*. (2009) examined EEM fluorescence spectra of foulants on membrane surface and found a protein-like substance at Ex/Em of 270/320nm. In this study, the cake layer content was extracted from an aerobic SCMBR system (with or without carriers) fed with primary settling

tank wastewater without any pretreatment. Thus, the results obtained were different from those reported in previous studies.

It is noted that different operating conditions operated in MBR will lead to significantly different organic composition in bulk mixed liquor (Ng *et al*., 2006; Meng *et al*., 2007). The organic composition of biofilm/cake layer was closely related to the soluble organic materials in the supernatant of mixed liquor as discussed in Section 6.1.6. Therefore, the different operating conditions applied in the previous studies might result in slightly different EEM fluorescence spectra being detected in the membrane foulants. In the cake layer of EEM fluorescence spectra obtained from this investigation, R1 (without carriers) had two evident peaks at Ex/Em=250/390 with the intensity of 158.4 and Ex/Em=250/420 with the intensity of 178.2. R2, on the other hand, had three peaks at Ex/Em=270/390 with intensity of 284.9, Ex/Em=250/430 with the intensity of 244.7 and Ex/Em=245/460 with the intensity of 183.1. These data indicated that although the profiles of the EEM fluorescence spectra of the extracted foulants were similar, the relative dominance of the protein-like substance was relatively higher in R2. This trend in EEM fluorescence spectra agreed well with those found in EPS concentration and LC-OCD measured for biofilm/cake layer foulants, indicating that the EEM fluorescence spectra could be a proper indicator for membrane fouling in SCMBR.

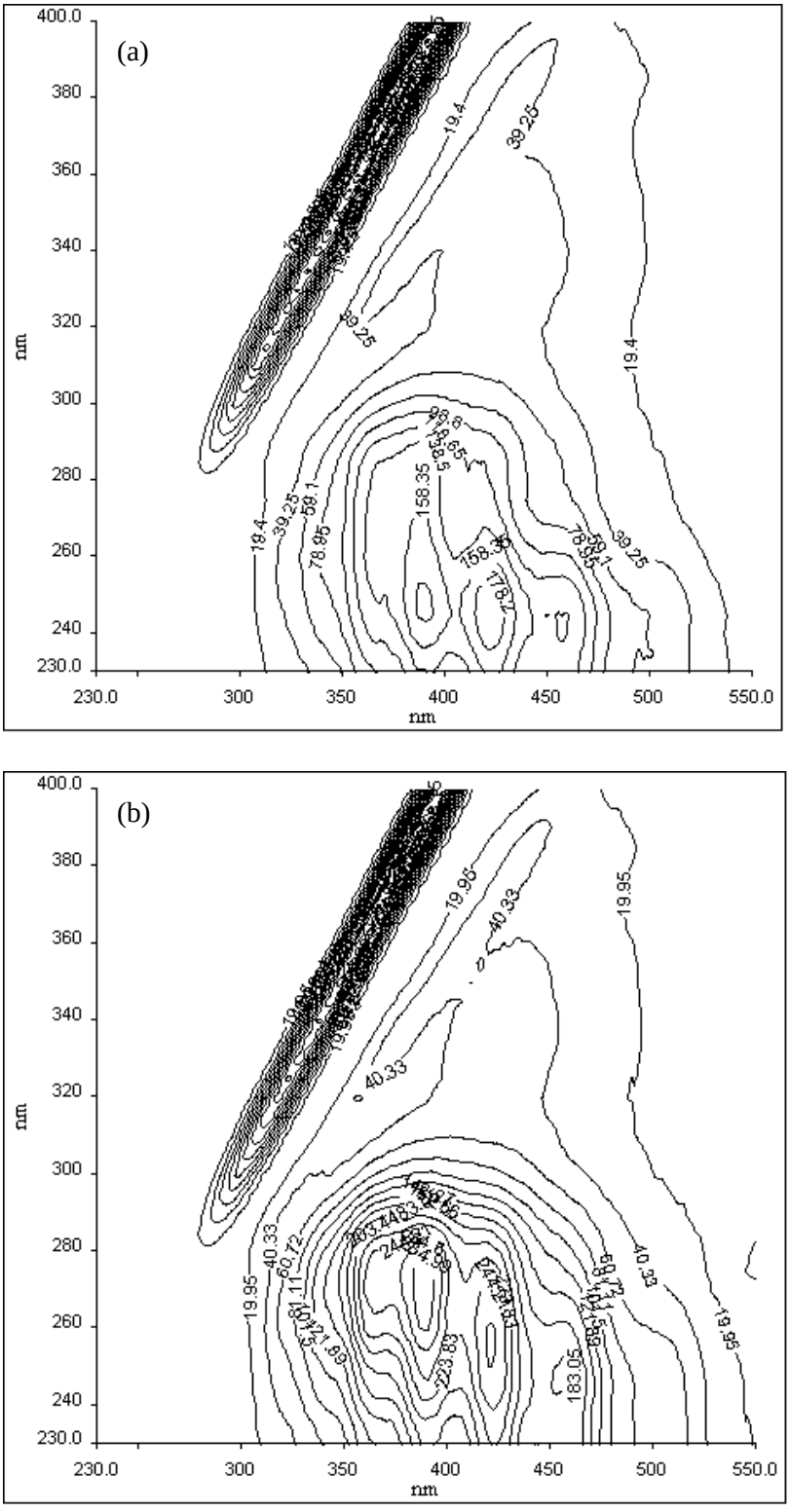

Figure 6.6 EEM fluorescence Spectra of the organics in cake layer. (a) R1; (b R2.

6.1.7 Optimum Dosage of Bioflm Carriers

The fouling control mechanisms by different dosage of biofilm carriers were also investigated by repeating all the analyses in Phase 1 and part of the results are summarized (see Table 6.2, 6.5 and Fig. 6.1b). All the results obtained were in good accordance with the results obtained in Phase I, indicating that more carriers addition significantly contributed to scouring of cake layer off the membrane surface. Consequently, R4 with a higher biofilm carrier dosage did not encounter fouling after 43 d of operation, while R3 reached TMP of 30 kPa.

As discussed in the previous sections, the positive effect of bioflm carrier addition was demonstrated. Huang *et al*., (2008) reported that there was an optimum dosage of carriers in SMBR by using a series of bench tests with MLSS concentrations of 5, 8 and 11 g/L. In the second phase of this study, two SCMBRs (R3 with 2.85% biofim carrier dosage and R4 with 5.70% carrier dosage) were started up again with the same raw mixed liquors from the water reclamation plant. Due to the adsorption of biomass on the biofilm carrier surface, the duration for the reactor to reach steady state was unclear. Therefore, the fouling trends were investigated from the day of SCMBRs reseeding. As reported by Huang *et al*. (2008) under a certain MLSS, there existed an effective carrier dose range for mitigating membrane fouling effectively. Similarly, under a certain carrier dose, there existed a minimum MLSS concentration, higher than which suspended carriers showed the whole positive effect on membrane fouling control. By interpolating the results from Huang and his co-workers' study (2008) to the average MLSS data collected (ie., R1 of 6.5 g/L, R2 of 5.9 g/L), a comparison was made to verify the effective carrier dosage observed in this case. The results showed that the carrier dosage of 5.70% in R3 agreed well with Huang *et al*. (2008)

interpolated results of 5.85% at MLSS of 6,500 mg/L. However, the carrier dosage of 2.89% in R4 was actually halved of that required amount for effective positive scouring to work effectively, indicating that an optimum effective dosage exists in each SCMBR system. In this SCMBR system with a mean MLSS of 6,000 mg/L, the optimum biofilm carrier dosage was 5.70% based on the dosage selection of 2.85 and 5.70% by volume ratio of carrier volume to reactor working volume.

6.2 Backwash

Membrane in-situ backwash was operated in this phase to investigate the effect of backwash on membrane fouling mitigation. Two SCMBRs operated under the same conditions will be referred as R1 (without backwash) and R2 (with backwash).

6.2.1 Membrane Fouling Behavior and Backwash Pressure

Figure 6.7 shows the TMP of the SCMBR system with (R2) or without (R1) backwash and the backwash pressure for R2 in the biomass acclimization period (Fig. 6.7a) and the process period (Fig. 6.7b). It could be seen from Fig. 6.7a that backwash was able to retard the TMP increase, and eventually lengthen the operation timespan of the SCMBR system. The TMP started to increase once the operation began, which indicated that under a high flux of 11.89 LMH, the conditional fouling in which the TMP does not increase, was not obvious. From Day 1 onwards, a gradual TMP increase, which was about 0.6 kPa per day, could be observed in both SCMBRs. From Day 9 onwards, an obvious TMP increase was observed for R1, and after that an exponential TMP increase (following the equation of $TMP=0.0004\ day^{4.324}$) occurred and R1 was seriously fouled on Day 13. Overall, R2 reached a TMP of 30 kPa on Day 23, which suggested that fouling cycle could be extended by10 days by adding the backwash system. In addition, exponential TMP increase was not observed in R2, although the TMP increase rate changed from 0.55 to 2.50 kPa per day. These results indicated that backwash was able to retard the membrane fouling process. The TMP increase in the SCMBR with the backwash system was gradual and turned out to be a linear increase. These observations are supported by some previous studies that a suitable periodic backwash may alleviate membrane fouling by reducing internal

clogging as well as cake layer fouling (Xu *et al*., 1995; Kuberkar *et al*., 1998; Hong *et al*., 2005; Hwang *et al*., 2009).

Once the SCMBR reached a TMP of 30 kPa, the ceramic membranes were taken out of the reactor and physically cleaned by a sponge to remove the biofilm/cake layer on the membrane surface in order to see the distribution of irreversible and reversible fouling. Results showed that after physical cleaning, the TMP could drop to 5.9 kPa for R1; however, TMP increased exponentially in the following days for R1 and reached 30 kPa in just two days. On the contrary, TMP could drop to 3.4 kPa for R2 and the reactor could run for another twelve days after physical cleaning. Fig. 6.7a also demonstrates the backwash pressure (BWP) in R2. As it can be seen from the figure, an obvious BWP was observed in the first two days and after that no significant BWP increase was noted. Once the physical cleaning was done for R2, BWP decreased to 5.4 from 9.4 kPa, and after that significant BWP was observed in R2 and finally reached 31.4 kPa when R2 encountered serious fouling after physical cleaning on Day 34. These results indicated that compared to R1, R2 had a longer operation timespan due to the effect of backwash during the process and after physical cleaning. This phenomenon might be attributed to the effect of backwash which was able to partially remove the irreversible and reversible foulants by the backwash pressure. The increase of BWP indicated the fouling resistance increase, which suggested fouling resistances contributed by biofilm/cake layer and pore blocking increased. The fouling resistance contributed by cake layer is always defined as reversible fouling, while the resistance contributed by pore blocking/clogging is always considered as irreversible fouling. It can be seen from Fig. 6.7a that after physical cleaning, the BWP decreased to 3.4 kPa; however, after 5-d operation, BWP increased to 9.5kPa, which was the same as the BWP before chemical cleaning. This

observation indicated that although physical cleaning was able to remove reversible fouling and partially remove the irreversible fouling, the TMP of BWP of R2 continued to increase significantly after physical cleaning. The significant BWP increase after the physical cleaning also indicated that once membrane irreversible fouling occurs significantly, backwash cannot mitigate fouling effectively.

Fig.6.7b shows the TMP of R1 and R2 and BWP of R2 during the treatment process. Overall, the fouling trend was similar to Fig. 6.7a that R2 could run for a longer period due to the addition of backwash system. However, compared to the fouling cycle in the biomass acclimization period, both R1 and R2 could run for a long operation timespan, with R1 reached a TMP of 30 kPa on Day 26 and R2 reached a TMP of 30 kPa on Day 40. This might be due to the different condition of mixed liquor in two stages. In the biomass accilimization period, the mixed liquor status was not stable and the microorganisms in the mixed liquor were facing more environmental stress. Therefore, more microbial by-products were released according to SMP analysis, leading to the faster fouling during the biomass acclimization period. The stable biomass condition after the biomass acclimization period rendered a long operation timespan possible. Consequently, R1 in this phase experienced a liner TMP increase within the first 13 d with a TMP increase rate of 0.21 kPa per day. After that, an exponential increase was observed in R1 which followed the relationship of $Y=0.0029X^{2.8147}$ ($R^2=0.9924$). Compared to R1, R2 in this phase did not have any obvious TMP increase within the first 8 days of operation with only 0.6 kPa of TMP increase observed. After that, a linear TMP increase was observed with increment of about 0.86k Pa per day. The BWP observed in this phase was different from what has been observed in the sludge acclimization period. It could be seen from Figs. 6.7a and

6.7b, when R1 reached a TMP of 30kPa in the biomass acclimization period, the BWP was only 9.5 kPa, while in this phase when R1 reached TMP of 30 kPa the BWP was 44.7 kPa. Besides the sludge condition being difference, this difference might also be due to the affecting mechanism of backwash process, during which the fouling resistance was the main contributor for the BWP increase. However, fouling resistance increase was due to foulants accumulation into the membrane pores and on the membrane surface, which is a function of operation time. In the process phase, the system could run for a longer period (39 d) than the biomass accilimization period (23 d), which indicated more soluble organics were either trapped into the membrane pores or deposited on the membrane surface.

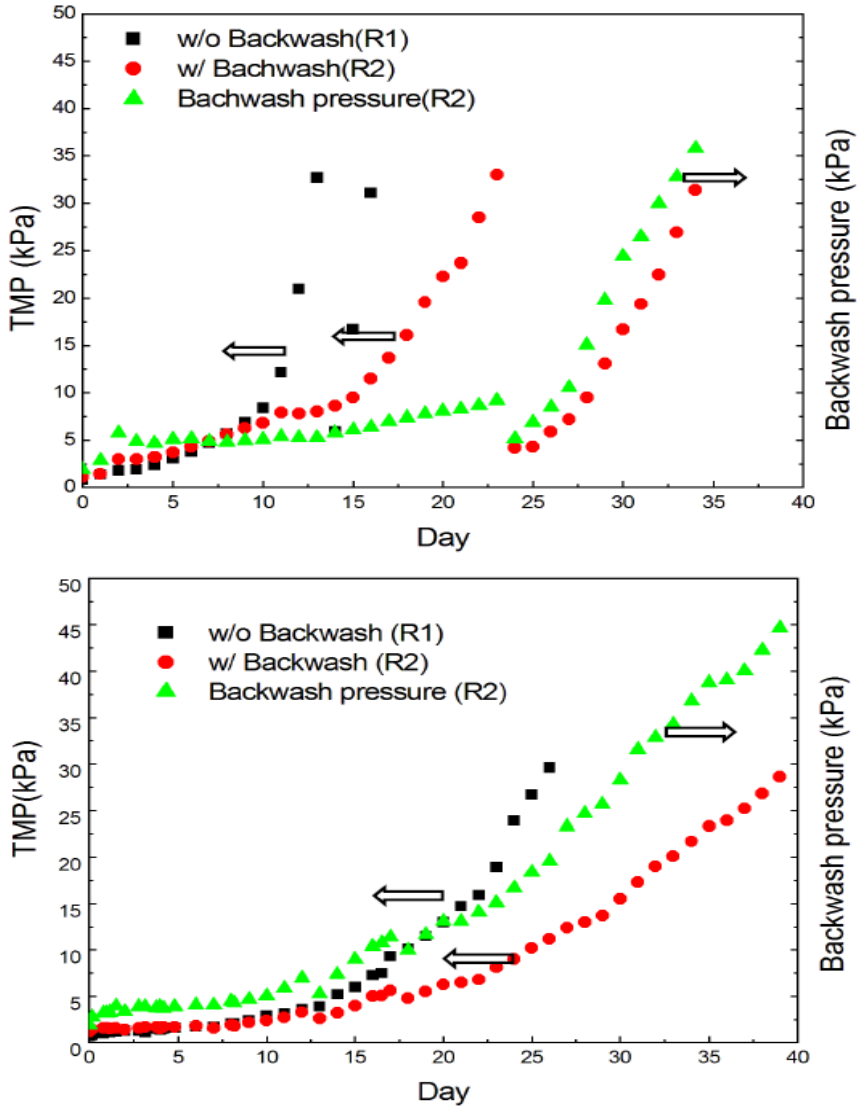

Fgure 6.7 TMP and BWP profiles for SCMBR with (R2) and without (R1) backwash: a) Biomass acclimization period; b) Fouling cycle analysis period.

When TMP of R1 and R2 reached 30kPa, the membrane was taken out of reactor to test clean water TMP before and after the physical cleaning, and the results are shown in Fig. 6.8. From this figure, it can be seen that once the membrane fouled, the total fouling resistance and the membrane internal resistance were similar, while the distribution of the fouling resistance for resistance contributed by biofilm/cake layer and pore blocking differed. R2, with the backwash, had a higher pore resistance at 2.33×10^{12} m^{-1}, accounted for 28.33% of the total membrane resistance in R2, which was also almost two times higher than that of R1. On the other hand, R1, without

backwash system, had a higher cake layer resistance when membrane fouled. This differnece between two SCMBRs might be attributd to two aspaects. It is reported that a formed cake layer may prevent further pore bolcking efficiently (Hwang *et al*., 2009), while the backwash system was able to partly dislodge the biofilm/cake layer by the BWP. Eventually, the final contribution of the pore resisntace was higher in the SCMBR with backwash. On the oterh hand, although the BWP was able to partly remove the solutes and colloidal towards the backwash direction, the longer operation timespan of R2, 40 d compared to 26 d in R1, gave more chances to the solutes and small particulates to accumulate in the membrane pores.

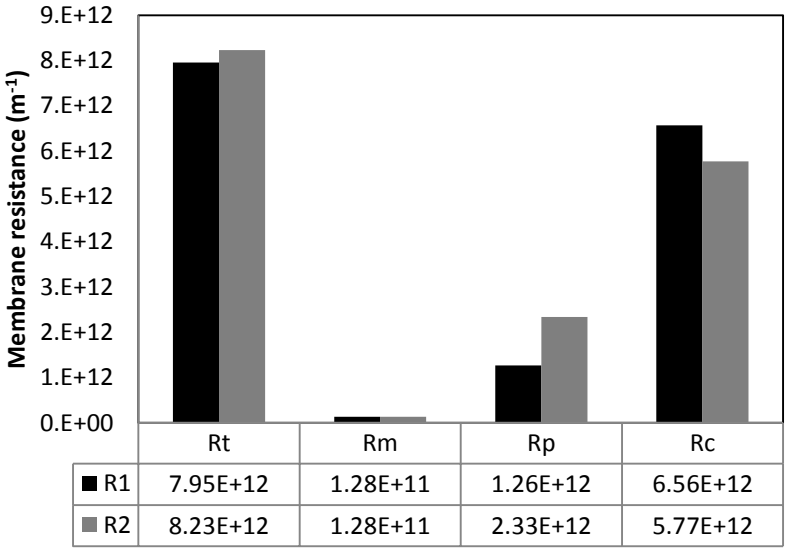

	Rt	Rm	Rp	Rc
R1	7.95E+12	1.28E+11	1.26E+12	6.56E+12
R2	8.23E+12	1.28E+11	2.33E+12	5.77E+12

Figure 6.8 Fouling resistance distributions of SCMBRs with backwash (R1) and without backwash (R2).

6.2.2 EPS and SMP in Mixed Liquors in Two SCMBRs

The biomass characteristics of two SCMBRs were monitored during the operation in terms of the components of SMP and EPS, and the results are summarized in Table 6.7. From this table, it can be observed that proteins and carbohydrates were the major components of both SMP and EPS. Slightly higher proteins and carbohydrates in SMP were detected in the SCMBR with backwash. This might be due to the effect of

backwash for 15 s in each 10-min cycle, while during this period a volume of 23.8 mL of membrane permeate was backwashed into the SCMBR. The slight operation condition might to some extent affect the environmental stress to the microbes, and consequently slightly more microbial products were produced. Other than the individual concentration of proteins and carbohydrates in SMP and EPS, the P/C ratio and total SMP and EPS concentrations were also analyzed, and results showed that no obvious differences were observed between two SCMBRs. It was reported that EPS, SMP as well as P/C ratio were the major fouling indicators of biological system. Wilén *et al*. (2003) reported that the proteins had a significant effect on the surface charge of biomass, and higher surface charge finally led to severe fouling. Ng *et al*. (2006) reported that higher total EPS (including soluble EPS –SMP) contributed to the faster fouling in a MBR system with low SRT. However, the same conclusion cannot be drawn in this study. Comparing the fouling propensities of the two SCMBRs, it could be identified that slightly higher SMP did lead to faster fouling in R2. On the contrary, due to the effect of the backwash, R2 reached a TMP of 30 kPa 14 d after R1 did. Therefore, it could be concluded that the minor difference in SMP might not lead to difference of membrane fouling characteristics observed in this study, and SMP concentration difference was not the major fouling affecting mechanisms. It was other affecting mechanism leading to different fouling characteristics.

Table 6.7 EPS, SMP and P/C ratio in the two SCMBRs.

	SMP			EPS			Total SMP	Total EPS	Total Protein	Total Carbohydrate
	Protein (mg/g MLVSS)	Carbohydrate (mg/g MLVSS)	P/C	Protein (mg/g MLVSS)	Carbohydrate (mg/g MLVSS)	P/C				
R1	2.46±1.17	2.29±0.54	1.07±0.50	12.99±3.99	4.12±1.38	3.57±1.57	4.75±1.45	17.1±4.25	15.45±4.12	6.41±1.42
R2	3.34±1.30	3.07±0.98	1.14±0.59	13.67±3.66	4.14±1.76	3.74±1.58	6.41±1.95	17.81±4.34	17.02±3.69	7.21±1.53

Note: Number of sampling =8

6.2.3 Microscopic Observation

SEM images were also employed to determine the micro-morphology of the fouling layer formed on the membrane surface. SEM technology is able to provide high resolution images of the fouling layer structure and give some clues to the origin of foulants. Figure 6.9 shows the SEM images of fouled ceramic membrane surface to characterize the fouling layer formation for R1 and R2, respectively. It is clearly observed that a thick and non-porous fouling layer consisting of various bacteria covered by a cluster of biopolymer were found on the membrane surface in R1. These biopolymer and bacteria could cover the membrane surface and block the membrane pores, leading to the severe membrane biofouling on the membrane surface (Ng et al., 2006; Meng *et al*., 2007). On the contrary, Fig. 6.9b shows the fouled membrane surface of R2 with backwash system, no obvious fouling layer was observed and the clusters of microbial cells were much fewer. In addition, in some areas the membrane pores still could be seen. It is reported by Hwang *et al*., (2009) that the filtered cake layer could be completely washed away by even a low backwash flux after 15 min filtration in a ceramic membrane system. In our study, it is a long operation system instead of a short time batch test, the accumulation of a small portion of bio-clusters still could be seen. Compared to membrane in R1, a clearer particle (either organic or inorganic) distribution could be observed on the fouled membrane in R2. There were some crystal-like particles observed in Fig. 6.9b, which are considered as inorganic foulants on the membrane surface (Choo *et al*., 2003). Biofouling can be attributed to a process of mature biofilm formation and/or biopolymer/EPS accumulation on the membrane surface in the membrane system. Higher amount of organic substrate available on the membrane surface could initiate and support the growth of biofilm. Besides, higher concentration of biopolymer/EPS content on the membrane surface

could allow more microbial cells adsorption onto the membrane surface to promote biofilm formation, leading to severe biofouling. The contents of SMP and EPS were analyzed in Section 6.2.2, and results shows that no significant differences were found in these two SCMBRs. With the similar mixed liquor, the significant difference of the fouling layer morphology could be attributed to the backwash effect in R2. The addition of backwash system could effectively prevent the initiation of biofilm/biocake layer on the membrane. Consequently, the adsorption of biopolymer onto the membrane surface was also relieved. This finding is supported by various studies. Al-Halbouni *et al*., (2008) studied the correlation of EPS contents with membrane fouling in a full-scale MBR system, and found that membrane fouling was mainly caused by the deposition of a fouling layer that was porous and did not embedded by large quantities of microbial cells due to the frequent membrane backwash during the process. Likewise, similar findings were also reported by Geng (2006) and Hwang *et al*., (2009). Therefore, it is assumed that the frequent backwash applied in the SCMBR system would help prevent and mitigate the microbial attachment onto membrane surface to a degree whereby biofilm/biocake development was not the dominant factor leading to severe fouling.

SEM is not only a useful tool to diagnose the origin of foulants on the membrane surface (i.e., bacteria, biopolymers), but also can be used to monitor the effectiveness of the membrane cleaning (Meng *et al*., 2010). In order to determine the effectiveness of the physical cleaning on the fouled ceramic membranes in both SCMBRs, the SEM images of the physically cleaned membranes were taken. In Figures 6.9c-d, the SEM images show that clear membrane pores were observed after the physical cleaning, indicating an effective performance of physical cleaning. Compared to the SEM images of fouled membrane surface of R1 in Fig. 6.9a and Fig. 6.9c, effective

physical cleaning efficiency was very obvious. However, not all the bio-clusters could be removed on the membrane surface in R1. Under a 5,000× magnification, small portion of microbial cells still could be observed. In addition, there were some glue-like substances (probably biopolymers) embedding the micro – cells diagnosed. These results indicated that, physical cleaning could remove most of the biopolymers and a large cluster of microbes, unless those hardly attached ones. In contrast, in Fig. 6.9d, the SEM image shows that no obvious bacteria clusters were observed after membrane physical cleaning. Instead, more crystal particles could be observed. Compared to the SEM images of fouled membrane surface of R2 shown in Fig. 6.9b and Fig. 6.9d, it was found that the differences between the SEM images of the membrane surface before and after physical cleaning were not significant.

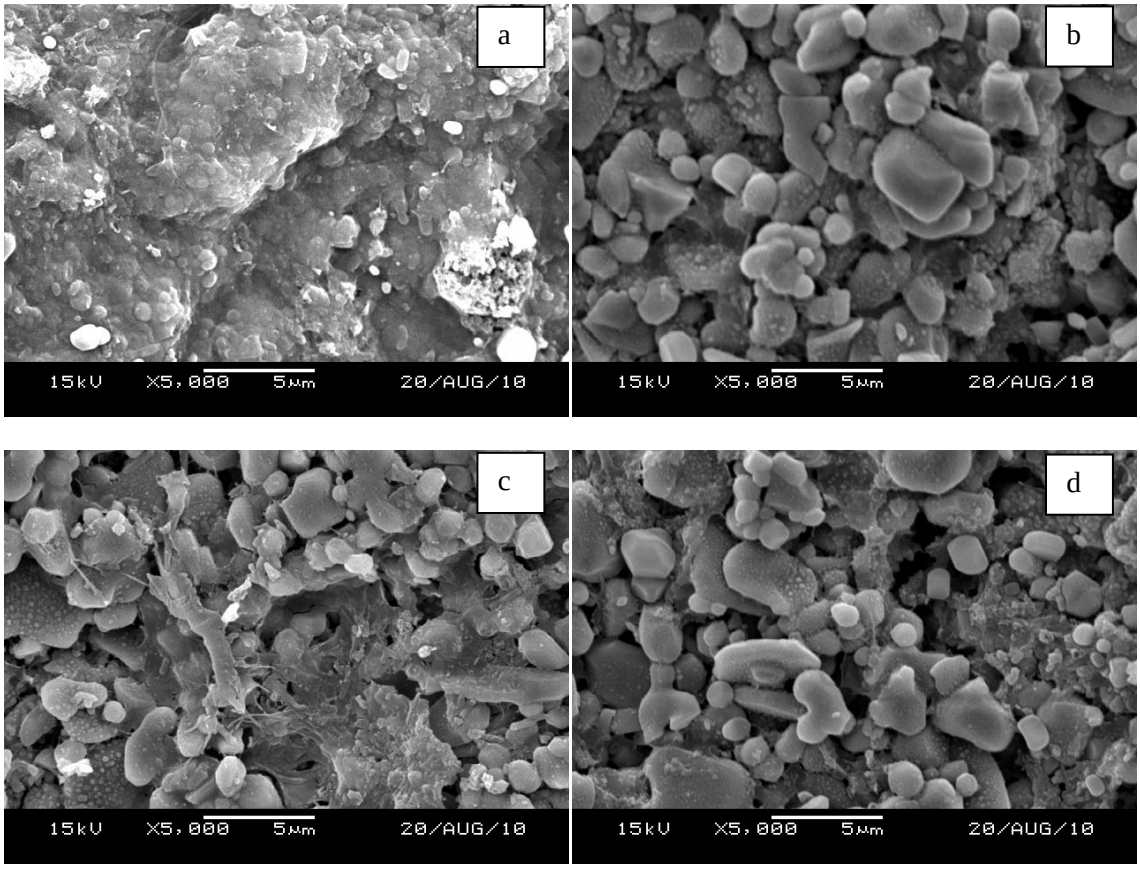

Figure 6.9 a). fouled membrane R1; b). fouled membrane R2; c) physically cleaned membrane R1; d) physically cleaned membrane R2.

6.2.4 Organic Compositions in the Biofilm/Cake Layer

As discussed in Section 6.2.1, biofilm/cake layer was the major fouling resistance contributor when ceramic membrane fouls. In order to elucidate the difference fouling mechanism of the SCMBR with or without backwash system, biofilm/cake layer was removed by a sponge and dissolved in 500 ml of ultrapure water. The organic components of the cake layer were analyzed, and the obtained results are summarized in Table 6.8.

Generally, the biomass was the major composition of biofilm/cake layer, which accounted for over 85% of the total organics in both SCMBRs. The proportion of other organics like the colloidal particles and solutes were also similar, which indicated that most of the biofilm/cake layers were originated from the mixed liquor. The VSS/SS ratio was higher than 80% in both SCMBRs (results not shown), which was a bit higher than that of the mixed liquor. This finding indicated that other than the origination from the sludge, the microbial activities also occured on the membrane surface. The microbial activities on the membrane surface produced more microbial by-products and induced higher the VSS/SS ratio of the biofilm/cake layer than that of the mixed liquor (around 0.75). The second largest portion of the cake layer was colloidal particles, which accounted for 9.23% and 11.47% in R1 and R2, respectively. Colloidal particles were reported to have strong impacts on membrane fouling as their deposition and precipitation on membrane surface will cause severe membrane pore clogging along the course of operation (Meng *et al*., 2007).The solutes of TOC accounted less than 5% of the total organics cake layer; however, solutes played a major role in enhancing membrane fouling by reducing the biofilm/cake layer

porosity and compacting the structure of the biofilm/cake layer. Proteins and carbohydrates were the major components of the solutes.

Comparing the amount of organic compositions of R1 and R2, it could be seen that SCMBR without backwash (R1) had organic concentrations with respect to the biomass, colloidal particles and solutes, the total specific cake layer concentration of 5.997 g/m^2 compared to 3.885 g/m^2 in R2. The higher concentration of the organics led to the faster and more severe membrane fouling in SCMBR system. Proteins and carbohydrates were reported to be the major membrane foulants in various studies (Chang and Lee, 1998; Lee *et al*., 2003; Ng *et al*., 2006; Al-Halbouni *et al*., 2007). The specific concentration of proteins and carbohydrates in R1 cake layer was three times and two times higher than those of R2 cake layer, respectively. Again, the more protein and carbohydrate contents might partly be due to the organic accumulation by the drag force and partly be due to the more microbial activities on the membrane surface in R1. The more the biomass existed onto the membrane surface, the more opportunities for the organics to attach and adhere on the membrane surface. All these affecting mechanism contributed to the faster membrane fouling discussed in Section 6.2.1 and thick fouling layer observed in the SEM images (Section 6.2.3).

Table 6.8 Biofilm/Cake layer organic compositions of R1 and R2

	VSS (g/m^2)	TOC$_c$(g/m^2)	TOC$_s$(g/m^2)			Total(g/m^2)
			Carbohydrate	Protein	Others	
R1	5.219(87.02[a])	0.553(9.23)	0.077(1.29)	0.133 (2.22)	0.014 (0.24)	5.997 (100)
R2	3.344(86.08)	0.445(11.47)	0.048 (1.23)	0.042(1.09)	0.005(0.14)	3.885(100)

Note: TOC$_c$= colloidal TOC; TOC$_s$= soluble TOC

[a]= Percentage of the organics out of the total organics.

6.2.5 EEM Fluorescence Spectra and LC-OCD Analysis

The organic characteristics of soluble part of biofilm/cake layer were analyzed by advanced technologies like LC-OCD and EEM fluorescence spectra. Figure 6.10 shows the LC-OCD chromatography of soluble contents of cake layer in R1 and R2 cake layers. As reported, the peaks of the chromatography can be integrated to obtain the equivalent amount of organic compounds such as biopolymers, humics and LWM substances in terms of carbon or nitrogen contents (Zheng *et al*., 2009; Halle *et al*., 2009; Zheng *et al*., 2010). Form this figure it could be seen that the major components of soluble contents of cake layer were biopolymers (HMW protein and polysaccharides), with retention time from 25-35 mins. The peak at elution time at around 45 mins that represents humic substances was not detectable. Small fraction of LMW substances like building blocks and acids were detected with low peak. These observations are in agreement with Zheng *et al*. (2009) who reported that accumulation of biopolymers on the membrane surface was very significant when treating secondary effluent by UF membranes. Comparing to the LC-OCD chromatography of biofilm/cake layer contents in R1 and R2, it could be observed that the biofilm/cake layer in R2 had a higher concentration of biopolymers. This finding is in good accordance with the carbohydrate and protein concentration analysis present in Section 6.2.4. The detailed components of the soluble content of biofilm/cake layer showed that soluble content of the biofilm/cake layer in R1 has a higher biopolymer concentration of 13.32g/m^2 than that of R2. It was reported by Zheng *et al*. (2010) that most of the fouling caused by biopolymers was reversible. The results obtained in this study indicated that the backwash system in R2 could effectively remove part of the biopolymers on the membrane surface, and lengthen the operation timespan by 14 days in R2.

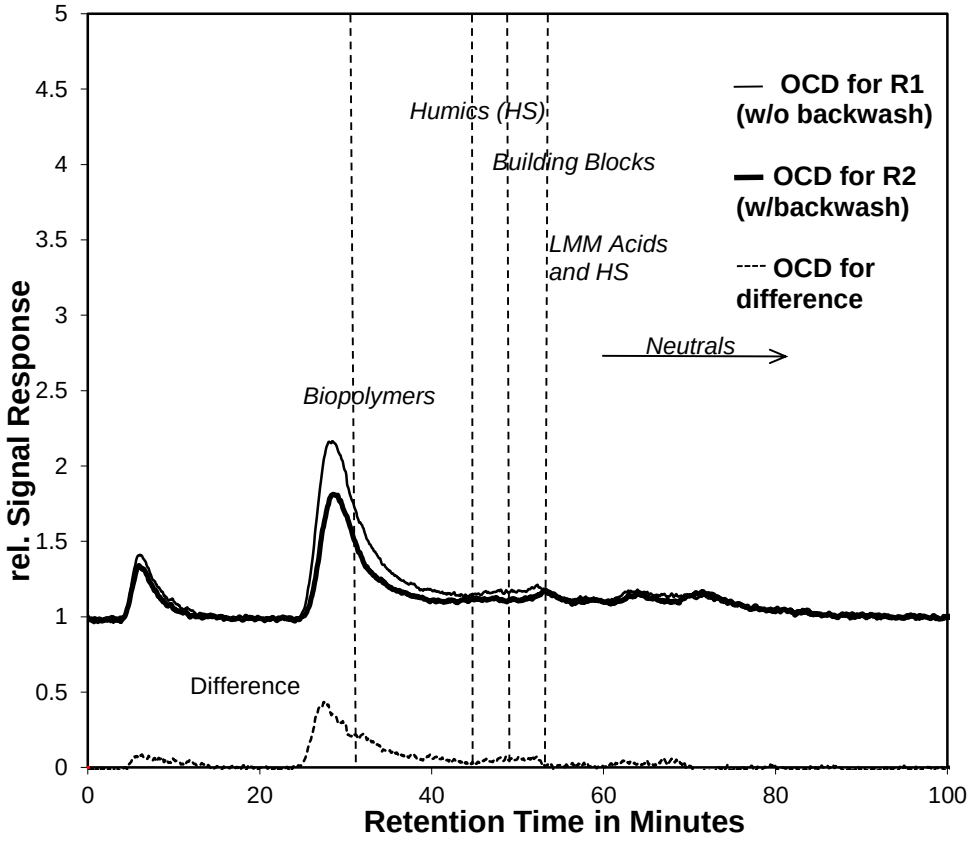

Figure 6.10 LC-OCD chromatograms of biofilm/cake layer in R1, R2, and the difference between them (10x dilution).

EEM fluorescence spectra of the solube biofilm/cake layer content was also measured by a luminenence spectrophotometer, and the results are shown in Figure 6.11. From Fig. 6.11a, it is noted that two peaks at the wavelength of Ex/Em of 240-280/380-400 and Ex/Em of 240-260/410-440 were very obvious in the biofilm/cake layer in R1. However, only one distinct peak at the wavelength of Ex/Em of 240-250/420-430 was observed in biofilm/cake layer in R2 (Fig. 6.11b). This finding indicated that the organic fraction differed slightly.

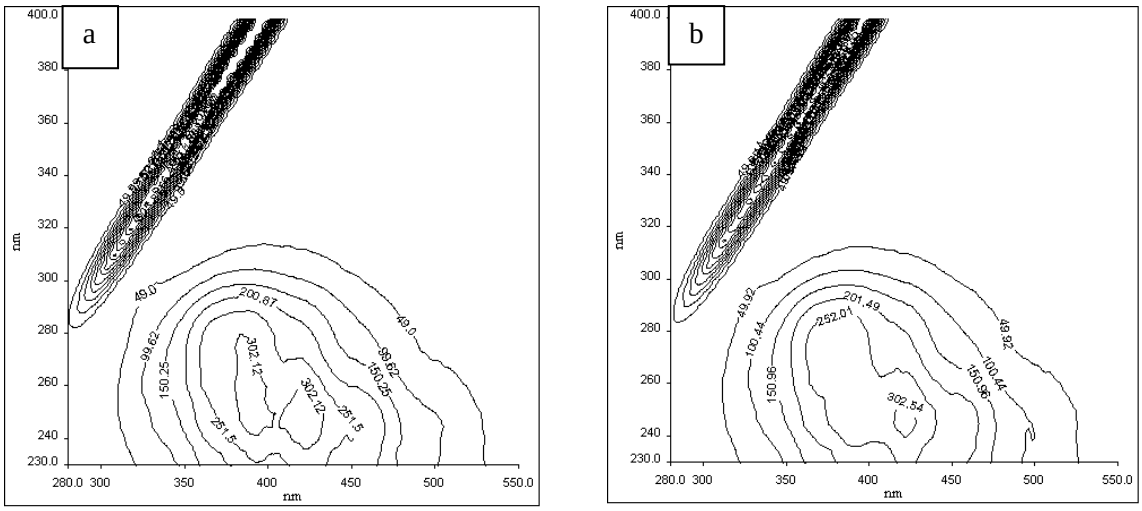

Figure 6.11 EEM spectra of soluble contents of biofilm/cake layer. a) R1; b) R2.

In Fig. 6.11, it can be observed that there are several peaks with relatively low fluorescence intensity which could not be obviously observed in the EEM spectra. Those peaks mainly appeared in the region of Ex 230–250 nm and Em > 380 nm, which represent fulvic acid-like substances. To understand the in-depth EEM fluorescence characteristics of DOM samples, the fluorescence regional integration (FRI) method was applied to characterize the five excitation–emission regions (Chen *et al*., 2003). In general, peaks at shorter wavelengths (<250 nm) and shorter emission wavelengths (<350 nm) are associated with simple aromatic proteins such as tyrosine and tryptophan (Regions I and II) (Ahmad and Reynolds, 1999). Peaks at intermediate excitation wavelengths (250–280 nm) and shorter emission wavelengths (<380 nm) corresponds to soluble microbial by-product-like material (Region IV) (Coble, 1996; Reynolds and Ahmad, 1997); while peaks located at the wavelengths of excitation (200–250 nm) and the emission (>380 nm) is related to fulvic acid-like substances (Region III). Peaks at longer excitation wavelengths (>280 nm) and longer emission wavelengths (>380 nm) are related to humic acid-like organics (Region V) (Artinger *et al*., 2000; Mounier *et al*., 1999). The distributions of FRI of DOM samples on the membrane surfaces of two SCMBRs are shown in Fig. 6.12. The different FRI

distribution of the soluble cake layer observed indicated the different compound structures in R1 and R2 biofilm/cake layer. The higher fraction of Region IV and Region V in biofilm/cake layer in R1 indicated the high retention of the fluorescence substances in a membrane with thick biofilm/cake layer. More Region IV fluorescence substances in R1 biofilm/cake layer also implied that more microbial by-products existed on the membrane surface in R1, which might be either due to the higher retention rate of these substances by the membrane or more active microbial activities on the membrane with thick biofilm/cake layer. The more fraction of Region III observed in R2 cake layer indicated that backwash was more capable of releasing HMW substances back to the bulk solution and eventually the higher fraction of LMW compounds such as fulvic acid-like substances in the biofilm/cake layer.

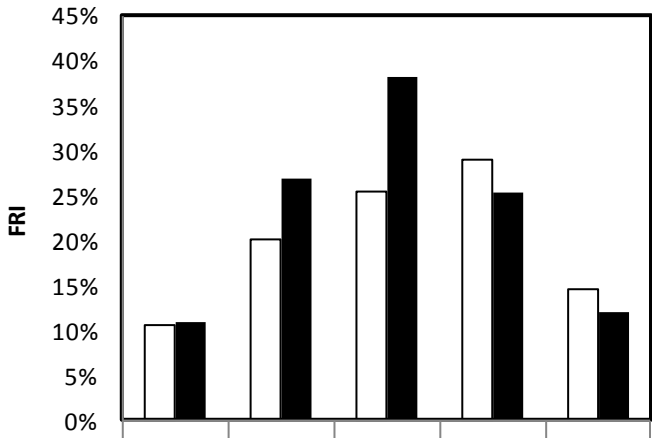

	I	II	III	IV	V
□ R1 cake layer	10.68%	20.15%	25.49%	28.98%	14.69%
■ R2 cake layer	10.88%	26.88%	38.12%	25.47%	12.04%

Figure 6.12 FRI distributions of soluble biofilm/cake layers in two SCMBRs.

6.2.6 FTIR Analysis

The LC-OCD as well as the EEM can only measure the organic characteristics in the solubilized fraction. However, as discussed in Section 6.2.5 biomass consisted of over

80% of the total biofilm/cake layer. In this case, the analysis of the dry matters of the biofilm/cake layer becomes highly important. The FTIR technology was used in this study to know the functional groups in the organic matters. In Fig. 6.13, it can be seen that the FTIR spectrum for cake layer content has several spectrum peaks at 670, 1,030, 1,100, 1,240, 1,400, 1,540, 1,650, 2,850, 2,920, 3,300 and 3450 cm^{-1} . This finding was in good agreement with what has been reported by An *et al*. (2008) who studied the membrane foulants characterization in an anaerobic non-woven fabric MBR for municipal wastewater treatment. A broad band spectrum detected between 3,450 and 3,300 cm^{-1} could be attributed to O–H stretching of the O–H bond in hydroxyl functional groups (Meng *et al*., 2007; Wang *et al*., 2008). The two sharp bands (observed in R1 cake layer) at around 2,920 and 2,850 cm^{-1} represented aliphatic C–H stretching (Smidt and Meissl., 2007; Marcato *et al*., 2009). These two peaks were not so obvious in R2 cake layer, indicating that foulants consists of C-H stetching bonds were more reversible and could be partially removed by the backwash. The three bands at about 1,652, 1,540 and 1,240 cm^{-1} in the spectrum indicated the presence of protein in the biofilm/cake layer, since the three peaks are the unique spectrum for the protein secondary structure, which was named as amides I (C=O stretching), II (N–H in plane) and III (C–N stretching) (Smidt and Parravicini; 2009). The sharper peak observed in the R1 biofilm/cake layer spectrum indicated that more protein was detected on the membrane surface of R1.Again, membrane backwash system helped to alleviate membrane fouling by partially removing the proteins and protein-like substances. The broad peak present at around 1,100 cm^{-1} was attributed to the symmetrical and asymmetrical stretches of C=O, indicating the presence of polysaccharides and polysaccharides-like substances. The dramatic difference of the spectrum for the biofilm/cake layer from the two SCMBRs suggested the

effectiveness of backwash to remove the HWM substances such as polysaccharides. The peak at around 1400 cm^{-1} corresponded to the symmetrical stretches of $–COO^-$ associated with amino acid (Omoike and Chorover, 2004; Kimura *et al*., 2005). As it can be observed from Fig 6.13, a sharper band of spectrum could be observed in R2 biofilm/cake layer, which was different from the other peaks. This observation indicated that the backwash was able to remove most of the bigger molecules with HMW such as polysaccharides and HMW proteins, while the removal of the small molecules like amino acids was not effective. The intense band at about 1,030 cm^{-1} in spectrum in R2 biofilm/cake layer could be attributed to Si–O stretch of clay minerals (Carballo *et al*., 2008; Smidt and Parravicini, 2009). Therefore, it could be concluded that the major components of the biofilm/cake layer were identified as proteins, polysaccharides and clay materials through the FTIR spectra. The presence of clay materials in the biofilm/cake layer was also evaluated by the SEM-EDX observation which will be discussed in the next section.

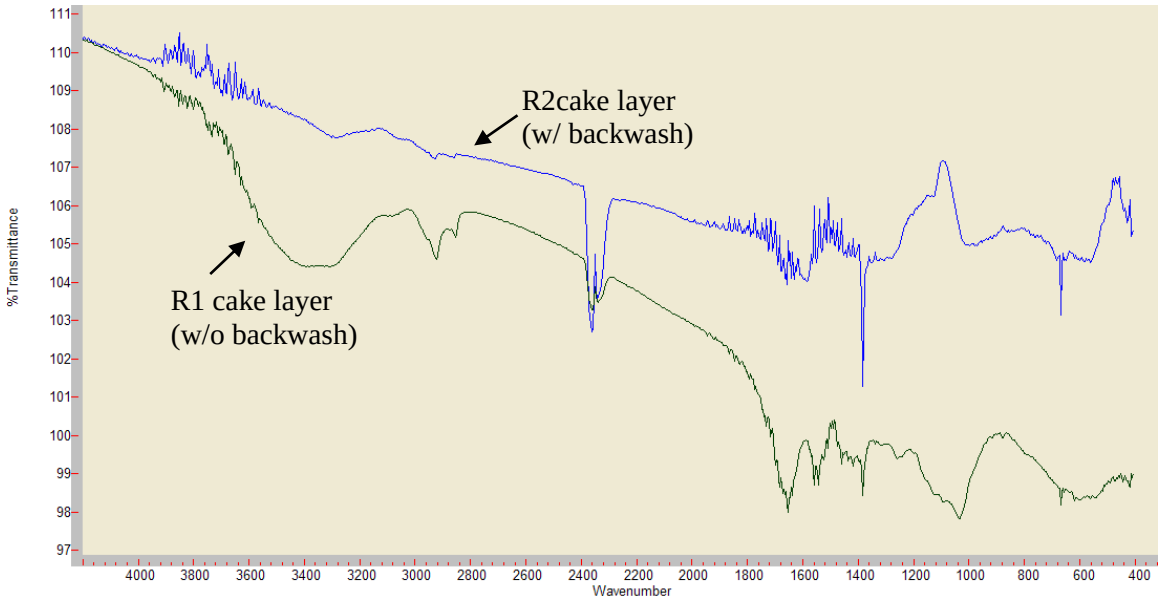

Figure 6.13 FTIR spectra of biofilm/cake layers in two SCMBRs.

6.2.7 Inorganic Element Analysis

Elemental analysis of the biofilm/cake layers was conducted by SEM-EDX to determine the chemical components of the biofilm/cake layers on the membrane surface, which was able to identify the major element composition of the fouling layers. The elements of C, O, Mg, Al, S, Si, P, Ca, and Fe were detected by SEM-EDX system (see Fig. 6.14). Comparing Figs. 6.14a and 6.14b, the general profiles of the elemental composition on the membrane surface were similar, with all elements of C, O, Mg, Al, S, Si, P, Ca, and Fe detected. The major inorganic elements detected in the biofilm/cake layer were P, Al and Si, followed by the Ca, S, Mg and Fe. It is noted that Mg, Si, Al, Fe and Ca are considered as the origin of the inorganic fouling in the system (Meng *et al*., 2007; Wang *et al*., 2008), and the presence of these elements in the biofilm/cake layer indicated the occurring of inorganic fouling. As discussed in Chapter 4, various metal ions were detected in the influent wastewater and the activated sludge. Therefore, it could be concluded that inorganic components on the membrane surface were originated from the influent wastewater and the mixed liquor, and were accumulated gradually during the operation of the MBR. Some researchers have studied the inorganic compositions of biofilm/cake layer by SEM-EDX. It has been shown that the inorganic element of Mg, Ca, S, P, Al, Si and Fe played an important role in the membrane fouling development. $MgNH_4PO_4{\cdot}6H_2O$ (struvite) is identified as the major inorganic foulants in an anaerobic MBR system (Choo and Lee, 1996) and cake layer characteristics analysis in an aerobic MBR system (Meng *et al*., 2007). The cations like Mg^{2+}, Fe^{3+}, Al^{3+} and Ca^{2+} may produce a cation bridge with COO- and become the major component of biopolymers. In addition, this cation bridge played an important role in reducing the porosity of the biofilm/cake layer, tighten the biofilm/cake layer attachment onto membrane surface and enhance the

membrane fouling eventually (Seidel and Elimelech, 2002). Recently, it is also reported that $CaCO_3$ scaling could lead to severe membrane irreversible fouling as the precipitate of $CaCO_3$ is very difficult to be removed by aeration and backwash (Kim *et al*., 2009).

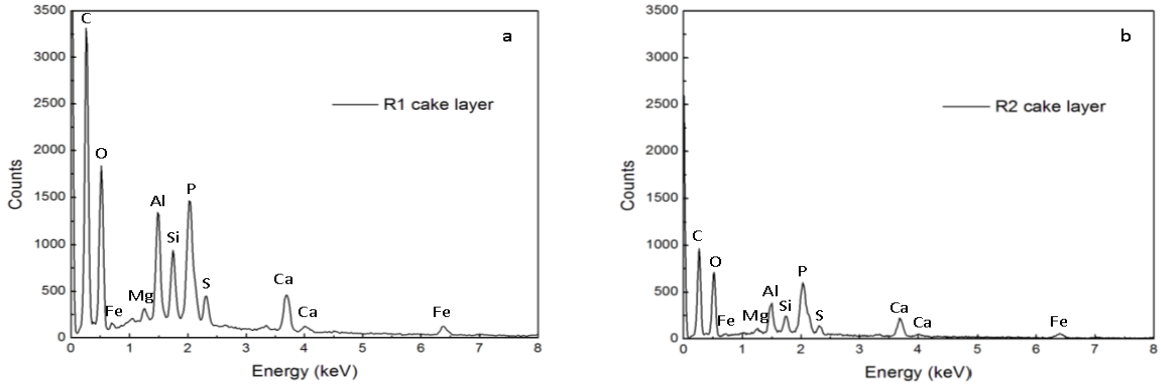

Figure 6.14 SEM-EDX profile. a) biofilm/cake layer in R1; b) biofilm/cake layer in R2

In Fig. 6.14, it can be seen that although the general profiles of the elements in the biofilm/cake layer were similar, the absolute counts of each elements in R1 biofilm/cake layer was significantly higher than those of R2. Especially for C, Al, Si O and Mg, the absolute counts in R1 biofilm/cake layer was three time higher than those of R2 biofilm/cake layer. This observation was in good agreement with the FTIR results (Section 6.2.6) that clay materials was also a major component of cake layer, and the backwash in R2 was able to remove most of these clay materials. The presence of element C in the biofilm/cake layer could be attributed to the accumulation of the components in the mixed liquor and the microbial byproducts originated from the microbial cell growth or decay on the membrane surface. It was reported that the major components of the mixed liquor were organic carbon other than the inorganic carbon. Therefore, the C elements detected could convey the organic contents in the cake layer. The higher percentage of C in R1 biofilm/cake

layer indicated the higher organic composition in the biofilm/cake layer. More inorganic elements found in R1 biofilm/cake layer indicated more severe inorganic fouling occurred on the membrane surface. However, as reported in Section 6.1.1, the inorganic foulants in the biofilm/cake layer affected fouling differently from that of the organic foulants in the membrane pores. The inorganic foulants in the biofilm/cake layer could account for the tightening of the porous biofilm/cake layer and the clustering of the biopolymer, contributing to a strongly attached biofilm/cake layer on the membrane surface. Compared to R1 that was covered by a thick and non-porous biofilm/cake layer, the thin cake layer observed (SEM image) in R2 did not initiate and support the attachment of inorganic components a lot. Consequently, although R2 had been operated for a longer period with more chance for the inorganic accumulation, fewer inorganic elements counts were detected by the end of the fouling cycle. The affecting mechanism by the backwash to relieve the formation of cake layer eventually contributed to the longer operation time of SCMBR.

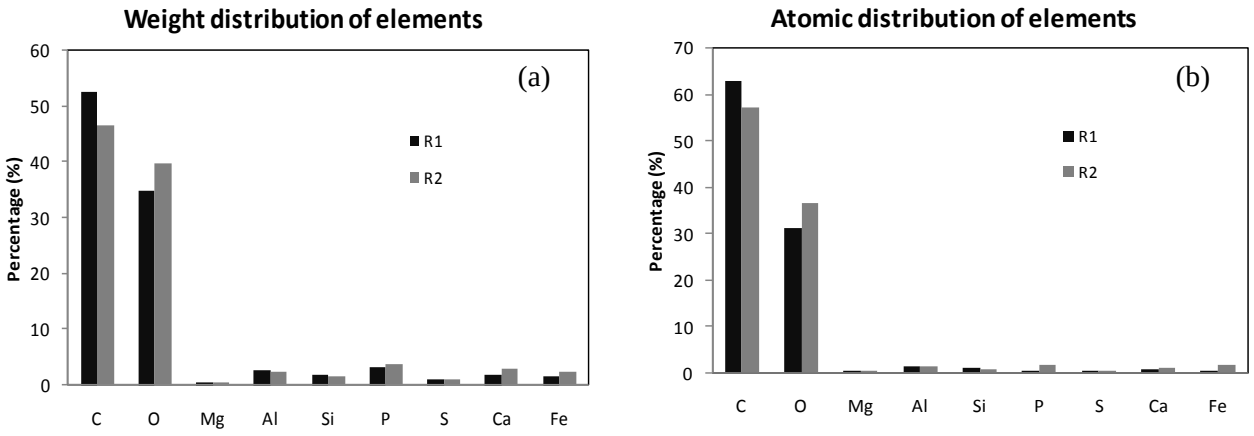

Figure 6.15 a) Weight distribution of elements in biofilm/cake layer in two SCMBRs; b) Atomic distribution of elements in biofim/cake layer in two SCMBRs

Other than the absolute counts of the elements, the weight distribution and the atomic distribution of the elements were also analyzed, and the results are shown in Fig. 6.15.

R1 had higher percentage of C indicated higher percentage of organic components in R1 biofilm/cake layer as discussed before. It was found that the percentage of O was higher in R2 than that of R1. The element of O was partially from the organic components and partially from the inorganic component. Results showed that the relative atom distributions on the biofilm/cake layer from the SCMBRs with or without backwash were different. The slightly higher percentage of O in R2 cake layer might be explained by the hypothesis that the pure origination of inorganic fouling by the accumulation of inorganic foulants onto the membrane surface was more severe in the backwash system, although the absolute O concentration was lower in the biofilm/cake layer from R2. The formation of the biofilm/cake layer on the membrane surface impacted on the function of the inorganic foulants. The inorganic components could affect the biofilm/cake layer structure as a biofilm/cake layer is the porous multilayer. The relative higher percentage of atomic distribution of O, P, Ca and Fe atoms found in R2 biofilm/cake layer indicated that these elements were more prone to deposit onto the membrane surface, while they might not contribute a lot to the biofilm/cake layer formation.

6.3 Summaries of Phase 3 Research

Fouling minimization strategies such as the addition of biofilm carriers and in-situ backwash were applied in this stage. Results showed that both strategies were very effective in retarding TMP increase in terms of continuously mitigating biofilm/cake layer formation. The compositions of biofilm/cake layer in the SCMBRs with or without biofilm carriers (Part 1) and SCMBRs with or without backwash (Part 2) were analyzed by some advanced DOM detector technologies (i.e. EEM fluorescence spetra, FTIR, LC-OCD) and inorganic detector (i.e. SEM-EDX). Results in Part 1 demonstrated that the major fouling contributors were biofilm/cake layer, and addition of biofilm carriers not only affected the biomass characteristics but also relieved membrane fouling by biofilm/cake layer mitigation. However, up to now, the application of different biofilm carriers in different studies makes it unclear whether the biofilm addition could continuously relieve membrane fouling. Further studies could be conducted to evaluate the affecting fouling mechanism by different types and different dosage of biofilm carriers. In Part 2 studies, results demonstrated that cake layer in the backwash system consisted of fewer inorganic components (i.e., Al, Mg, Ca, Si, etc) as well as organic compounds (i.e., polysaccharides, protein, lipid, amino acid, etc). Consequently, the introduction of backwash in SCMBR could retard membrane fouling and lengthen the total operation period by 60% by exploring the proposed backwash mode. However, due to time constraints, the selection of optimum backwash mode was not investigated in this study. Further studies in the area could pave way to implementation of optimal backwash protocol in the pilot- and full-scale SCMBRs.

Chapter 7. Conclusions and Recommendations

7.1 Conclusions

In this study, the application of the submerged ceramic membrane bioreactor was investigated in treating domestic wastewater, which was divided into three phases. Phase 1 focused on the treatment performance of SCMBR in treating domestic wastewater and the membrane fouling propensities of difference pore-sized membranes. Phase 2 focused on the in-depth fouling mechanisms in terms of biofilm/biocake structure and compositions and the non-traditional organic detection by LC-OCD, EEM spectra and HPLC. The development of microbial communities in the biofim/biocake was also investigated regularly. Phase 3 focused on the fouling minimization strategies, such as the biofilm carrier addition (Part 1) and backwash (Part 2). In Part 1, different fouling mechanisms occurred in systems with or without biofilm carrier were elucidated in terms of the biomass characteristics and the biofim/cake layer compositions. In Part 2, different fouling mechanisms induced by the system with or without backwash were evaluated in terms of the membrane surface morphology (SEM), foulants distribution (SEM-EDX) and the composition of the biofilm/cake layer (FTIR, LC-OCD, EEM).

Results obtained in Phase 1 could be summarized as follows:

- All SCMBRs with different pore sizes could obtain an average of 94.5% TCOD and over 98% of NH_3-N removal when operated under 10 d SRT and 6 h HRT in treating real sewage.
- The profiles of MWD and PSD were slightly different in the early stage of the operation and appeared to be similar for the SCMBRs with different pore sizes. An active layer might have developed on the membrane surface, which would achieve sieving of colloidal particles that contributed to COD rejection, resulting in similar PSD and MWD profiles in the later phase.
- R80 with the smallest pore size and smoothest membrane surface was the last one to exhibit serious membrane fouling, while R300 with the opposite membrane properties fouled fastest.
- Results of the effect of mixed liquor characteristics (MLSS, CST, Zeta Potential, EPS and SMP) on fouling showed that mixed liquor properties were not the dominant factors leading to various fouling behaviors with different pore-sized SCMBRs operated under similar conditions in this study.
- Both membrane pore sizes and membrane surface properties affected membrane fouling significantly. Membrane fouling potential was in good accordance with the sequence of membrane surface roughness: R80 < R200 < R100 < R300.

Results obtained in Phase 2 could be summarized as follows:

- A biofilm/biocake layer has developed after a period of 7 d. Within the first 7 days of operation, membrane resistance was the dominant factor. From Day 7

onwards, the formation of biofilm/biocake was the dominant fouling contributor.

- The sequence of the biofilm/biocake coverage ratio was in good accordance with the TMP increase rate after the early stage (first 7 days), with M80 had the lowest dp/dt while M300 had the highest dp/dt.
- A bioflm/biocake layer formed on the membrane surface after a period of time base on the LC-OCD, EEM spectra and HLPC results of the membrane permeates and mixed liquor supernatant of the sample after 1 h and 14 d operation period. This biofilm/biocake layer enhanced the organic rejection for ceramic membranes, especially for M300.
- The results of HPLC, LC-OCD and EEM fluorescence spectra indicated that the different profile of the supernatant and the membrane permeates could be attributed partly to the membrane rejection and partly to the biological function (mostly hydrolysis) by the biofilm/biocake on the membrane surfaces. Consequently, more fraction of the smaller MWD substances were observed in membrane permeates, since some HMW compounds were hydrolyzed by the biofilm into the LMW compounds.
- Membrane pore size, surface roughness, and suction pressure jointly affected the microbial communities. The smoother the membrane surface, the higher the possibility to induce microbial ecology dominance in the early stage.

Results obtained from Part 1 of Phase 3 could be summarized as follows:

- Addition of biofilm carrier was able to delay the membrane fouling in R1 (with carriers) by the co-effect of effectively scouring the cake layer on the membrane surface and changing the mixed liquor characteristics.

- SCMBR without carriers (R2) had 5 times higher cake resistance and 2.5 times higher total resistance than that of the one with carriers. The cake layer, compositions of biomass, colloidal particles, solutes and inorganic matters, was the main contributor to membrane fouling.
- Both the higher concentration of biomass and inorganic matters in biofilm/cake layer facilitated TMP increment in R2 (without carriers).The bridging effect between the biopolymers and the inorganic matters contributed to the biofilm/cake layer tightening, reducing the cake layer porosity and eventually contributing to faster membrane fouling in R2 (without carriers).
- Higher concentration of LMW compounds (less than 1000) in the biofilm/cake layer contributed to the faster fouling in R2 (without carriers). EEM fluorescence spectra and LC-OCD in biofilm/cake layer could be a potential indicator for membrane fouling in SCMBR.
- Majority of the biomass in biofilm/cake layer were resulted from the mixed liquor EPS. Protein contents in the mixed liquor EPS and biofilm/cake were not the dominant affecting factors.

Results obtained in Part 2 of Phase 3 could be summarized as follows:

- Backwash was an effective method to alleviate membrane fouling in terms of partially dislodging the foulants from the membrane surface and membrane inner pores by the backwash. Backwash force was able to dislodge most of the foulants back into the bulk solution. However, when membrane was seriously fouled by pore blocking, backwash cannot alleviate membrane fouling.

- An exponential TMP increase was observed in the SCMBR without backwash (R1) after 13 d operation, while SCMBR with backwash (R2) did not have obvious TMP increase within the first 8 d and a linear increase was found.
- A glue-like substances (biopolymers) embedding the microcells have developed on the membrane surface in R1 (without backwash), which could account for a cluster of the microcells, bacteria and organic and inorganic foulants coexisting in the biofilm/cake layer. On the contrary, no obvious clusters of biopolymers could be observed by SEM images for the membrane surface in R2 (with backwash).
- Biopolymers and clay materials (contributed by Si) were the main foulants on the membrane surfaces. The protein-like substances at the wavelength of Ex/Em of 240-280/380-400 and Ex/Em of 240-260/410-440 were the major foulant in R1(without backwash), and the one at the wavelength of Ex/Em of 240-250/420-430 was the dominant protein-like substances in R2 (with backwash). FTIR results indicated the higher concentration of polysaccharides, polysaccharide-like substances, proteins and protein-like substances in the biofilm/cake layer in R1 (without backwash), while fouling contributed by these foulants were more reversible. The removal of small molecules on the membrane surface like amino acids was not effective in backwash systems.
- Elemental analysis by the SEM-EDX showed that major inorganic elements detected in the biofilm/cake layer were P, Al and Si, followed by the Ca, S, Mg and Fe. The presence of these elements indicated the origin of the inorganic fouling, and the existing of a cation bridge between Mg^{2+}, Fe^{3+}, Al^{3+}, Ca^{2+} and COO^{-} component of biopolymers. This interaction between the

inorganic and biopolymer further reduced the cake layer porosity and enhanced the membrane pore blocking.

7.2 Recommendations

7.2.1 Selection of Operating Condition for Pilot-scale System

Experimental results in this study demonstrated that SCMBR could provide continuous excellent quality of effluent in treating domestic wastewater. The investigation of the membrane surface properties on fouling showed that the membrane with smoother membrane surface could have longer operation duration. In addition, the fouling control strategies discussed also indicated that biofilm carrier addition and backwash were able to retard membrane fouling by mitigating and alleviating the cake layer formation. However, due to the time constraints, the selection of an optimum operating conditions including the operating parameters (i.e., SRT, HRT, flux, aeration rate) and the selection of fouling control strategies (i.e., biofilm carrier dosage, backwash mode) were not conducted in this study. In order to implement the SCMBR in a pilot- or full-scale, studies on selection of optimum operating parameters and fouling strategies are necessary and crucial. More efforts could be made in the future to optimize the SCMBR in treating domestic wastewater, and in the end the overall cost for SCMBR will be lowered.

7.2.2 In-depth Fouling Mechanism by Advanced Technologies

Findings obtained in this study showed that biofilm/biocake development corresponded well with membrane fouling in terms of the 2-D analysis by ISA-2 software. The higher the biofilm/biocake coverage ratio increase rate, the faster the membrane fouled. However, the membrane coverage ratio was a 2-D analysis, and

was not able to provide the detail information about the biofilm/biocake volume as well as the porosity which could be analyzed by 3-D analysis using ISA-2 software. It was recently reported by Ng and Ng (2010) that CLSM coupled with biofilm/biocake structural analysis was a good strategy to investigate the effect of characteristics (i.e. biovolume, porosity and heterogeneity) and compositions (lipids, DNA, polysaccharides and proteins) of biofilm on membrane fouling. The correlations between the developments of these components on the membrane surface also provided an insight into the fouling mechanisms illustration. Due to the constraints of the ceramic materials (hard membrane surface), the implementation of experiments in this area is very difficult in continuous operated system. The investigation of the biofim/biocake development on ceramic membrane surface in the batch system might give some implications for the pilot- and full-scale system.

7.2.3 Application of Ceramic Membranes in Other Systems

The mechanical, thermal, biological and chemical stability of ceramic membrane makes it very popular in food industries. The findings in this study showed that fouling increment of ceramic membrane was gradual instead of exponential increment typically found in the polymeric MBR system operating under sub-critical flux conditions. The gradual TMP increment mode might be due to the hydrophilic membrane nature. These characteristics of ceramic membranes make it potential usage as a pre-treatment for seawater desalination. The pretreatment of seawater by MF/UF is crucial before the RO process in order to remove large quantities of suspended solids - the major foulants that lead to frequent RO membrane cleaning. The gradual TMP increment mode could lengthen the operation period. In addition, the in-situ backwash/backflush/backpulse realized in the ceramic membrane system

also makes implementation of membrane cleaning convenient. Eventually, the total operating cost of the seawater desalination could be reduced. A study regarding the evaluation of ceramic membrane in the application as a pretreatment for seawater desalination will be promising from the cost-effective perspective.

References

Ahmad, S.R., and Reynolds, D.M., 1999. Monitoring of water quality using fluorescence technique: prospect of on-line process control. *Water Res*., 33 (9), 2069–2074.

Ahmed, Z., Cho, J., Lim, B.R., Song K.G., and Ahn K.H., 2007. Effects of sludge retention time on membrane fouling and microbial community structure in a membrane bioreactor. *J. Membr. Sci*., 287 (2), 211–218.

Al-Halbouni, D., Traber, J., Lyko, S., Wintgens, T., Melin, T., Tacke, D., Janot, A., Dott, W., and Hollender, J., 2008. Correlation of EPS content in activated sludge at different sludge retention times with membrane fouling phenomena. *Water Res*., 42 (6-7), 1475–1488.

An, Y., Wang, Z.W., Wu, Z.C., Yang, D.H., and Zhou, Q., 2009. Characterization of membrane foulants in an anaerobic non-woven fabric membrane bioreactor for municipal wastewater treatment. *J . Chem. Engineering*, 155 (3), 709-715.

An, Y.H., and Friedman, R.J., 1998. Concise review of mechanisms of bacterial adhesion to biomaterial surfaces. *J. Biomed. Mater. Res.* , 43(3), 338-348.

APHA, AWWA, and WEF, 2005. Standard Methods for the Examination for Water and Wastewater, 21st ed. APHA, Washington DC, USA.

Artinger, R., Buckau, C., Geyer, S., Fritz, P., Wolf, M., and Kim, J.I., 2000. Characterization of groundwater humic substances: influence of sedimentary organic carbon. *Applied Geochemistry* 15 (1), 97–116.

Baker, A., 2001Fluorescence excitation–emission matrix characterization of some sewage-impacted rivers. *Environ. Sci. Technol.*, 35, 948–953.

Bai, R.B., and Leow, H.F., 2002. Microfiltration of activated sludge wastewater—the effect of system operation parameters, *Sep. Purif. Technol*., 29(2), 189–198.

Ben Aim, R.M. and Michael, J.S., 2003. Membrane bioreactors for wastewater treatment and reuse: a success story, *Water Sci. Technol*., 47 (1), 1-6.

Beyenal, H., Donovan, C., Lewandowski, Z., and Harkin, G., 2004. Three-dimensional Biofilm Structure Quantification. *Journal of Microbiological Methods*, 59, 395 – 413.

Blöche, C., Bunse, U., Seβler, B., Chmiel, H., and Janke, H. D., 2004. Continuous regeneration of degreasing solutions from electroplating operations using a membrane bioreactor. *Desalination*, 162, 315-326.

Bouhabila, E.H., Aim, R.B., and Buisson, H., 2001. Fouling characterisation in membrane bioreactors. *Sep. Purif. Technol*., 22–23, 123–132.

Bouhabila, E.H., Ben Aim, R., and Buisson, H., 1998. Microfiltration of activated sludge using submerged membrane with air bubbling (application to wastewater treatment), *Desalination*, 118 (1-3), 315–322.

Bourgeous, K.N., Darby, J.L., and Tchobanoglous, G., 2001. Ultrafiltration of wastewater: effects of particles, mode of operation, and backwash effectiveness, *Water Res.* 35 (1), 77–90.

Braker, G., Ayala-del-Rio, H.L., Devol, A.H., Fesefeldt, A., and Tiedje, J.M., 2001. Community Structure of Denitrifiers, Bacteria, and Archaea along Redox Gradients in Pacific Northwest Marine Sediments by Terminal Restriction Fragment Length Polymorphism Analysis of Amplified Nitrite Reductase (nirS)and 16S rRNA Genes. *Applied and Environmental Microbiology*, 67, 1893-1901.

Brockmann, M., and Seyfried, C.F., 1997. Sludge activity under the conditions of crossflow microfiltration, *Water Sci. Technol.* 35 (10), 173–181.

Brookes, A., Jefferson, B., Guglielmi, G., and Judd, S.J., 2006. Sustainable flux fouling in a membrane bioreactor: impact of flux and MLSS, *Sep. Sci. Technol.* 41 (7), 1279–1291.

Cabassud, C., Massé, A., Espinosa-Bouchot, M., and Spérandio, M., 2004. Submerged membrane bioreactors: interactions between membrane filtration and biological activity, *Proceedings of the Water Environment-Membrane Technology Conference* Seoul, Korea..

Carballo, T., Gil, M.V., Gomez, X., Gonzalez-Andres, F., and Moran, A., 2008. Characterization of different compost extracts using Fourier-transform infrared spectroscopy (FTIR) and thermal analysis, *Biodegradation* 19 (6), 815–830.

Chae, S.R., Ahn, Y.T., Kang, S.T., and Shin, H.S., 2006. Mitigated membrane fouling in a vertical submerged membrane bioreactor (VSMBR), *J. Membr. Sci*., 280 (1-2), 572–581.

Chang I.S., Lee, C.H., and Ahn, K.H., 1999. Membrane filtration characteristics in membrane coupled activated sludge system — the effect of floc structure of activated sludge on membrane fouling. *Separation Sci. and Technol*., 34 (9), 1743–1758.

Chang I.S., and Lee, C. H., 1998. Membrane filtration characteristics in membrane coupled activated sludge system: the effect of physiological states of activated sludge on membrane fouling. *Desalination*, 120 (3), 221–233.

Chang, I.S., and Kim, S.N., 2005. Wastewater treatment using membrane filtration — effect of biosolids concentration on cake resistance. *Process Biochem*., 40(3-4), 1307-1314.

Chang, I.S., Gander, M., Jefferson, B., and Judd, S.J., 2001. Low-cost membranes for use in a submerged MBR. *Proc. Saf. Environ. Protect*., 79, 183–188.

Chang, S., and Fane, A.G., 2002. Filtration of biomass with laboratory-scale submerged hollow fibre modules—effect of operating conditions and module configuration, *J. Chem. Technol. Biotechnol.* 77, 1030–1038.

Characklis, W.G., and Marshall, K.C., 1990. Biofilms: A basis for and interdisciplinary approach, in: W.G. Characklis, K.C. Marshall (Eds.), Biofilms, Wiley-Interscience, New York, 3-16.

Chen, J., Gu, B., Le-Boeuf, E.J., Pan, H., and Dai, S., 2002. Spectroscopic characterization of the structural and functional properties of natural organic matter fractions. *Chemosphere*, 48 (1), 59–68.

Chen, V., 1998. Performance of partially permeable microfiltration membranes under low fouling conditions, *J. Membr. Sci*., 147 (2), 265–278.

Chen, W., Westerhoff, P., Leenheer, J.A., and Booksh, K., 2003. Fluorescence excitation–emission matrix regional integration to quantify spectra for dissolved organic matter. *Environ Sci. & Technol.* 37 (24), 5701–5710.

Chen, W., Westerhoff, P., Leenheer, J.A., and Booksh, K., 2003. Fluorescence excitation–emission matrix regional integration to quantify spectra for dissolved organic matter, *Environ Sci. & Technol*., 37 (24), 5701–5710.

Chiemchaisri, C., and Yamamoto, K., 1994. Performance of membrane separation bioreactor at various temperatures for domestic waste-water treatment, *J. Membr. Sci*., 87 (1-2), 119–129.

Chiemchaisri, C., Yamamoto, K., and Vigneswaran, S., 1994. Household membrane bioreactor in domestic wastewater treatment. *Water Sci. Technol*., 27, 171-178.

Chin, Y.P., Aiken, G.R., and O'Loughlin, E., 1994. Molecular weight, polydispersity, and spectroscopic properties of aquatic humic substances. *Environ. Sci. Technol*. 28(11), 1853–1858.

Cho, J., Amy, G., Pellegrino, J., and Yoon, Y., 1998. Characterization of clean and natural organic matter (NOM) fouled NF and UF membranes, and foulants characterization, *Desalination*, 118 (1-3), 101–108.

Cho, J.W., Song, K.G., Lee, S.H., and Ahn, K.H., 2005. Sequencing anoxic/anaerobic membrane bioreactor (SAM) pilot plant for advanced wastewater treatment. *Desalination*, 178, 219–225.

Choo, K.H., and Lee, C.H., 1996. Membrane fouling mechanisms in the membrane coupled anaerobic bioreactor, *Water Res*., 30 (8), 1771–1780.

Cicek, N., Franco, J.P., Suidan, M.T., Urbain, V., and Manem, J., 1999. Characterization and comparison of a membrane bioreactor and a conventional activated sludge system in the treatment of wastewater containing high-molecular weight compounds, *Water Environ. Res*., 71, 64–70.

Coble, P.G., 1996. Characterization of marine and terrestrial DOM in seawater using excitation–emission matrix spectroscopy. *Marine Chemistry* , 51 (4), 325–346.

Côté, P., Siverns, S., and Montib, S., 2005. Comparison of Membrane-based Solutions for Water Reclamation and Desalination. *Desalination*, 182 (1-2), 251-257.

Davey, M.E., and O'Toole, G.A., 2000. Microbial Biofilms: from Ecology to Molecular Genetics. *Microbiology and Molecular Biology Reviews*, 64 (4), 847 – 867.

Defrance, L., and Jaffrin, M.Y., 1999a. Reversibility of fouling formed in activated sludge filtration, *J. Membr. Sci.*, 157 (1), 73–84.

Defrance, L., and Jaffrin, M.Y., 1999b. Comparison between filtrations at fixed transmembrane pressure and fixed permeate flux: application to a membrane bioreactor used for wastewater treatment, *J. Membr. Sci*., 152, 203–210.

Defrance, L., Jaffrin, M. Y. , Gupta, B., Paullier, P., and Geaugey, V., 2000. Contribution of various constituents of activated sludge to membrane bioreactor fouling, *Biosource tech.*, 73 (2), 105-112.

Donlan, R.M., 2002. Biofilms: Microbial Life on Surfaces. *Emerging Infectious Diseases*, 8 (9), 881 – 890.

Dubois, M., Gilles, K.A., Hamiltin, J.K., Rebers, P.A., and Smith, F., 1956. Colorimetric Method for Determination of Sugars and Related Substances. *Anal. Chem*., 28, 350–356.

Dufresne, R., Lebrun, R. E., and Lavallee, H. C., 1997. Comparative study on fluxes and performances during papermill wastewater treatment with membrane bioreactor, *Can. J. Chem,Eng*., 75, 95-103.

Eriksson, A.E., Baase, W.A., Zhang, X.J., Heinz, D.W., Blaber, M., Baldwin, E.P., and Matthews, B.W., 1992. Response of a protein structure to cavity-creating mutations and its relation to the hydrophobic effect. *Science*, 255, 178–183.

Evans, P.J., Bird, M.R., Pihlajamäki, A., and Nyström, M., 2008. The influence of hydrophobicity, roughness and charge upon ultrafiltration membranes for black tea liquor clarification. *J. Membr.Sci*., 313(1-2), 250–262.

Falk, M.W., Song, K.G., Matiasek, M.G., and Wuertz, S., 2009. Microbial community dynamics in replicate membrane bioreactors – natural reproducible fluctuations. *Water Research*, 43, 842-852.

Fane, A.G., and Fell, C.J.D., 1987. A review of fouling and fouling control in ultrafiltration, *Desalination*, 62, 117–136.

Fane, A.G., Fell, C.J.D., Hodgson, P.H., Leslie, G., and Marshall, K.C., 1991. Microfiltration of biomass and biofluids effect of membrane morphology and operating conditions. *Filtr. Sep*., 28 (5), 332- 340.

Fang, H.H.P., and Shi, X., 2005. Pore Fouling of Microfiltration Membranes by Activated Sludge. *J. Membr. Sci.* (1-2), 264, 161 – 166.

Fawehinmi, F., Lens, P., Stephenson, T., Rogalla, F., and Jefferson, B., 2004. The influence of operating conditions on EPS, SMP and bio-fouling in anaerobic MBR. *in Proceedings of the Water Environment-Membrane Technology Conference*, Seoul, Korea.

Flemming, H.-C., Schaule, G., McDonogh, R., and Ridgway, H.F., 1994. Effects and Extent of Biofilm Accumulation in Membrane Systems. In: Geesey G.G., Lewandowski Z., and Flemming H.-C. (eds) Biofouling and Biocorrosion in Industrial Water Systems. *Lewis Publishers*, Boca Raton, 62 – 87.

Flint, S.H., Brooks, J.D., and Bremer, P.J., 2000. Properties of the stainless steel substrate, influencing the adhesion of thermo-resistant streptococci. *J. Food Eng*., 43 (3), 235-242.

Gander, M.A., Jefferson, B., and Judd, S., 2000. Membrane bioreactors for use in small wastewater treatment plants: membrane materials and effluent quality, *Water Sci. Technol*., 41(1), 205–211.

Geng, Z., 2006. Study of membrane fouling in a membrane enhanced biological phosphorus removal process. The faculty of graduate studies (Civil Engineering), University of Bristish Columbia, 179.

Ghayeni, S.B.S., Beatson, P.J., Schneider, R.P., and Fane, A.G., 1998. Adhesion of wastewater bacteria to reverse osmosis membranes. *J. Membr. Sci*., 138 (1), 29–42.

Ghayenia, S. B. Sadr, Beatsona, P. J., Schneiderb, R. P., and Fane, A. G., 1998. Water reclamation from municipal wastewater using combined microfiltration-reverse osmosis (ME-RO): Preliminary performance data and microbiological aspects of system operation. *Desalination*, 116(1), 65-80.

Götzinger, E., Pircher, M., Dejaco-Ruhswurm, I., Kaminski, S., Skorpik, C., and Hitzenberger, C.K., 2007. Imaging of birefringent properties of keratoconus corneas by polarization-sensitive optical coherence tomography, *Investigative Ophthalmology & Visual Science* 48, 3551–3558.

Growth expected for MBR market. 2005. *Membr. Technol*., 2, 4.

Gunder, B., and Krauth, K.. 1998. Replacement of secondary clarification by membrane separation—results with plate and hollow fibre modules, *Water Sci. Technol*., 38 (4-5), 383–393.

Halle, C., Huck, P.M., Peldszus, S., Haberkamp, J., and Jekel, M., 2009. Assessing the performance of biological filtration as pretreatment to low pressure membranes for drinking water, *Environ Sci and Technol*, 43 (10), 3878–3884

Han, S.S., Bae, T.H., Jang, G.G., and Tak, T.M., 2005. Influence of sludge retention time on membrane fouling and bioactivities in membrane bioreactor system, *Process Biochemistry*, 40 (7), 2393–2400.

Hanaki, K., Wantawin, C., and Ohgaki, S., 1990. Effects of the activity of heterotrophs on nitrification in a suspended growth reactor. *Water Res*. 24(3), 289-296.

Hanft, S., 2006. C-240 Membrane Bioreactors in the Changing World Water Market. Business Communications Company Inc..

He, Y., Xu, P., Li, C., and Zhang, B., 2005. High-concentration food wastewater treatment by an anaerobic membrane bioreactor. *Water Res*., 39(17), 4110–4118.

Holbrook, R.D., Higgins, M.J., Murthy, S.N., Fonseca, A.D., Fleischer, E.J., Daigger, G.T., Grizzard, T.J., Love, N.G., and Novak, J.T., 2004. Effect of alum addition on the performance of submerged membranes for wastewater treatment, *Water Environ. Res*., 76 (7), 2699–2702.

Hong, S., Krishna, P., Hobbs, C., Kim, D., and Cho, J., 2005. Variations in backwash efficiencyduring colloidal filtration of hollow-fiber microfiltration membranes, *Desalination*, 173 (3), 257-268.

Hong, S.P., Bae, T.H., Tak, T.M., Hong, S., and Randall, A., 2002. Fouling control in activated sludge submerged hollow fiber membrane bioreactors, *Desalination*, 143 (3), 219–228.

Huang, X., Wei, C. H., and Yu, K.C., 2008. Mechanism of membrane fouling control by suspended carriers in a submerged membrane bioreactor. *J. Membr. Sci*. 309 (1-2), 7-16.

Hwang, K.J., Chana, C. S., and Tung, K.L., 2009. Effect of backwash on the performance of submerged membrane filtration. *J. Membr.Sci*, 330 (1-2), 349-356.

Jefferson, B., Brookes, A., Le-Clech, P. and Judd, S.J., 2004. Methods for understanding organic fouling in MBRs, *Water Sci. Technol*., 49 (2), 237–244.

Ji, L., and Zhou, J., 2006. Influence of aeration on microbial polymers and membrane fouling in submerged membrane bioreactors, *J. Membr. Sci.*, 276 (1-2), 168–177.

Jiang, T., Kennedy, M.D., Guinzbourg, B.F., Vanrolleghem, P.A., and Schippers, J.C., 2005. Optimising the operation of an MBR pilot plant by quantitative analysis of the membrane fouling mechanism, *Water Sci. Technol.* 51 (6-7), 19–25.

Judd, S., 2006. *The MBR book.* Elsevier.

Kane, M.D., Poulsen, L.K., and Stahl, D.A., 1993. Monitoring the enrichment and isolation of sulfate-reducing bacteria by using oligonucleotide hybridization probes designed from environmentally derived 16S rRNA sequences. *Applied and Environmental Microbiology*, 59(3), 682-686.

Kang, I.J., Yoon, S.H., and Lee, C.H., 2002. Comparison of the filtration characteristics of organic and inorganic membranes in a membrane-coupled anaerobic bioreactor *Water Res*., 36 (7), 1803–1813..

Kang, S., Hoek, E.M.V., Choi, H., and Shin, H., 2006. Effect of membrane surface properties during the fast evaluation of cell attachment, *Sep. Sci. Technol.*, 41 (7), 1475–1487.

Khawaji, A.D., Kutubkhanah, I.K., and Wie, J.M., 2008. Advances in seawater desalination technologies. *Desalination*, 221, 47-69.

Kim J.S., Lee, C.H., and Chun, H.D., 1998. Comparison of ultrafiltration characteristics between activated sludge and BAC sludge. *Wat Res.*, 32 (1), 3443–3451.

Kim, H.Y., Yeon, K.M., Lee, C.H., Lee, S., and Swaminathan, T., 2006. Biofilm structure and extracellular polymeric substances in low and high dissolved oxygen membrane bioreactors, *Sep. Sci. Technol.*, 41(7), 1213–1230.

Kim, J., Lee, M., and Yoon, T.L., 2009, Membrane autopies to investigate scale fouling: pilot scale MBR tests in wastewater treatment application, in: 5th IWA specialized membrane technology conference for waste and wastewater treatment, Beijing.

Kim, J.S., and Lee, C.H., 2003. Effect of powdered activated carbon on the performance of an aerobic membrane bioreactor: comparison between cross-flow and submerged membrane systems, *Water Environ. Res*., 75 (4), 300–307.

Kimura, K., Naruse, T., and Watanabe, Y., 2009. Changes in characteristics of soluble microbial products in membrane bioreactors associated with different solid retention times: Relation to membrane fouling, *Water Res*. 43 (4) 1033-1039.

Kimura, Y., Mizusawa, N., Ishii, A., and Ono, T.A., 2005. FTIR detection of structural changes in a histidine ligand during S-state cycling of photosynthetic oxygen-evolving complex. *Biochemistry*, 44(49), 16072-16078.

Knoblock, M.D., Sutton, P.M., Mishra, P.N., Gupta, K., and Janson, A., 1994. Membrane biological reactor system for treatment of oily wastewaters. *Water Environ Res*., 66(2), 133–139.

Knoell, T., Safarik, J., Cormack, T., Riley, R., Lin, S.W., and Ridgway, H., 1999. Biofouling potentials of microporous polysulfone membranes containing a sulfonated

polyether-ethersulfone/polyethersulfone block copolymer: correlation of membrane surface properties with bacterial attachment. *J. Membr. Sci*., 157 (1), 117–138.

Korshin, G.V., Kumke, M.U., Li, Ch.-W., and Frimmel, F.H., 1999. Influence of chlorination on chromophores and fluorophores in humic substances. *Environ. Sci. & Technol*., 33(8), 1207–1212.

Kuberkar, V., Czekaj, P., and Davis, R., 1998. Flux enhancement for membrane filtration of bacterial suspensions using high-frequency backpulsing, *Biotechnol. Bioeng*. 60 (1) 77-87.

Kumar, M., Adham, S. S., and Pearce, W.R., 2006. Investigation of seawater reverse osmosis fouling and its relationship to pretreatment type, *Environ. Sci. Technol*., 40(6) 2037–2044.

Kwok, W.K., Picioreanu, C., Ong, S.L., van Loosdrecht, M.C.M., Ng, W.J., and Heijnen J.J., 1998. Influence of Biomass Production and Detachment Forces on Biofilm Structures in a Biofilm Airlift Suspension Reactor. *Biotechnology and Bioengineering*, 58 (4), 400 – 407.

Lacoste, B., Drakides, C., and Rumeau, M., 1992. *Proc. Interfltra*, 92, Paris, 287-292.

Laspidou, C.S., and Rittmann, B.E., 2002. A unified theory for extracellular polymeric substances, soluble microbial products, and active and inert biomass. *Water Res*. 36 (11), 2711-2720.

Le Roux, I., Krieg, H.M., Yeates, C.A., and Breytenbach, J.C., 2005. Use of chitosan as an antifouling agent in a membrane bioreactor, *J. Membr. Sci*., 248 (1-2), 127–136.

Le-Clech, P., Chen, V., and Fane, T.A.G., 2006a. Fouling in membrane bioreactor used in wastewater treatment. *J. Membr. Sci*.,284 (1-2), 17–51.

Le-Clech, P., Fane, A., Leslie, G. and Childress, A., 2005. The operator's perspective, *Filt. Sep*.,42, 20–23.

Le-Clech, P., Jefferson, B., Chang, I.S. and Judd, S.J., 2003. Critical flux determination by the flux-step method in a submerged membrane bioreactor, *J. Membr. Sci.* ,227 (1-2), 81–93.

Le-Clech, P., Jefferson, B., and Judd, S.J., 2003. Impact of aeration, solids concentration and membrane characteristics on the hydraulic performance of a membrane bioreactor. *J. Membr. Sci*. ,218 (1-2), 117–129.

Le-Clech, P., Metzger, U., Stuetz, R., and Chen, V., 2006b. Modes of filtration in membrane bioreactors and its effects on polymeric fouling. *Proceedings of the Eurombra Workshop on Biofouling in membrane systems Trondheim*, Norway.

Lee, J., Ahn, W.Y., and Lee, C.H., 2001. Comparison of the filtration characteristics between attached and suspended growth microorganisms in submerged membrane bioreactor, *Water Res.*, 35 (10), 2435–2445.

Lee, W., Kang, S., and Shin, H., 2003. Sludge characteristics and their contribution to microfiltration in submerged membrane bioreactors. *J. Membr. Sci*. 216(1-2) , 217–227.

Lesjean, B., Rosenberger, S., Schrotter, J., and Recherche, A., 2004. Membrane-aided biological wastewater treatment — an overview of applied systems. *Membr. Technol*., 2004(8), 5-10.

Leslie, G.L., Schneider, R.P., Fane, A.G., Marshall, K.C., and Fell, C.J.D., 1993. Fouling of a Microfiltration Membrane by 2 Gram-Negative Bacteria. *Colloids Surf. A: Physicochem. Eng. Aspects*, 73, 165–178.

Li, M.S., Zhao, Y.J., Zhou, S.Y., Xing, W.H., and Wong, F.S., 2007. Resistance analysis for ceramic membrane microfiltration of raw soy sauce, *J. Membr. Sci.*, 299 (1-2), 122–129.

Li, W., Xing, W., Jin, W., and Xu, N., 2006. Effect of pH on microfiltration of Chinese herb aqueous extract by zirconia membrane, *Sep. Purif. Technol*., 50 (1), 92–96.

Li, Y.Z., He, Y.L., Liu, Y.H., Yang, S.C., and Zhang, G.J., 2005. Comparison of the filtration characteristics between biological powdered activated carbon sludge and activated sludge in submerged membrane bioreactors, *Desalination*, 174 (3), 305–314.

Liang, S., Liu, C., and Song, L.S., 2007. Soluble microbial products in membrane bioreactor operation: Behaviors, characteristics, and fouling potential. *Water Res*., 41(1), 95-101.

Liao, X. Z., Zou J., Cockayne, D. J. H., Jiang, Z. M., and Wang, X., 2001. Extracting composition and alloying information of coherent Ge(Si)/Si(001) islands from [001] on-zone bright-field diffraction contrast images. *J. Appl. Phys.*, 90, 2725-2729.

Liu, R., Huang, X., Chen, L., Wen, X., and Qian, Y., 2005. Operational performance of a submerged membrane bioreactor for reclamation of bath wastewater, *Process Biochem.*, 40 (1), 125–130.

Liu, R., Huang, X., Wang, C.W., Chen, L.J., and Qian, Y., 2000. Study on hydraulic characteristics in a submerged membrane bioreactor process, *Process Biochem*., 36 (3), 249–254.

Liu, W. T., Marsh, T. L., Cheng, H., and Forney, L. J., 1997. Characterisation of microbial diversity by determining terminal restriction fragment length polymorphisms of genes by encoding 16S rRNA. *Applied and Environmental Microbiology*, 63, 4516-4522.

Lowry, O., Rosebrough, N., Farr, A., and Randall, R., 1951. Protein Measurement with the Folin Phenol Reagent. *J. Biolog. Chem*., 193 (1), 265–275.

Lyko, S., Al-Halbouni, D., Wintgens, T., Janot, A., Hollender, J., Dott, W., and Melin, T., 2007. Polymeric compounds in activated sludge supernatant – characterization and

retention mechanisms at a full-scale municipal membrane bioreactor, *Water Res*. 41, 3894–3902.

Ma, L., Li, X., Du, G., Chen, J., and Shen, Z., 2005. Influence of the filtration modes on colloid adsorption on the membrane in submerged membrane bioreactor, Colloid Surf. A: *Physiochem. Eng. Asp.,* 264 (1-3), 120–125.

Madaeni, S.S., 1997. The effect of operating conditions on critical flux in membrane filtration of latexes, *Process Safety Environ. Protection* ,75 (4), 266–269.

Madaeni, S.S., Fane, A.G., and Wiley, D.E., 1999. Factors influencing critical flux in membrane filtration of activated sludge, *J. Chem. Technol. Biotechnol*., 74 (6), 539–543.

Marcato, C.E., Mohtar, R., Revel, J.C., Pouech, P., Hafidi, M., and Guiresse M., 2009. Impact of anaerobic digestion on organic matter quality in pig slurry, *Int. Biodeterior. Biodegrad.* 63 (3), 260–266.

Marshall, A.D., Munro, P.A., and Tragard, G., 1993. The effect of protein fouling in microfiltration and ultrafiltration on permeate flux, protein retention and selectivity: a literature review, *Desalination*, 91 (1), 65–108.

Maruyama, T., and Katoh, S., 2001. FTIR analysis of BSA fouled on ultrafiltration and microfiltration membranes, *J. Membr. Sci*., 192 (1-2), 201-207.

Massé, A., Sperandio, M., and Cabassud, C., 2006. Comparison of sludge characteristics and performance of a submerged membrane bioreactor and an activated sludge process at high solids retention time. *Water Res.*,40 (12), 2405–2415.

Matthiasson, E., 1983. The role of macromolecular adsorption in fouling of ultrafiltration membranes, *J. Membr. Sci.,* 16, 23–36.

Mattias, N., Gun, T., and Karin, Ö., 2008. Influence of temperature and cleaning on aromatic and semi-aromatic polyamide thin-film composite NF and RO membranes, *Separation Sci Tech*., 62 (3), 719–728.

Meng , F.G., Zhang, H.M., Yang, F.L., and Liu, L.F., 2007. Characteristics of cake layer in submerged membrane bioreactor, *Environ. Sci. Technol*., 41 (11), 4065-4070.

Meng F.G., Yang, F.L., Shi, B.Q., and Zhang, H.M., 2008. A comprehensive study on membrane fouling in submerged membrane bioreactors operated under different aeration intensities, *J. Membr. Sci*., 59 (1), 91–100.

Meng, F., Zhang, H., Yang, F., Li, Y., Xiao, J., and Zhang, X., 2006. Effect of filamentous bacteria on membrane fouling in submerged membrane bioreactor. *J. Membr. Sci*., 272 (1–2), 161–168.

Metsamuuronen, S., Howell, J. and Nystrom, M., 2002. Critical flux in ultrafiltration of myoglobin and baker's yeast, *J. Membr. Sci.*, 196 (1), 13–25.

Mikkelsen, L. H., and Keiding, K., 2001. Effects of solids concentration on activated sludge deflocculating, conditioning and dewatering. *Water Sci. and Technol.*, 44(2-3), 417-425.

Morgan, S.L., Baggott, J.E., Vaughn, W.H., Young, P.K., Austin, J.V., Krumdieck, C.L., and Alarcon, G.S., 1990. The effect of folic acid supplementation on the toxicity of low-dose methotrexate in patients with rheumatoid arthritis. *Arthritis Rheum* , 33, 9-18.

Mounier, S., Braucher, R., Benaim, J.Y., 1999. Differentiation of organic matter's properties of the Rio Negro basin by crossflow ultra-filtration and UV-spectrofluorescence. *Water Res*, 33(10), 2363-2373.

Muller, E.B., Stouthamer, A.H., van Verseveld, H.W., and Eikeiboom, D.M., 1995. Aerobic domestic wastewater treatment in a pilot plant with complete sludge retention by cross-flow filtration, *Water Res*., 29 (4), 1179-1189.

Ng, C.A., Sun, D., Zhang, J., Chua, H.C., Bing, W., Tay, S., and Fane, A., 2005. Strategies to improve the sustainable operation of membrane bioreactors, *Proceedings of the International Desalination Association Conference*, Singapore .

Ng, H.Y., and Hermanowicz, S.W., 2005. Membrane bioreactor operation at short solids retention times: performance and biomass characteristics. *Water Res.* 39 (6), 981–992.

Ng, H.Y., Tan, T.W., and Ong, S.L., 2006. Membrane fouling of submerged membrane bioreactors: impact of mean cell residence time and the contributing factors. *Environ. Sci. Technol*., 40 (8), 2706–2713.

Ng, T.C.A., and Ng, H.Y., 2010. Characterisation of initial fouling in aerobic submerged membrane bioreactors in relation to physic-chemical characteristics under different flux consitions. Water Res., 44, 2336-2348.

Ognier, S., Wisniewski, C., and Grasmick, A., 2002a. Membrane fouling during constant flux filtration in membrane bioreactors, *Membr. Technol*., 2002 (7), 6–10.

Ognier, S., Wisniewski , C., and Grasmick, A., 2002b. Influence of macromolecule adsorption during filtration of a membrane bioreactor mixed liquor suspension, *J. Membr. Sci*., 209 (1), 27–37.

Omoike, A., and Chorover, J., 2004. Spectroscopic study of extracellular polymeric substances from *Bacillus subtilis*: aqueous chemistry and adsorption effects, *Biomacromolecules* , 5 (4), 1219–1230.

Orantes, J.C., Wisniewski, C., Heran, M., and Grasmick, A., 2004. Influence of total sludge retention on the performance of a submerge membrane bioreactor, *Proceedings of the Water Environment-Membrane Technology Conference*, Seoul, Korea.

Ousman, M., and Bennasar, M., 1995. Determination of various hydraulic resistances during crossflow filtration of a starch grain suspension through inorganic membranes, *J. Membr. Sci.*, 105 (1-2), 1–21.

Pasmore, M., Todd, P., Smith, S., Baker, D., Silverstein, J.A., Coons, D., and Bowman, C.N., 2001. Effects of ultrafiltration membrane surface properties on *Pseudomonas aeruginosa* biofilm initiation for the purpose of reducing biofouling, *J. Membr. Sci.*, 194 (1), 15–32.

Qin, J., Kekre, K.A., Tao, G., Oo, M.H., Wai, M.N., Lee, T.C., Viswanath, B., and Seah, H., 2006. New option of MBR-RO process for production of NEWater from domestic sewage. *J. Membr. Sci*., 272(1-2), 70-77.

Quirynen, M., van der Mei, H.C., Bollen, C. M., Schotte. A, Marechal, M., Doornbusch, G. I., Naert, I., Busscher, H. J., and van Steenberghe, D., 1993. An in vivo study of the influence of the surface roughness of implants on the microbiology of supra- and subgingival plaque. *J. Dent. Res.*, 72 (9), 1304-1309.

Rahman, M.M., and Al-Malack, M.H., 2006. Performance of a crossflow membrane bioreactor (CF-MBR) when treating refinery wastewater. Desalination, 191, 16–26.

Reynolds, D.M., and Ahmad, S.R., 1997. Rapid and direct determination of wastewater BOD values using fluorescence technique. *Water Res*., 31 (8), 2012–2018.

Rojas, M.E. H., Kaam, R. V., Schetrite, S., and Albasi, C., 2005. Role and variations of supernatant compounds in submerged membrane bioreactor fouling, Desalination, 179 (1-3), 95-107.

Rosenberger, S., Evenblij, H., te Poele, S., Wintgens, T., and Laabs, C., 2005. The importance of liquid phase analyses to understand fouling in membrane assisted activated sludge processes-six case studies of different European research groups, *J. Membr. Sci.*, 263 (1-2), 113–126.

Rosenberger, S., Krüger, U., Witzig, R., Manz, W., Szewzyk, U., and Kraume, M., 2002. Performance of a bioreactor with submerged membranes for aerobic treatment of municipal wastewater, *Water. Res.*, 36(2), 13–20.

Rosenberger, S., Laabs, C., Lesjean, B., Gnirss, R., Amy, G., Jekel, M., and Schrotter, J.C., 2006. Impact of colloidal and soluble organic material on membrane performance in membrane bioreactors for municipal wastewater treatment, *Water Res.*, 40 (4), 710–720.

Rosenberger, S., Laabs, C., Lesjean, B., Gnirss, R., Amy, G., Jekel, M., and Schrotter, J.C., 2006. Impact of colloidal and soluble organic material on membrane performance in membrane bioreactors for municipal wastewater treatment, *Water Res.*, 40 (4), 710–720.

Seidel, A., and Elimelech, M., 2002. Coupling between chemical and physical interactions in natural organic matter (NOM) fouling of nanofiltration membranes: implications for fouling control. . *J. Membr. Sci*., 20(3), 245-255.

Senesi, N., 1990. Molecular and quantitative aspects of the chemistry of fulvic acid and its interactions with metal ions and organic chemicals. Part II. The fluorescence spectroscopy approach. *Anal. Chim. Acta*., 232, 77–106.

Shimizu, Y., Rokudai, M., Tohya, S., Kauawake, E., Yazawa, T., Tanaka, H., and Eguchi, K., 1989. Effect of pore size on the filtration characteristics of ceramic membrane for membrane bioreactors. *Kagaku Kogaku Ronbu nshu*, 15, 322.

Shin, H.S., and Kang, S.T., 2003. Characteristics and fates of soluble microbial products in ceramic membrane bioreactor at various sludge retention times, *Water Res.,* 37 (1), 121–127.

Singh, K.K., and Vincent, W.S., 1987. Clumping characteristics and hydrophobic behavior of an isolated bacterial strain from sewage sludge. *Appl. Microbiol. Biotechnol*. 25, 396–398.

Smidt, E., and Parravicini, V., 2009. Effect of sewage sludge treatment and additional aerobic post-stabilization revealed by infrared spectroscopy and multivariate data analysis, *Bioresour. Technol.* 100 (5), 1775–1780.

Smidt, E., and Meissl, K., 2007. The applicability of Fourier transform infrared (FTIR) spectroscopy in waste management, *Waste Manage.* 27 (2), 268–276.

Sofia, A., Ng, W.J., and Ong, S.L., 2004. Engineering design approaches for minimum fouling in submerged MBR, *Desalination*, 160 (1), 67–74.

Sondhi, R., and Bhave, R., 2001, Role of backpulsing in fouling minimization in crossflow filtration with ceramic membranes. *J. Membr. Sci*. 186 (1), 41–52.

Sondhi, R., Lin, Y.S., and Alvarez, F., 2000. Crossflow filtration of chromium hydroxide suspensions by ceramic membranes: Fouling and its minimization by backpulsing, *J. Membr. Sci*. 174, pp. 111–122.

Stoodley, H.L., Costerton, J.W., and Stoodley, P., 2004. Bacterial Biofilms: From the Natural Environment to Infectious Diseases. *Nature Reviews Microbiology*, 2, 95-108.

Stoodley, P., Sauer, K., Davies, D.G., and Costerton, J.W., 2002. Biofilms as Complex Differentiated Communities. *Annual Reviews in Microbiology*, 56, 187 – 209.

Sun, D. D., Hay, C. T., and Khor, S.L., 2006. Effects of hydraulic retention time on behavior of start-up submerged membrane bioreactor with prolonged sludge retention time. *Desalination*., 195, 209-225.

Swietlik, J., Dabrowska, A., Raczyk-Stanis1awiak, U., and Nawrocki, J., 2004. Reactivity of natural organic matter fractions with chlorine dioxide and ozone. *Water Res*., 38 (3), 547–558.

Tan, T.W., and Ng, H. Y., 2008. Influence of mixed liquor recycle ratio and dissolved oxygen on performance of pre-denitrification submerged membrane bioreactors, *Water Res*., 42 (4-5), 1122 – 1132.

Tardieu, E., Grasmick, A., Geaugey, V., and Manem, J., 1996. Fouling mechanisms in membrane bioreactors applied to wastewater treatment. In: *Proceedings of the Seventh World Filtration Congress,* Budapest, 571-575.

Tardieu, E., Grasmick, A., Geaugey, V., and Manem, J., 1999. Influence of hydrodynamics on fouling velocity in a recirculated MBR for wastewater treatment. *J. Mem Sci*., 156 (1), 131-140.

Trouve, F.W., Urbain, V., and Manem, J., 1994. Treatment of municipal wastewater by membrane bioreactor: results of a semi-industrial pilot scale study. *Water Sci. Technol*., 30, 151-157.

Trussell, R.S., Merlo, R.P., Hermanowicz, S.W., and Jenkins, D., 2006. The effect of organic loading on process performance and membrane fouling in a submerged membrane bioreactor treating municipal wastewater, *Water Res.,* 40 (14), 2675–2683.

Ueda, T., Hata, K., Kikuoka, Y., and Seino, O., 1997. Effects of aeration on suction pressure in a submerged membrane bioreactor, *Water Res*., 31 (3), 489–494.

Valin, S.D., and Sutherland, D.J., 1982. Predicting previous termbioflocculation: new developments in the application of flocculation theory. *Environ. Technol. Lett.* 3, 363–374.

Visvanathan, C., Choudhary, M. K., Montalbo, M. T., and Jegatheesan, V., 2007. Landfill leachate treatment using thermophilic membrane Bioreactor. *Desalination* , 204 (1-3), 8–16.

Wang, X.M., Li X.Y., and Huang, X., 2007. Membrane fouling in a submerged membrane bioreactor (SMBR): characterisation of the sludge cake and its high filtration resistance, *Sep. Purif. Technol*., 52 (3), 439–445.

Wang, Y., Tang S., and Zhang J., 2004. Clarification of soy sauce by the inorganic ceramic membrane ultrafitration, *China Condiment* (Chinese) ,1, 140–143.

Wang, Z.W., Wu, Z.C., Mai, S.H., Yang, C.F., Wang, X.H., An, Y., and Zhou, Z., 2008a. Research and applications of membrane bioreactors in China: Progress and prospect. *Sep. Purifi. Technol.*, 62 (2), 249–263.

Wang, Z.W., Wu, Z.C., and Tang, S.J., 2009. Characterization of dissolved organic matter in a submerged membrane bioreactor by using three-dimensional excitation and emission matrix fluorescence spectroscopy, *Water Res*., 43 (6), 1533-1540.

Wang, Z.W., Wu, Z.C., Yin, X., and Tian, L.M., 2008b. Membrane fouling in a submerged membrane bioreactor (MBR) under sub-critical flux operation : Membrane foulant and gel layer characterization. *J. Membr. Sci.*, 325 (1), 238-244.

Wei, C.H., Huang, X., Wang, C.W., and Wen, X.H., 2006. Effect of a suspended carrier on membrane fouling in a submerged membrane bioreactor, *Water Sci. Technol*., 53 (6), 211–220.

Wen, X., Bu, Q., and Huang X., 2004. Study on fouling characteristic of a axial hollow fibers cross-flow microfiltration under different flux operations, *Proceedings of the Water Environment-Membrane Technology Conference* Seoul, Korea.

White, D.A., and Asaadi, M., 1989. Fouling behavior in inorganic tubular membranes, in: *Proceedings of the International Technical Conference on Membrane Separation Process*, Brighton, UK.

Wisniewski, C., and Grasmik, A., 1998. Floc size distributuion in a membrane bioreactor and consequences for membrane fouling. *Colloids Surfaces A: Physicochem Eng Aspects*, 138 (2-3), 403–411.

Wilén, B.M., Jin, B., and Lant, P., 2003. The influence of key chemical constituents in activated sludge on surface and flocculating properties, *Water Res*. 37 (9), 2127–2139.

Wu, D., Howell, J.A., and Field, W., 1999. Critical flux measurement for model colloids, *J. Membr. Sci.*, 152 (1), 89–98.

Xing, C.H., 1998. Ceramic membrane bioreactor for urban wastewater treatment and membrane fouling mechanism, Ph.D. Thesis, Department of Environmental Science and engineering, Tsinghua University, (in Chinese).

Xing, C.H., Tardieu, E., Qian, Y., and Wen, X.H., 2000. Ultrafiltration membrane bioreactor for urban wastewater reclamation. *J. Mem Sci*., 177(1-2), 73-82.

Xing, C.H., Wen, X.H., Qian, Y., and Tardieu, E., 2001. Microfiltration-membrane-coupled bioreactor for urban wastewater reclamation. *Desalination*, 141, 63-73.

Xu, Y., Dodds, J., and Leclerc, D., 1995. Optimization dissontinuous microfiltration backwash process, *J. Chem. Eng*., 57 (3), 247-251.

Yamagishi, T., Matsuda, M., Masuda, H., Kamisawa, C., Iizumi, S., Oomura, T., Nagura, K., Ito, S., Taked, A.H., Suzuki, T., Toyohara, H., and Okada, T., 1990. Crossflow filtration for anaerobic wastewaters. *Polution Jpn*, 5, 291.

Yamamoto, K., Hiasa, M., and Mahmood, T., 1989. Direct solid–liquid separation using hollow fiber membrane in an activated sludge aeration tank, *Water Sci. Technol*., 21 (4-5), 43-54.

Yamashita, Y., and Tanoue, E., 2003. Chemical characterization of protein-like fluorophores in DOM in relation to aromatic amino acids. *Marine Chemistry* 82 (3–4), 255–271.

Yamato, N., Kimura, K., Miyoshia, T., and Watanabe, Y., 2006. Difference in membrane fouling in membrane bioreactors (MBRs) caused by membrane polymer materials. *J. Mem Sci.*, 280(1-2), 911-919.

Yang, Q.Y., Chen, J.H., and Zhang, F., 2006. Membrane fouling control in a submerged membrane bioreactor with porous, flexible suspended carriers, *Desalination*. 189 (1-3) 292–302.

Yigit, N.O., Civelekoglu, G., Harman, I., Koseoglu, H., and Kitis, M., 2009. Effects of various backwash scenarios on membrane fouling in a membrane bioreactor, *Desalination*, 237 (1-3), 346–356.

Yun, M.A., Yeon, K.M., Park, J.S., Lee, C.H. , Chun, J., and Lim, D.J., 2006. Characterization of biofilm structure and its effect on membrane permeability in MBR for dye wastewater treatment, *Water. Res*, 40 (1), 45-52.

Zhang, J., Chua, H.C., Zhou, J., and Fane, A.G., 2006. Factors affecting the membrane performance in submerged MBR, *J. Membr. Sci*., 284 (1-2), 54–66.

Zheng, X., Ernst, M., and Jekel, M., 2010. Pilot-scale investigation on the removal of organic foulants in secondary effluent by slow sand filtration prior to ultrafiltration, *Water Res.*, 44 (10), 3203–3213.

Zheng, X., Mehrez, R., Jekel, M., and Ernst, M., 2009. Effect of slow sand filtration of treated wastewater as pre-treatment to UF, *Desalination*, 249 (2), 591–595.

Zhou, J., Yang, F.L., Meng, F.G., An, P., and Wang, D., 2007. Comparison of membrane fouling during short-term filtration of aerobic granular sludge and activated sludge, *J. Environ. Sci.*, 19 (11), 1281-1286.

Publication lists:

Journal:

L. Jin, H. Y. Ng and S. L. Ong, 2009. Performance and fouling characteristics of different pore-sized submerged ceramic membrane bioreactors (SCMBR), *Water Science & Technology-WST*, 59(11), 2213-2218.

L. Jin, S. L. Ong and H. Y. Ng, 2010. Comparison of fouling characteristics in different pore-sized submerged ceramic membrane bioreactors. *Water Res*., 44(20), 5907-5018.

L. Jin, H. Y. Ng and S. L. Ong, Fouling characteristics of ceramic membranes in submerged membrane bioreactors systems. (Under preparation)

L. Jin, H. Y. Ng and S. L. Ong, Effect of in-situ backwash on membrane fouling in submerged ceramic membrane bioreactors. (Under preparation)

International Conferences:

L. Jin, H. Y. Ng and S. L. Ong, The performance and fouling characteristics of different pore-size submerged ceramic membrane bioreactors in treating domestic wastewater. *Proceedings of 2008 IWA North American Membrane Research Conference*, 10-13 August 2008, University of Massachusetts, USA. (Poster presentation).

L. Jin, H. Y. Ng and S. L. Ong, Performance and fouling characteristics of different pore-size submerged ceramic membrane bioreactors (SCMBR). *Proceedings of the IWA 1st Asia-Pacific Regional Young Water Professional Conference*, 8-10 December 2008, Gwangju, South Korea. (Oral Presentation).

L. Jin, H. Y. Ng and S. L. Ong, Effect of pore size on treatment performance and fouling in ceramic membrane bioreactors. *Proceedings of 5th IWA Specialist Membrane Technology Conference and Exhibition for Water and Wastewater Treatment*, 1-3 September 2009, Beijing, China. (Oral presentation).

L. Jin, H. Y. Ng and S. L. Ong, Effect of membrane pore size on membrane biofouling in ceramic membrane bioreactors. The 82nd Annual Water Environment Federation Technical Exhibition and Conference, 10-14 October 2009, Orlando, USA. (Oral presentation).

L. Jin, H. Y. Ng and S. L. Ong, Performance and fouling potential of different pore-sized ceramic membrane bioreactors. *Proceedings of 3rd IWA-ASPIRE Conference & Exhibition*, 18-22 October 2009, Taipei. (Oral presentation).

L. Jin, S. L. Ong and H. Y. Ng, Effect of dissolved organic matters on fouling in submerged ceramic membrane bioreactors. The water congress 2010, Montréal, Canada, 18-24 September 2010. (Poster presentation).